NASA TECHNICAL MEMORANDUM

NASA TM X-53499

August 26, 1966

NASA TM X-53499

LUNAR THERMAL ENVIRONMENT

By James K. Harrison, Daniel W. Gates,
James R. Watkins, Billy P. Jones

Research Projects Laboratory

NASA

George C. Marshall
Space Flight Center,
Huntsville, Alabama

TECHNICAL MEMORANDUM X-53499

LUNAR THERMAL ENVIRONMENT

by

James K. Harrison
Daniel W. Gates
James R. Watkins
Billy P. Jones

George C. Marshall Space Flight Center
Huntsville, Alabama

ABSTRACT

This report provides current quantitative data on photometric, light polarization, luminescence, color, microwave temperature, and infrared temperature properties of the moon. No theoretical models or deductions from them are included; only selected experimental data obtained from measurements made from earth are included.

NASA-GEORGE C. MARSHALL SPACE FLIGHT CENTER

NASA-GEORGE C. MARSHALL SPACE FLIGHT CENTER

TECHNICAL MEMORANDUM X-53499

LUNAR THERMAL ENVIRONMENT

by

James K. Harrison
Daniel W. Gates
James R. Watkins
Billy P. Jones

RESEARCH PROJECTS LABORATORY
RESEARCH AND DEVELOPMENT OPERATIONS

TABLE OF CONTENTS

TECHNICAL MEMORANDUM X-53499

LUNAR THERMAL ENVIRONMENT

SUMMARY

This report provides current quantitative data on photometric, light polarization, luminescence, color, microwave temperature, and infrared temperature properties of the moon. No theoretical models or deductions from them are included; only selected experimental data obtained from measurements made from earth are included.

author

INTRODUCTION

This report gives scientific guidelines that may be regarded as a definition of the lunar thermal environment as determined by measurements made from earth. Specifically, it provides current quantitative data on photometric, light polarization, luminescence, color, microwave temperature, and infrared temperature properties of the moon.

The purpose of the report is to present facts concerning the thermal environment of the moon in a handy reference form for designers of equipment to be used in lunar exploration, those trying to establish scientific experiments, and theorists attempting to arrive at a thermal model satisfying all measured data that enters into an energy balance on the moon's surface.

No theoretical models or deductions from them are included and neither is all experimental data. Only experimental data are included. In most cases, recently obtained data are used since they have been collected with refined instruments having improved resolution. However, this does not mean that measurements made earlier are of no value, but rather that the earlier measurements are more difficult to interpret. The primary reason for this is that the moon is heterogeneous in its thermal radiation properties and as the resolution decreases, the measurements tend to hide the heterogeneity. This aspect notwithstanding, it is sometimes useful to have such over-all information. For this reason, an attempt is made to provide data in each of the areas (photometric, etc.) giving over-all and some detailed features. For example, a single light polarization curve for the illuminated portion of the disk is given as well as a set of graphs showing polarization of specific local areas of the moon.

Although a relatively small number (31) of references are cited, stacks of scientific papers were used in the preparation of this report. These papers were accumulated systematically for several years; some of them are listed in two bibliographies[1,2] which were produced by concentrated effort on the part of the Redstone Scientific Information Center in cooperation with the Research Projects Laboratory of the Marshall Space Flight Center. The data actually chosen for this report represent a judgment by the authors, based upon a long and continuing review of the literature and combined with experience obtained over several years in the thermal design of spacecraft.

It is the present intent to revise this report as more information becomes available. In addition, a much more comprehensive and detailed report is in preparation. The latter will give the results of most of the experimental measurements that have been published in those thermal physics areas without regard to discriminatory judgment as to which is more accurate or more useful. The purpose of the more detailed report is to provide all experimental data under a single cover for easy access to a designer who wishes to dig deeper in order to make his own judgment about the moon's environment for his particular application. As it now stands, there exists a vast quantity of information which is scattered widely throughout many journals and publications. Because of this, the information is essentially inaccessible to a large number of persons who need it but do not have the time or inclination to dig it out.

---

[1] Shenk, C. F., H. P. Eckstein and W. P. McNutt: "Lunar Thermophysics," Redstone Scientific Information Center, U.S. Army Missile Command, Redstone Arsenal, Alabama, RSIC-419 (June 1965).

[2] McNutt, W. P., G. Caras, R. L. Langston, J. Terry and H. Hoop: "Lunar Thermophysics (Supplement to RSIC-419)," Redstone Arsenal, Alabama, RSIC-462 (Sept. 1965).

The authors would be glad to receive any constructive suggestions from users of the report, especially those comments which can be taken into account in future revisions.

PHOTOMETRIC ALBEDO

The albedo for prominent features on the lunar surface is presented in Table I [1] and Figure 1. Table I data are for full moon, while the data in Figure 1 are for a nearly full moon (7° phase). The columns in the table give: (1) the crater number and name, (2) the value of p, (3) the value of A, (4) the value of a, and (5) the value of p, as measured by Markov and by Sytinskaya. The figure gives p, obtained by Saari and Shorthill, from a calibration of their voltage values against the albedo data of Sytinskaya.

The factor p was originally defined by Russell [3] for a planet as: the ratio of the actual brightness of the planet at full phase to that of a self-luminous body of the same size and position, which radiates as much light from each unit of its surface as the planet receives from the sun under normal illumination. The tabular values of p (except for the whole moon), since they are for local regions, would require that this definition be altered from the entire planet viewpoint to that of the local regions for which the value applies. p is the fraction of light reflected toward the earth and is, therefore, a directional albedo. Russell gives p in equation form:

$$p = \frac{M_o R^2 \Delta^2}{r^2}$$

where,

M_o = ratio of radiation from full moon ($g = 0$) at distance Δ from earth to radiation of sun at 1 A. U.

R = distance from moon to sun

Δ = distance from moon to earth

r = moon's radius

The factor A is the albedo originally defined by Bond given in Van Diggelen's paper [1]. If a sphere is exposed to parallel light, its albedo A is the ratio of the whole amount of light reflected from the sphere to the whole amount incident on it. Again, since the values of A in the table are for local regions, the above definition requires a slight change of viewpoint. In equation form, Russell gives A as

$$A = pq$$

where,

$$q = 2 \int^{\pi} \frac{I(g)}{I(0)} \sin g \, dg \; ; \quad g = \text{phase angle.}$$

Expressed verbally, this function indicates how many times more light is reflected in all directions other than in the direction of the earth. Van Diggelen [1] uses the value 0.578 (after Rougier) for q.

LIGHT POLARIZATION

Some of the sunlight reflected from the moon is partially polarized. Lyot [4] is credited with making the first detailed and precise analysis of the polarization of light from the whole disk of the moon, primarily because of the high sensitivity of his polarimeter. Lyot concluded that the direction of polarization was always exactly perpendicular or exactly parallel to the plane of vision. He assigned a positive (+) sign to the portion of polarized light that is perpendicular to the plane of vision and a negative (-) sign to that portion that is parallel to the plane of vision. By plotting the phase angle along the abscissa and the proportion of polarized light, together with its sign along the ordinate, Lyot obtained a single curve describing the properties of the polarization of light from the whole disk of the moon (Fig. 2).

Gehrels, Coffeen, and Owings [5] made some photoelectric measurements of polarization on various lunar regions at various wavelengths, using diaphragms about 10 sec of arc in diameter. The polarization measurements obtained during three runs, April 1959, August 1959, and November 1963, with the McDonald 82-inch telescope are shown in Figure 3. The per cent polarization of the regions shown is plotted as a function of phase for observations with ultraviolet (3600 Å), green (5400 Å), and infrared (9400 Å) filters. The circles, squares, and crosses are for observations made in April 1959, August 1959, and November 1963, respectively. The phase dependence of polarization with the green (5400 Å) filter agrees with that found by Lyot (1929), but with the ultraviolet (3600 Å) filter the polarization generally was greater, and with the infrared (9400 Å) filter, smaller.

Figure 4 is included to illustrate the percentage polarization, percentage geometrical albedo, and scattering efficiency of particles with radius $0.8\,\mu$ and refractive index $1.34 - 0.01\,i$ as a function of the reciprocal of the wavelength in microns. In the figure, the solid line is for the percentage geometrical albedo of Mare Crisium for zero phase. The observed data are shown by dots, and the probable errors are indicated with vertical lines. The dashed line represents the scattering efficiency of particles with radius $0.8\,\mu$ and refractive index $1.34 - 0.01\,i$, as calculated from Mie theory.

As the figure shows, the polarization rises as the albedo drops. Gehrels, et al., found no rotation of the polarization position angles; neither did they find the polarization position angles to be wavelength dependent. From Mie scattering by particles, the polarization position angles are either 90° or 180° with respect to the plane of scattering. Except for regions close to the limb (Lyot, 1929), the polarization position angles are always observed close to either 90° or 180°. This infers that multiple scattering is absent on the lunar surface.

LUMINESCENCE

Lunar luminescence is a confirmed phenomena. In the observation of Gehrels, et al. [5] , luminescense was detected in the photometry and independently confirmed by the polarimetry. Their observations revealed that the lunar surface was 10 to 20% brighter in visible light in 1956/1959 near the maximum of the last solar-activity cycle than in 1963 November / 1964 January when solar activity was near its minimum. The effect, being localized and fairly constant from day to day, probably varies with the solar cycle. The luminescence effects appear to be similar at various wavelengths, but the amount of luminescence appears to vary appreciably with time, indicating some possible connection with the solar cycle as indicated above.

Since light tends to become polarized when it is reflected, the observation that the light of the moon is polarized to a greater extent when its brightness is at a minimum than when it is at a maximum suggests that moonlight at its brightest includes some light that is not reflected sunlight.

Figure 5 shows an example of the "line-depth" method employed to detect lunar luminescence [6]. This method utilizes a comparison of profiles of absorption lines in the spectrum of the sun (left) and moon (right). A measure of the per cent of the total moonlight attributed to lunar luminescence (arrow) is given by the increase in the residual intensity (brackets) of the profile for the moon.

Figure 6 gives the profiles of the H and K lines of Ca II in the ultraviolet part of the moon's spectrum [7]. The lunar H and K lines are not as dark (their traces are not as deep) as the solar H and K lines because of luminescence from the moon.

Figure 7 compares the contours of the line H (3968.6 Å) of the Ca^+ spectra of Aristarchus (circles) on October 4, 1955, and the sun (solid line) [8]. Figure 8 compares the intensity of the H line (3968.6 Å) in spectra of the Crater Aristarchus ($I_{☾}$) on October 4, 1955, and the sun $I_{\odot}$. Using the "line-depth" method, Kozyreu obtained a value of 13% for the percentage of luminescence in relation to the intensity of the constant spectrum which is reflected by Aristarchus. According to Kozyreu, the luminescence of Aristarchus is stronger after a full moon.

COLOR

Observations of the color of the moon provide data for additional information on which to form an acceptable model of the lunar surface. The color-phase observations of Gehrels, et al. [5], show a definite reddening of the moon with phase regardless of its color. The reddish color is a uniform, not a local, effect of the moon. This effect appears to have a linear dependence on phase of the moon α over the range $-45^{\circ} < \alpha < +35^{\circ}$; typical color-phase relations for the whole moon over this range are:

$$(G - I) = +0.251\ (\pm .007) + 0.0028\ (\pm .0002)\ /\alpha/$$

$$(U - G) = +0.386\ (\pm .007) + 0.0036\ (\pm .0004)\ /\alpha/$$

assuming that the observed regions are an average sample for lunar colors. The agreement of the colors of the moon with calculations based upon Mie theory indicates that particle scattering is responsible for the reddening of the moon with phase (Fig. 4).

In addition to the reddening-phase relation, the moon exhibits certain other different colors. Figure 9 shows the distribution of the most distrinctly reddish (shaded) and greenish (dotted) region on the moon (according to Barabashev and to Tchekirda) [9]. The reddish details are more pronounced in the mountainous regions (e.g., Tycho and the Wood Spot). The greenish areas are more pronounced in the dark region near Kepler and the region to the west of Plato. The more pronounced bluish areas are Mare Frigoris and the floor of Grimaldi. The absolute color differences are very small, making the entire lunar surface appear nearly the same color.

MICROWAVE TEMPERATURES

Temperatures derived from microwave thermal emission measurements may be compared with temperatures at various depths below the lunar surface. Some measurements are presented by the investigator as averaged over the entire lunar disk. Others are presented as average central brightness temperatures, depending upon the resolution (beam-width between half-power points) of the apparatus used in taking the measurements. The resolution has been improving in recent years, particularly at the shorter wavelengths, although it is far from that obtained with infrared systems.

Data of Salomonovich [10]; Salomonovich and Losovskii [11]; Gibson [12]; Piddington and Minnett [13]; Zelinskaya, Troitskii, and Fedoseev [14]; Salomonovich and Koshchenko [15]; Mayer, McCullough, and Sloanaker [16]; Troitskii and Zelinskaya [17]; and Akabane [18] for the central brightness temperature are given in Table II as a function of wavelength. The columns in the table correspond to factors in the terms of a truncated Fourier series representation of the measured data points of the following form

$$T = T_0 + T_1 \cos(\theta - B_1) + T_2 \cos(2\theta - B_2)$$

where,

$$\theta = \Omega t$$

$$\Omega = \frac{2\pi}{P}$$

$P = 2.55144 \times 10^6$ seconds (the lunation period)

T = central brightness temperature

T_o = constant component of temperatures

T_1 and T_2 = first and second variational components of temperature

B_1 and B_2 = phase angles of the fundamental heat wave (with respect to the solar insolation at the surface).

In addition, the constant temperature as determined by Grebenkemper [19], Medd and Broten [20], and Mezger and Strassl [21] is given in Table III.

Central brightness microwave temperatures (as a function of fraction of lunation period) are tabulated in Table IV using the above equation and the data from Table II. In Table II, zero time is at new moon; whereas, in Table IV, zero time is at full moon. Graphs of the data in Table IV are shown in Figures 10 - 19.

Recent central brightness temperatures for a lunation at 3.2-mm wavelength as measured by Tolbert and Coats [22] are shown in Figure 20. The resolution was 9' of arc using a Dicke-type radiometer.

Theoretically, the constant component of temperature, T_o, should be the same for all wavelengths. They are not the same due to a number of considerations, among which are: method of antenna calibration, reduction of the data (especially corrections for earth atmospheric effects), and apparatus performance (especially resolution). These data, together with the IR data of Sinton [23], Murray and Wildey [24], and Shorthill and Saari [25] compared with calculations made in Research Projects Laboratory, yield a recommended value for this constant component of $220^\circ K \pm 30^\circ K$. This tolerance is necessary because of the wide spread in its measured value in the microwavelength and the uncertainty regarding the IR measurements of the lunar nighttime temperatures.

The first and second variational components of temperature, T_1 and T_2, and the phase angles, B_1 and B_2, are dependent upon wavelength.

Measurements at the longer wavelengths have usually shown little change in the temperature during lunar eclipses due to lack of sensitivity and resolution, as well as the fact that the radiation measured comes from below the lunar surface. However, Epstein, et al. [26], have made measurements at 3.2 mm during the total lunar eclipse. In fact, a difference between mountainous and maria regions was observed at the resolution attained (2.8' at 70° elevation and 3.1' at 15° elevation). The data are shown in Figure 21.

INFRARED TEMPERATURES

Temperature Variations About the Subsolar Point. The brightness temperatures along concentric circles about the subsolar point (SSP) have been determined from the infrared data of Saari and Shorthill [27]. The temperatures were determined for 18 successive locations of the SSP phase angles -113° 20' to +135° 40'. Figures 22 through 39 are used to locate the coordinates at a given feature for a given phase. The coordinate system has as an axis the line connecting the SSP and the antisolar point. The prime meridian is the line connecting the SSP and the center of the visible disc as seen from the earth when the measurement was made. Positive longitudes are as indicated by the arrow. Zero degrees latitude is the terminator; 90° is the SSP. With the coordinates of this system and the phase angle, the temperature of any lunar feature can be obtained from Figures 40 through 57. In these figures the brightness temperature is plotted against longitude for constant latitudes (concentric circles about the SSP). Temperatures are given for the illuminated and visible surface only.

The coordinate system is superimposed on a lunar photograph which uses the USAF convention, i.e., the moon as viewed from earth with the naked eye. The photograph is for no libration, whereas the heavy grid lines used in the coordinate system are for the libration at the particular phase angle and date shown. This introduces some inaccuracies when correlating a given lunar feature with a temperature, especially near the limbs, and also explains the mismatch around the edge between the photograph and the superimposed grid lines.

Eclipse Temperatures. Investigations of brightness temperature during eclipse of the moon have shown that certain local regions are, in general, thermally enhanced; that is, their temperatures are higher than their environs. Figures 58 through 70 give brightness temperatures which were taken from various publications of Saari and Shorthill [28, 29, 30]. The resolution is about 10" of arc and has been shown to be very reproducible with the fast scans and comparisons of the data in repeats every 6 minutes, both during full moon and total eclipse. The assumption was made for all of these that the subsolar point is 374°K. However, the absolute values of temperature may be readily adjusted as better measurements are made of the subsolar point temperature. The relative value will remain the same with such adjustments. The black body assumption (emissivity of 1) may very well be revised, and recent suggestions for the temperature at the subsolar point have ranged from 374°K to above 400°K.

Figures 58 through 67 present isotherms for several regions where a temperature comparison can be made of the same region before and during an eclipse [31]. Figures 60 and 61 show the anomalous temperature behavior for the crater Aristarchus; immediately before (Fig. 59), the entire region was at approximately the same temperature. This effect is clearly demonstrated for the regions around Copernicus and Tycho in Figures 69 and 70. Figure 68 shows the hot spots for the entire surface.

Antisolar Point Temperature. The lunar midnight or antisolar point temperature has been estimated from the data of Shorthill and Saari [25] and Murray and Wildey, whose data are given in Figure 71.

REFERENCES

1. Van Digglen, J.: Photometric Properties of Lunar Crater Floors. Rec. Astr. Obs., Utrecht, Netherlands, Vol. XIV, No. 2, 1958, Translated into English by NASA, Report No. NASA-TT-F-209, Aug. 1964.
2. Saari, J. M.; and Shorthill, R. W.: Geo-Astrophysics Laboratory Review. Boeing Scientific Research Laboratories, Seattle, Wash., July - Dec. 1965, p. 37.
3. Russell, Henry Norris: On the Albedo of the Planets and Their Satellites. Astrophys. J., Vol. XLII, No. 3, April 1916, pp. 173-196.
4. Lyot, B.: Polarization of the Moon and of the Planets Mars and Mercury. Observatorie du Pic du Midi, Paris, France, Comptes Rendus, 178, 22, 1796-1798, 1924.
5. Gehrels, T.; Coffeen, T.; and Owings, D.: Wavelength Dependence of Polarization, Part III, The Lunar Surface. Astronom. J., 69, 10, 826-852, 1964.
6. Kopal, Z.: The Luminescence of the Moon. Sci. Am., 212, 28-37, May 1965.
7. Spinrad, H.: Lunar Luminescence in the Near Ultraviolet. Icarus, 3, 500 - 501, Dec. 1964.
8. Kozyreu, N. A.: The Luminescence of the Lunar Surface and the Intensity of Solar Corpuscular Radiation. Astronautics Information Translation, No. 18, AD-252-312, 1961.
9. Fessenkov, V. G.: Photometry of the Moon. Physics and Astronomy of the Moon, edited by Z. Kopal, Academic Press, N. Y. and London, pp. 121 - 125, 1962.
10. Salomonovich, A. E.: Radio Emission of the Moon at 8 Millimeters. Soviet – AJ, 2, 1, 112-118, Jan. - Feb. 1958.
11. Salomonovich, A. E.; and B. Ya Losovskii: Radio-Brightness Distribution on the Lunar Disk at 0.8 cm. Soviet – AJ, 6, 6, 833-839, May - June 1963.
12. Gibson, J. E.: Thermal Radiation of the Moon at 0.86 cm Wavelength. Naval Research Laboratory, Final Report, No. 4984, Aug. 29, 1957.
13. Piddington, J. H.; and Minnett, H. C.: Microwave Thermal Radiation from the Moon. Australian J. Sci. Res., A2:63, 63-77, 1949.

14. Zelinskaya, M. R.; Troitskii, V. S.; and Fedossev, L. I.: Lunar Radio Emissions at 1.63 cm Wavelength. Soviet – AJ, 3, 4, 628-632.
15. Salomonovich, A. E.; and Koshchenko, B. H.: Observations of the Thermal Radio Emission of the Moon at the 2 cm Wavelength. Radiofizida, 4, 4, 591-595, 1961.
16. Mayer, C. H.; McCullough, T. P.; and Sloanaker, R. M.: Radio Emission of the Moon and Planets. Chapter 12, Planets and Satellites: The Solar System, Vol. 3, University of Chicago Press, 442-472, 1961.
17. Troitskii, V. S.; and Zelinskaya, M. R.: Determination of Certain Properties of Surface Layers of the Moon from Its Radiowave Emission at 3.2 cm Wavelength. Translated by G. F. Hill and E. Lyssenko, Technical Library, ARGMA, Redstone Arsenal, Alabama, from Astronomicheskii Zhurnal, 32, 6, 550-554, Nov. - Dec. 1955.
18. Akabane, K.: Lunar Radiation at 3,000 Mc/s. Proc. Japan Acad., 31, 3, 161-165, 1955.
19. Grebenkemper, C. J.: Lunar Radiation at a Wavelength of 2.2 cm. U.S. Naval Research Laboratory, NRC Report No. 5151 (AD-162624), June 6, 1958.
20. Medd, W. J.; and Broten, N. W.: Lunar Temperature Measurements at 3200 Mc/s. National Research Council, Ottawa, Canada, Planetary and Space Science, 5, 307-313, 1961.
21. Mezger, P. G.; and Strassl, H.: The Thermal Radiation of the Moon at 1420 Mc/s. Bonn University Observatory, Planetary and Space Science, 1, 213-226 (Z. Astrophysik, 48, 27, 72-76, 1959).
22. Talbert, C. W.; and Coats, G. T.: Lunar Radiation at 3.2 Millimeters and a Lunar Model. Electrical Engineering Research Laboratory, University of Texas, Report No. 7-24, Aug. 15, 1963.
23. Sinton, W. M.: Observations of Solar and Lunar Radiation at 1.5 Millimeters. J. Opt. Soc. Am., 45, 11, 975-979, Nov. 1955.
24. Murray, B. C.; and Wildey, R. L.: Surface Temperature Variation During the Lunar Nighttime. Contribution No. 1173, Division of Geological Sciences, California Institute Technology, Pasadena, California, May 1963.
25. Saari, J. M.: The Surface Temperature of the Antisolar Point of the Moon. Icarus, 3, 161-167, July 1964.
26. Epstein, E. E.; Jacobs, E.; King, H. E.; Reber, E. E.; Shimabakuro, F. I.; and Stacey, J.; The Total Lunar Eclipse of December 30, 1963; Observations at 3.2 Millimeters. Aerospace Corporation, Report No. TDR-269(5250-41)-4 (AD-451758), Oct. 19, 1964.

27. Six, N. F.; Montgomery, C. G.; Shorthill, R. W.; and Saari, J. M.: Analysis of Lunar Brightness Temperatures Determined from Infrared Scan Data. Boeing Report, Boeing Scientific Research Laboratories (to be published).
28. Shorthill, R. W.; and Saari, J. M.: Lunar Infrared Temperature Measurements During September 4, 5, and 6, 1960. AF BMD-TR-59-9, Boeing Airplane Company, Jan. 30, 1961.
29. Shorthill, R. W.; and Saari, J. M.: Infrared Mapping of Lunar Craters During the Full Moon and the Total Eclipse of September 5, 1960. Boeing Scientific Research Laboratories, D1-82-0176, July 1962.
30. Shorthill, R. W.: Measurements of Lunar Temperature Variations During an Eclipse and Throughout a Lunation. Boeing Scientific Research Laboratories, D1-82-0196, August 1962.
31. Shorthill, R. W.; and Saari, J. M.: Lunar Radiation Measurements Program. Boeing Scientific Research Laboratories, D1-82-0456-1, Jan. - June 1965.

TABLE I

ALBEDO FOR VARIOUS FEATURES

(After Van Digglen)

nr name of the crater	$\rho = a$ v. Digg.	A v. Digg.	a Markov	$\rho = a$ Syt.
1 Albategnius	0.111	0.063		0.112
2 Alphonsus	0.107	0.062		
3 Archimedes	0.081	0.047	0.042	0.088
4 Aristarchus	0.152	0.088	0.084	0.176
5 Aristoteles	0.105	0.061		0.110
6 Aristyllus	0.080	0.047		
7 Arzachel	0.112	0.065		
8 Autolycus	0.082	0.048		
9 Billy	0.063	0.037		
10 Bonpland	0.087	0.050		
11 Bullialdus	0.114	0.060		
12 Campanus	0.089	0.052		
13 Cassini	0.110	0.063		
14 Catharina	0.115	o.067		
15 Clavius	0.137	0.079		
16 Cleomedes	0.090	0.052		
17 Copernicus	0.114	0.066	0.054	0.120
18 Cyrillus	0.110	0.063		
19 Firmicus	0.069	0.040		
20 Fracastorius	0.102	0.059		
21 Gassendi	0.091	0.053		
22 Grimaldi	0.063	0.037	0.026	0.062
23 Hevelius	0.108	0.063		
24 Hipparchus	0.109	0.063		
25 Julius Caesar	0.073	0.043		
26 Kepler	0.102	0.059		0.100
27 Landsberg	0.115	0.067		
28 Langrenus	0.110	0.063		0.144
29 Lemonnier	0.062	0.036		
30 Lubiniezcky	0.102	0.059		
31 Lyell	0.067	0.038		
32 Macrobius	0.097	0.056		
33 Manillius	0.081	0.047		0.122
34 Maraldi	0.066	0.038		
35 Marius	0.059	0.034		
36 Menelaos	0.085	0.049		0.158
37 Mercator	0.095	0.055		
38 Petavius	0.114	0.066		
39 Pitatus	0.068	0.040		
40 Plato	0.068	0.040	0.029	0.068
41 Posidonius	0.077	0.044		
42 Proclus	0.142	0.082	0.078	
43 Ptolemaeus	0.095	0.055	0.043	0.108
44 Riccioli	0.071	0.041		0.060
45 Schickard	0.087	0.050	0.042	0.078 and 0.099
46 Theophilus	0.108	0.063		
47 Tycho	0.131	0.076	0.076	0.154
48 Vendelinus	0.105	0.061		
Vesuvius sand 1830	0.033	0.019		
Asama Yama ash	0.079	0.046		
Vesuvius sand 1894	0.103	0.059		
Vesuvius ash 1906 A	0.171	0.099		
Vesuvius ash 1906 B	0.198	0.114		
whole moon	0.105	0.061		
Mare Crisium			0.029	0.062
Mare Foecunditatis			0.028	0.069
Oceanus Procellarum			0.076	0.051 - 0.070
Sinus Iridum			0.030	0.065
Mare Tranquillitatis				0.066
Mare Serenitatis				0.070
Mare Frigoris				0.069
Mare Imbrium				0.054 - 0.074
Mare Vaporum				0.060
Mare Nubium				0.062 - 0.073

TABLE II

SUMMARY OF MICROWAVE CENTRAL BRIGHTNESS TEMPERATURES

Wavelength (cm)	T_o	T_1	T_2	B_1	B_2	Author	Resolution
0.80	197	-32	0	$2\pi/9$	0	Salomonovich	18'
0.80	211	-40	+14	$\pi/6$	$11\pi/90$	Salomonovich & Losovskii	2'
0.86	225	-45	0	$2\pi/9$	0	Gibson	12'
1.25	249	-52	0	$\pi/4$	0	Piddington & Minnett	32'
1.25	215	-34	0	$\pi/4$	0	Piddington & Minnett *	32'
1.63	224	-36	0	$2\pi/9$	0	Zelinskaya, et al	26'
2.00	190	-20	0	$2\pi/9$	0	Salomonovich & Koshchenko	4'
3.15	195	-12	0	$11\pi/45$	0	Mayer, et al	9'
3.20	223	-17	0	$3\pi/16$	0	Troitskii & Zelinskaya	6.3'
10.00	315	-44.1	0	$\pi/4$	0	Akabane	-

*Salomonovich's [11] analysis of Piddington and Minnett's data.

TABLE III

CONSTANT MICROWAVE TEMPERATURES

Wavelength (cm)	Temp., K°	Author	Resolution
2.20	$200 \pm 10°$	Grebenkemper	6'
9.37	$220 \pm 5\%$	Medd & Broten	140'
20.11	$250 \pm 5°$	Mezger & Strassl	-

TABLE IV

CENTRAL BRIGHTNESS MICROWAVE TEMPERATURES FOR A LUNATION

	Salomonovich	Salomonovich/ Losovskii	Gibson	Piddington/ Minnett	Piddington/ Minnett (Salomonovich)	Zelinskaya/ Troitskii/ Fedoseev	Salomonovich/ Koshchenko	Mayer/ McCullough/ Sloanaker	Troitskii/ Zelinskaya	Akabane
F/P	CASE(1)	CASE(2)	CASE(3)	CASE(4)	CASE(5)	CASE(6)	CASE(7)	CASE(8)	CASE(9)	CASE(10)
0.	221.513	258.627	259.472	285.770	239.042	251.578	205.321	203.632	237.703	346.184
0.20000000E-01	223.898	261.753	262.825	290.088	241.865	254.260	206.811	204.609	238.656	349.846
0.39999999E-01	225.859	263.426	265.582	293.759	244.265	256.466	208.037	205.434	239.363	352.959
0.59999999E-01	227.364	263.619	267.699	296.723	246.204	258.160	208.978	206.095	239.812	355.473
0.79999998E-01	228.391	262.367	269.143	298.935	247.650	259.314	209.619	206.580	239.995	357.349
0.99999998E-01	228.922	259.769	269.890	300.360	248.581	259.912	209.951	206.883	239.911	358.557
0.11999999E-00	228.950	255.980	269.930	300.974	248.983	259.944	209.969	206.999	239.560	359.078
0.13999999E-00	228.474	251.197	269.261	300.769	248.849	259.409	209.671	206.925	238.948	358.904
0.15999999E-00	227.502	245.653	267.894	299.748	248.181	258.315	209.064	206.663	238.084	358.038
0.17999999E-00	226.049	239.600	265.850	297.926	246.990	256.680	208.156	206.218	236.982	356.493
0.19999999E-00	224.138	233.295	263.162	295.332	245.294	254.530	206.961	205.595	235.660	354.293
0.21999998E-00	221.798	226.989	259.873	292.008	243.121	251.898	205.499	204.806	234.138	351.474
0.23999999E-00	219.068	220.908	256.033	288.006	240.504	248.826	203.792	203.861	232.441	348.080
0.25999998E-00	215.989	215.246	251.704	283.388	237.485	245.363	201.868	202.777	230.594	344.164
0.27999998E-00	212.612	210.155	246.954	278.228	234.111	241.563	199.757	201.571	228.628	339.788
0.29999998E-00	208.987	205.735	241.857	272.607	230.436	237.486	197.492	200.260	226.573	335.021
0.31999998E-00	205.174	202.038	236.495	266.614	226.517	233.196	195.109	198.867	224.462	329.938
0.33999998E-00	201.232	199.062	230.952	260.343	222.417	228.761	192.645	197.413	222.328	324.620
0.35999998E-00	197.223	196.757	225.314	253.893	218.200	224.251	190.140	195.920	220.204	319.150
0.37999997E-00	193.211	195.032	219.672	247.366	213.932	219.738	187.632	194.414	218.124	313.615
0.39999998E-00	189.259	193.767	214.114	240.865	209.681	215.291	185.162	192.916	216.122	308.101
0.41999997E-00	185.428	192.819	208.727	234.492	205.514	210.982	182.768	191.451	214.227	302.696
0.43999997E-00	181.780	192.039	203.597	228.348	201.497	206.878	180.488	190.043	212.472	297.486
0.45999997E-00	178.372	191.280	198.805	222.530	197.693	203.044	178.358	188.712	210.882	292.551
0.47999997E-00	175.258	190.415	194.425	217.129	194.161	199.540	176.411	187.481	209.483	287.971
0.49999996E-00	172.487	189.345	190.528	212.230	190.958	196.423	174.679	186.368	208.297	283.817
0.51999997E 00	170.102	188.004	187.175	207.912	188.135	193.740	173.189	185.391	207.344	280.154
0.53999996E 00	168.141	186.373	184.418	204.241	185.735	191.534	171.963	184.566	206.637	277.041
0.55999997E 00	166.636	184.477	182.301	201.277	183.796	189.841	171.023	183.905	206.188	274.527
0.57999996E 00	165.609	182.384	180.857	199.065	182.350	188.686	170.381	183.420	206.005	272.651
0.59999996E 00	165.078	180.208	180.110	197.640	181.419	188.088	170.049	183.117	206.089	271.443
0.61999996E 00	165.050	178.094	180.070	197.026	181.017	188.056	170.031	183.001	206.440	270.922
0.63999996E 00	165.526	176.215	180.739	197.231	181.151	188.591	170.329	183.075	207.052	271.096
0.65999996E 00	166.498	174.757	182.106	198.252	181.819	189.685	170.936	183.337	207.916	271.962
0.67999996E 00	167.951	173.908	184.150	200.074	183.010	191.320	171.844	183.782	209.018	273.507
0.69999995E 00	169.862	173.844	186.838	202.668	184.706	193.470	173.039	184.405	210.340	275.707
0.71999995E 00	172.202	174.716	190.127	205.992	186.879	196.102	174.501	185.194	211.862	278.526
0.73999995E 00	174.932	176.637	193.967	209.994	189.496	199.174	176.208	186.139	213.559	281.920
0.75999995E 00	178.010	179.676	198.296	214.612	192.515	202.637	178.132	187.223	215.406	285.836
0.77999995E 00	181.388	183.846	203.046	219.772	195.889	206.437	180.243	188.429	217.372	290.212
0.79999994E 00	185.012	189.103	208.142	225.393	199.564	210.514	182.508	189.740	219.427	294.979
0.81999995E 00	188.826	195.344	213.505	231.386	203.483	214.804	184.891	191.133	221.538	300.062
0.83999994E 00	192.768	202.412	219.048	237.657	207.583	219.239	187.355	192.587	223.672	305.380
0.85999994E 00	196.776	210.098	224.686	244.106	211.800	223.748	189.860	194.080	225.796	310.850
0.87999993E 00	200.789	218.155	230.328	250.633	216.068	228.262	192.368	195.586	227.876	316.385
0.89999992E 00	204.741	226.306	235.886	257.135	220.319	232.709	194.838	197.084	229.878	321.899
0.91999991E 00	208.572	234.262	241.273	263.508	224.486	237.018	197.232	198.549	231.773	327.304
0.93999991E 00	212.220	241.730	246.403	269.652	228.503	241.122	199.512	199.957	233.528	332.514
0.95999990E 00	215.628	248.438	251.195	275.470	232.307	244.956	201.642	201.288	235.118	337.449
0.97999989E 00	218.742	254.138	255.575	280.871	235.839	248.460	203.589	202.519	236.517	342.029
0.99999989E 00	221.513	258.627	259.472	285.770	239.042	251.577	205.321	203.632	237.703	346.183

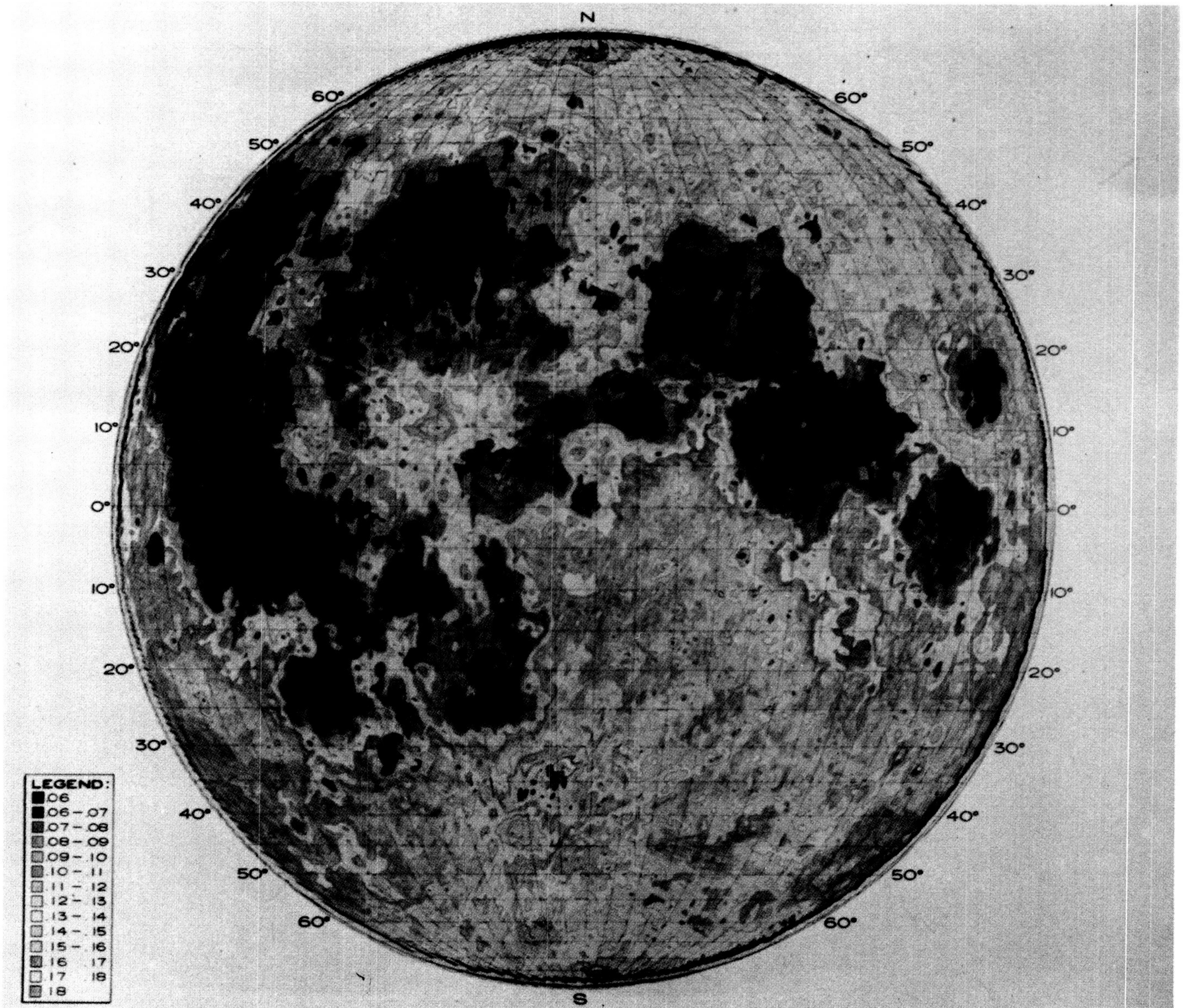

FIGURE 1 LUNAR SURFACE ALBEDO

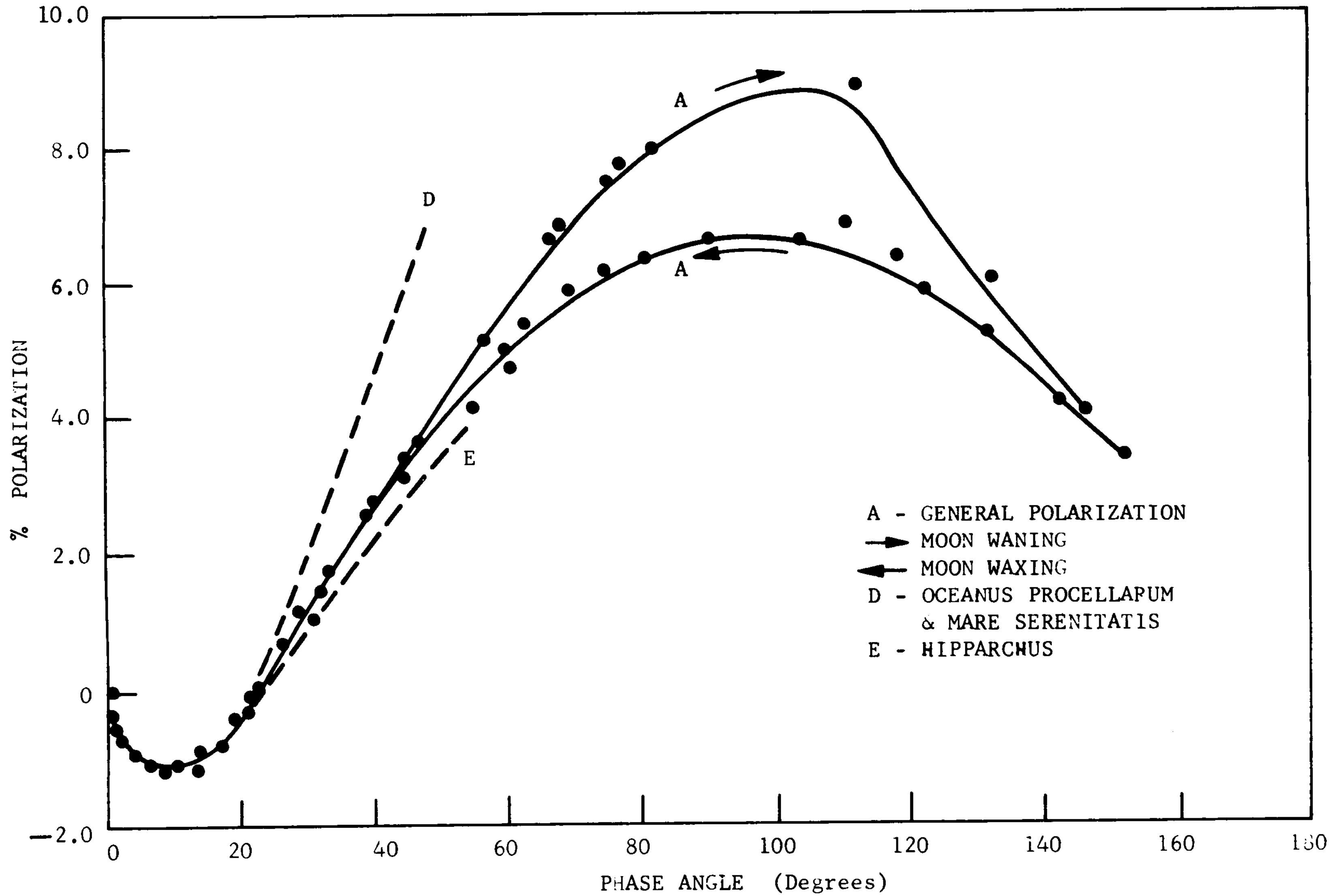

FIGURE 2 - THE POLARIZATION CURVE OF THE MOON (After Lyot)

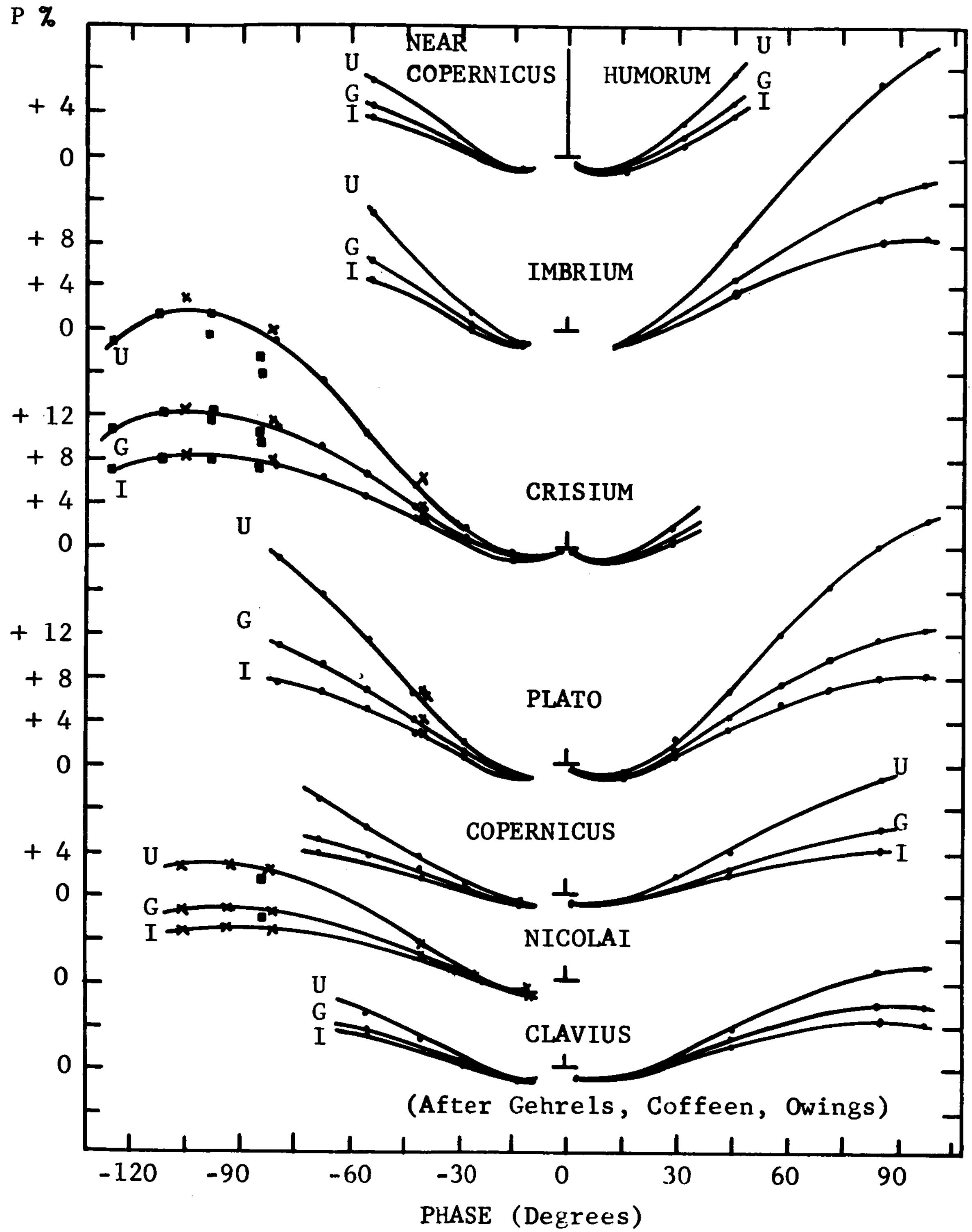

FIGURE 3 - LIGHT POLARIZATION FOR SEVERAL LUNAR REGIONS

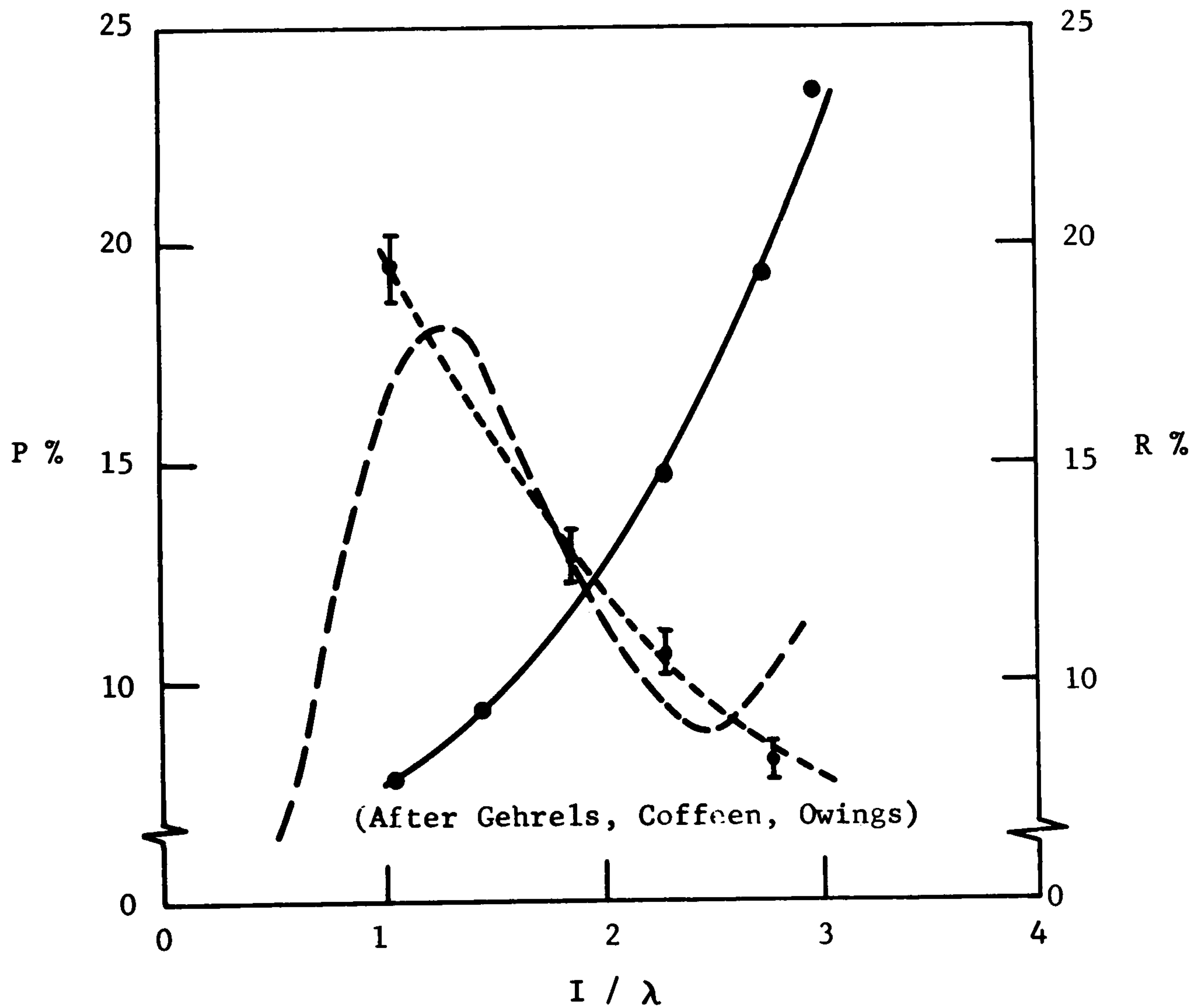

FIGURE 4 - POLARIZATION, ALBEDO, AND PARTICULATE SCATTERING

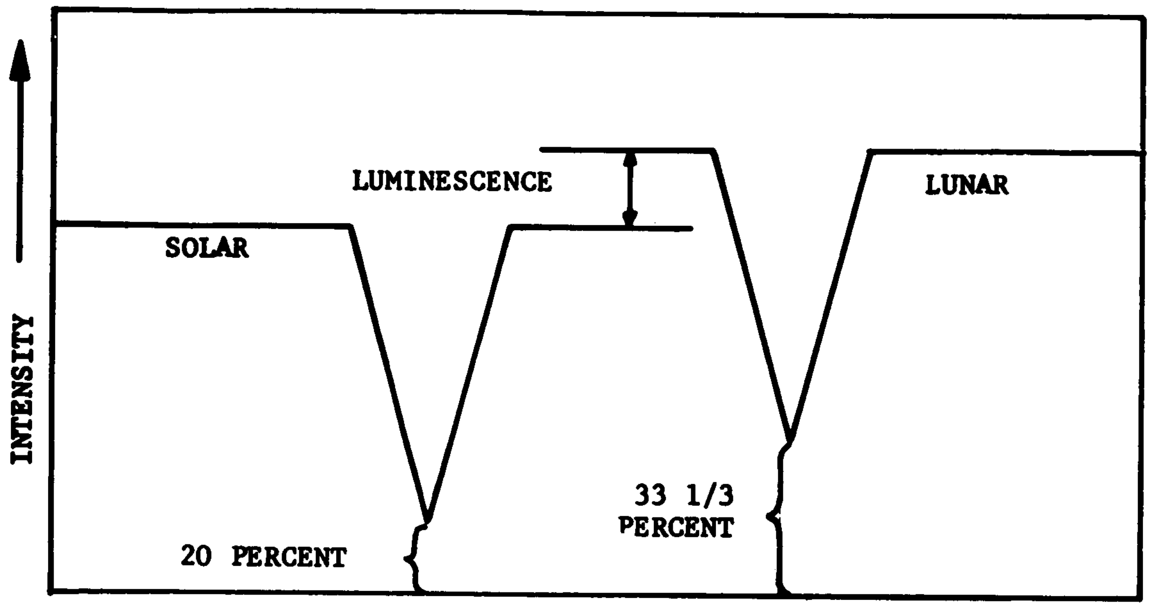

FIGURE 5 - LINE-DEPTH METHODS OF DETECTING LUMINESCENCE

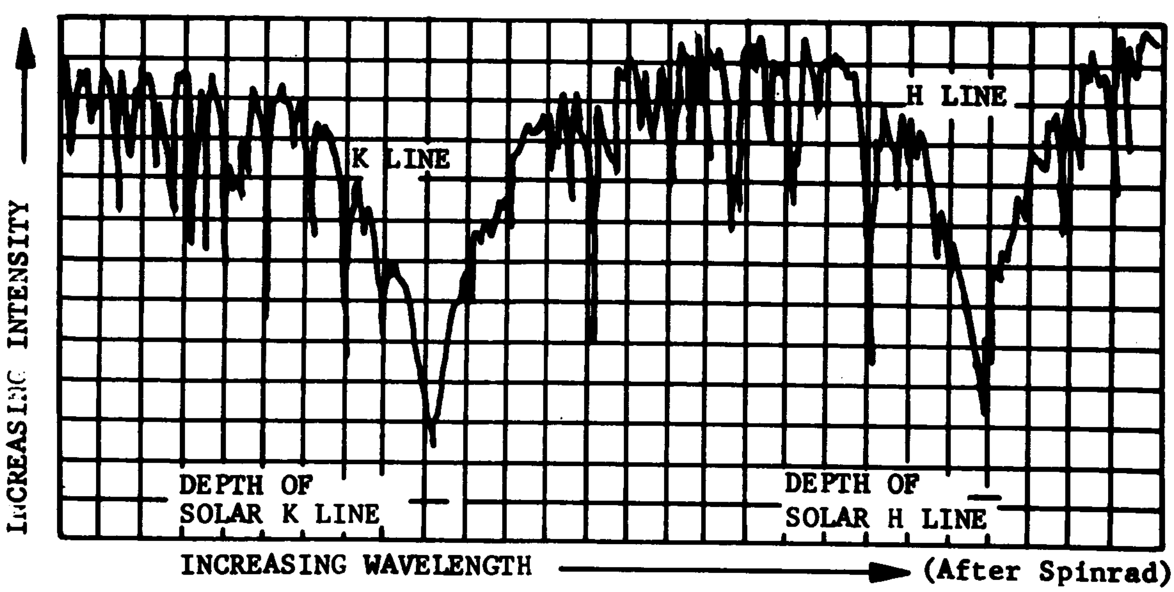

FIGURE 6 - PROFILES OF TWO LINES IN UV OF LUNAR SPECTRUM

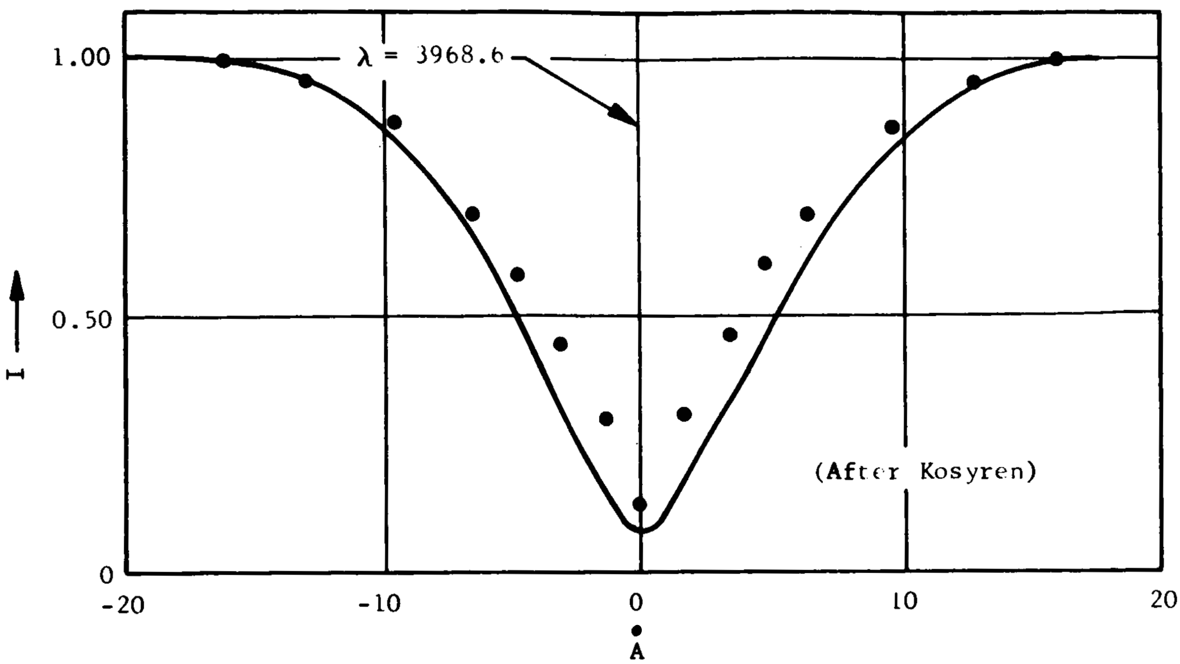

FIGURE 7 - LINE H (3968.6A) IN SPECTRA ARISTARCHUS

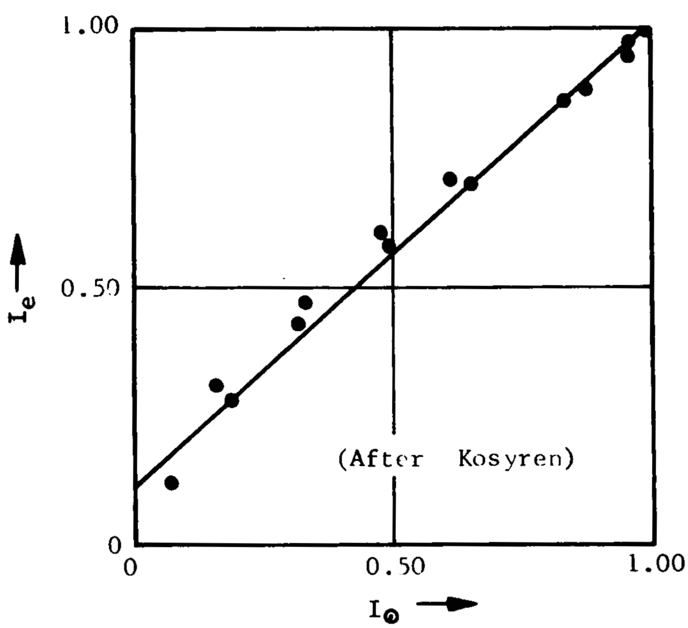

FIGURE 8 - INTENSITY OF H - LINE IN ARISTARCHUS

FIGURE 9 - COLOR REGIONS

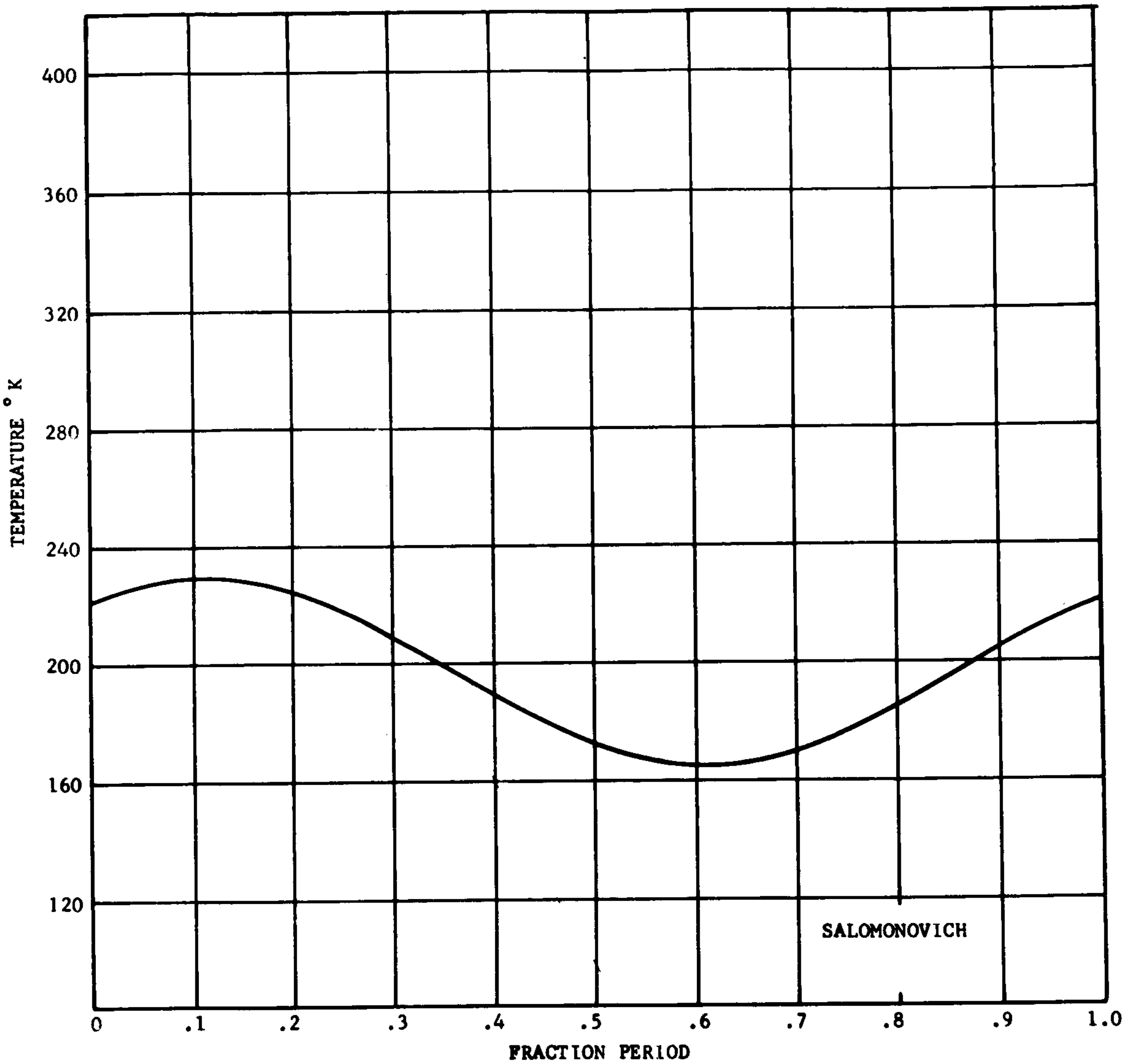

FIGURE 10 - LUNAR BRIGHTNESS TEMPERATURE AT 8 mm WAVELENGTH

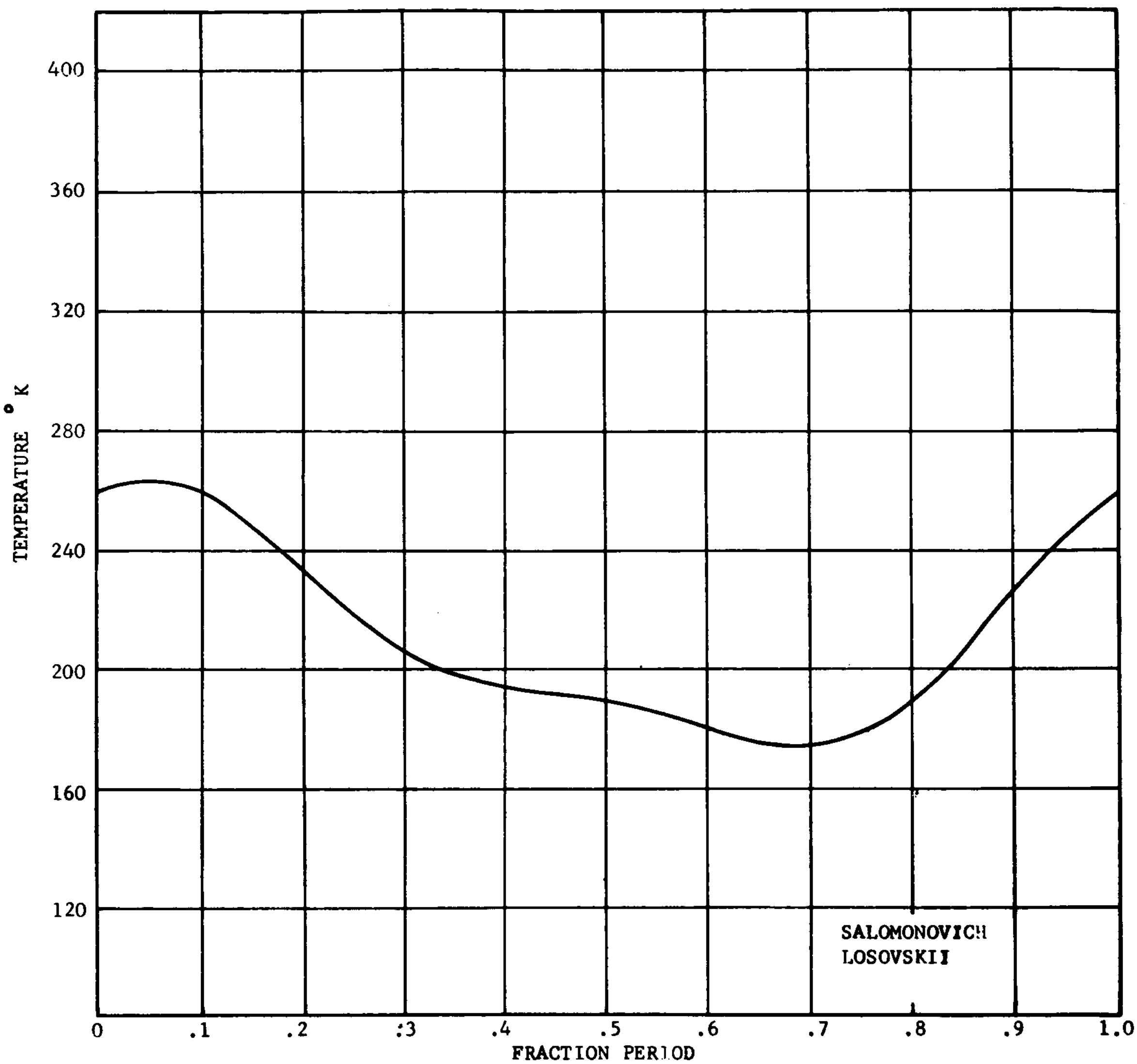

FIGURE 11 - LUNAR BRIGHTNESS TEMPERATURE AT 0.8 cm WAVELENGTH

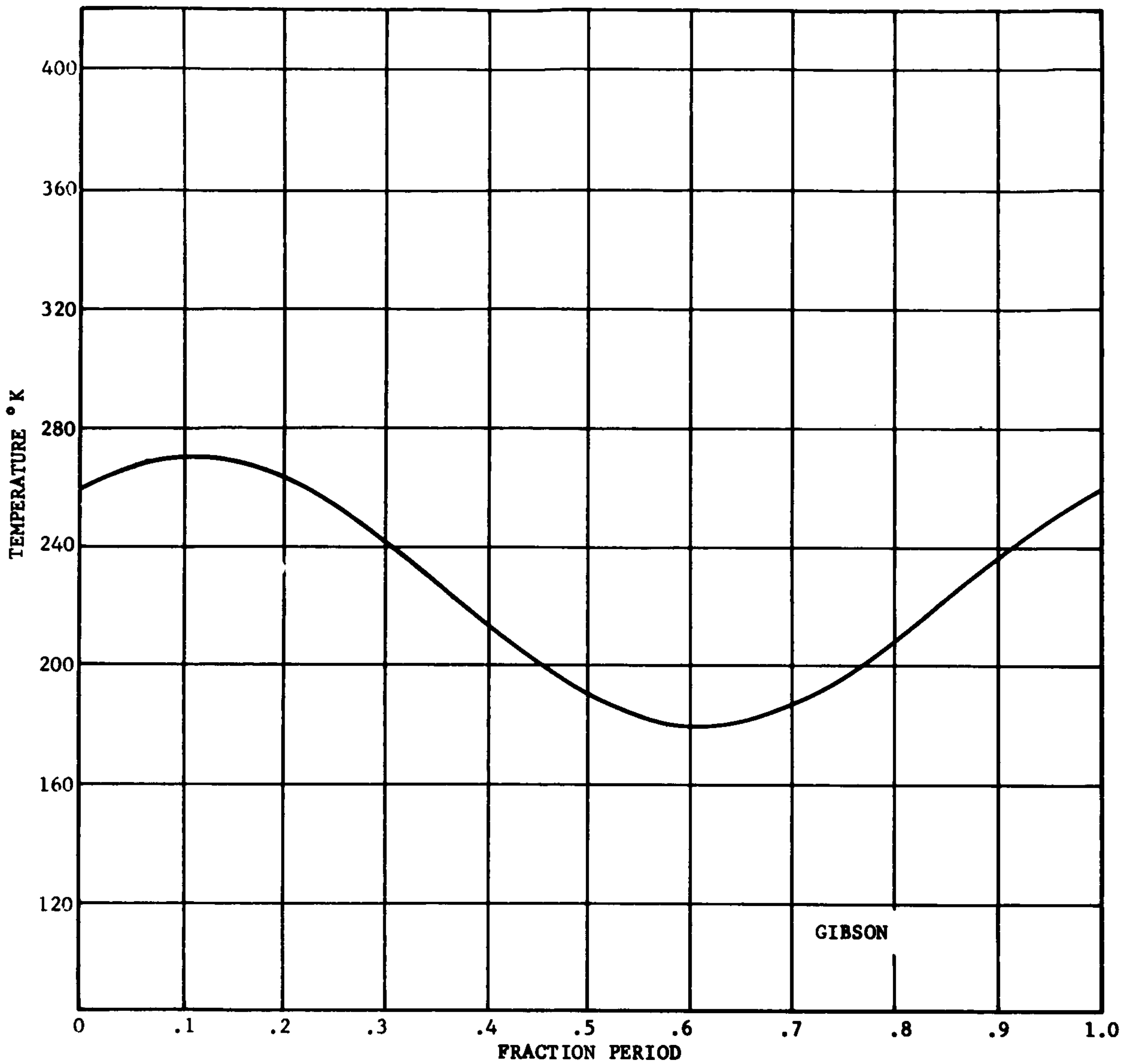

FIGURE 12 - LUNAR BRIGHTNESS TEMPERATURE AT 0.86 cm WAVELENGTH

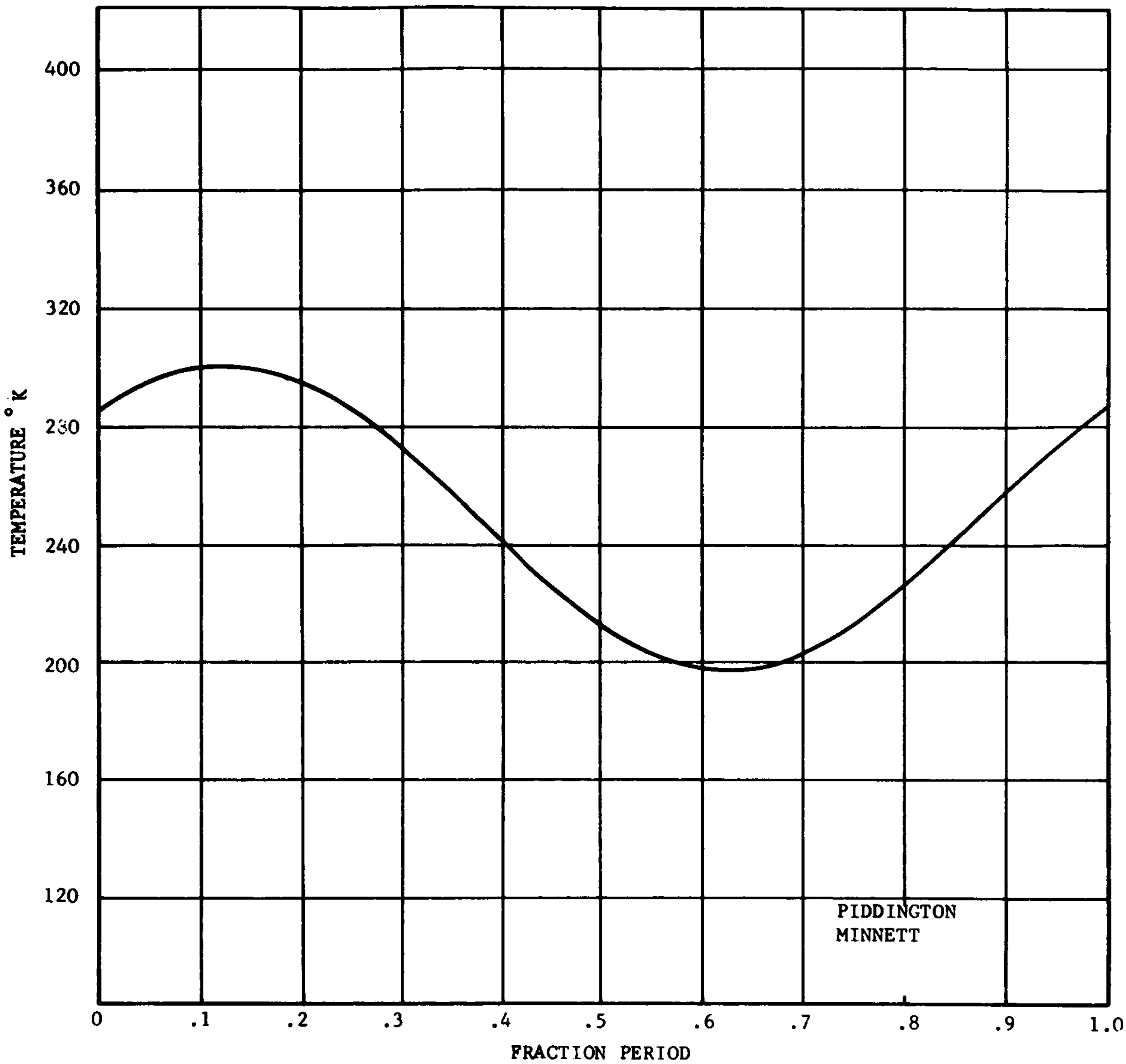

FIGURE 13 - LUNAR BRIGHTNESS TEMPERATURE AT 1.25 cm WAVELENGTH

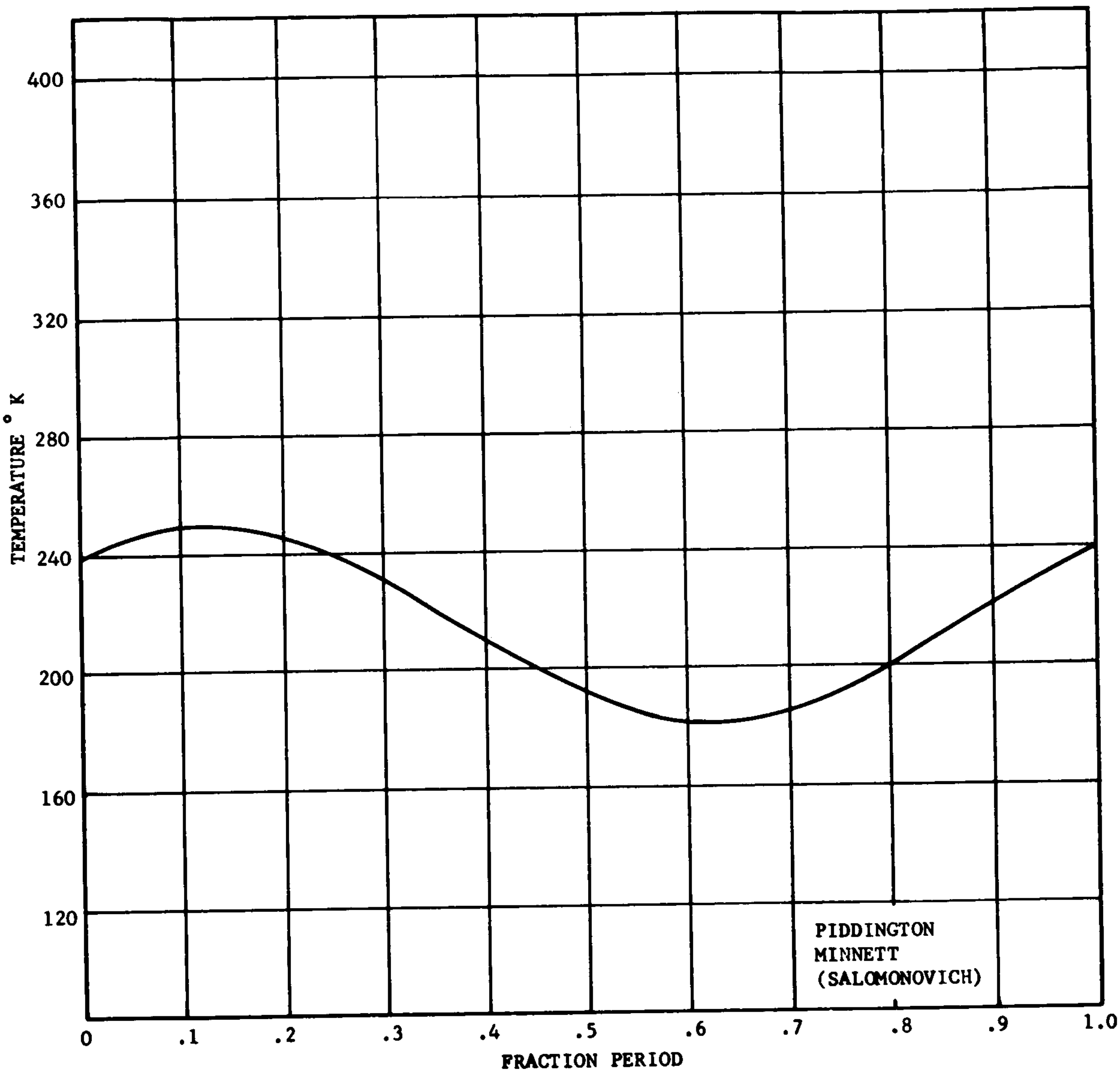

FIGURE 14 - LUNAR BRIGHTNESS TEMPERATURE AT 1.25 cm WAVELENGTH ACCORDING TO SALOMONOVICH

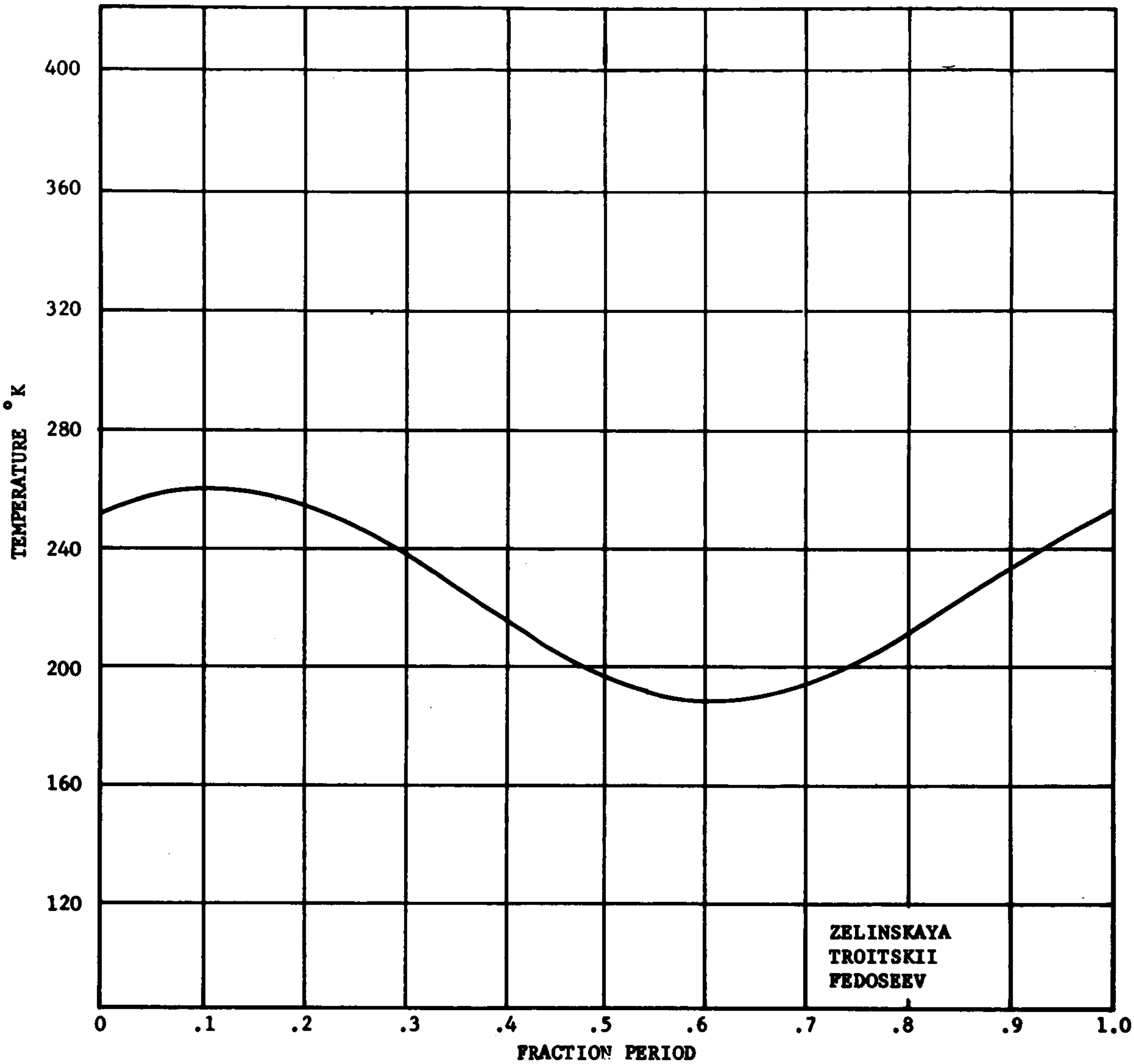

FIGURE 15 - LUNAR BRIGHTNESS TEMPERATURE AT 1.63 cm WAVELENGTH

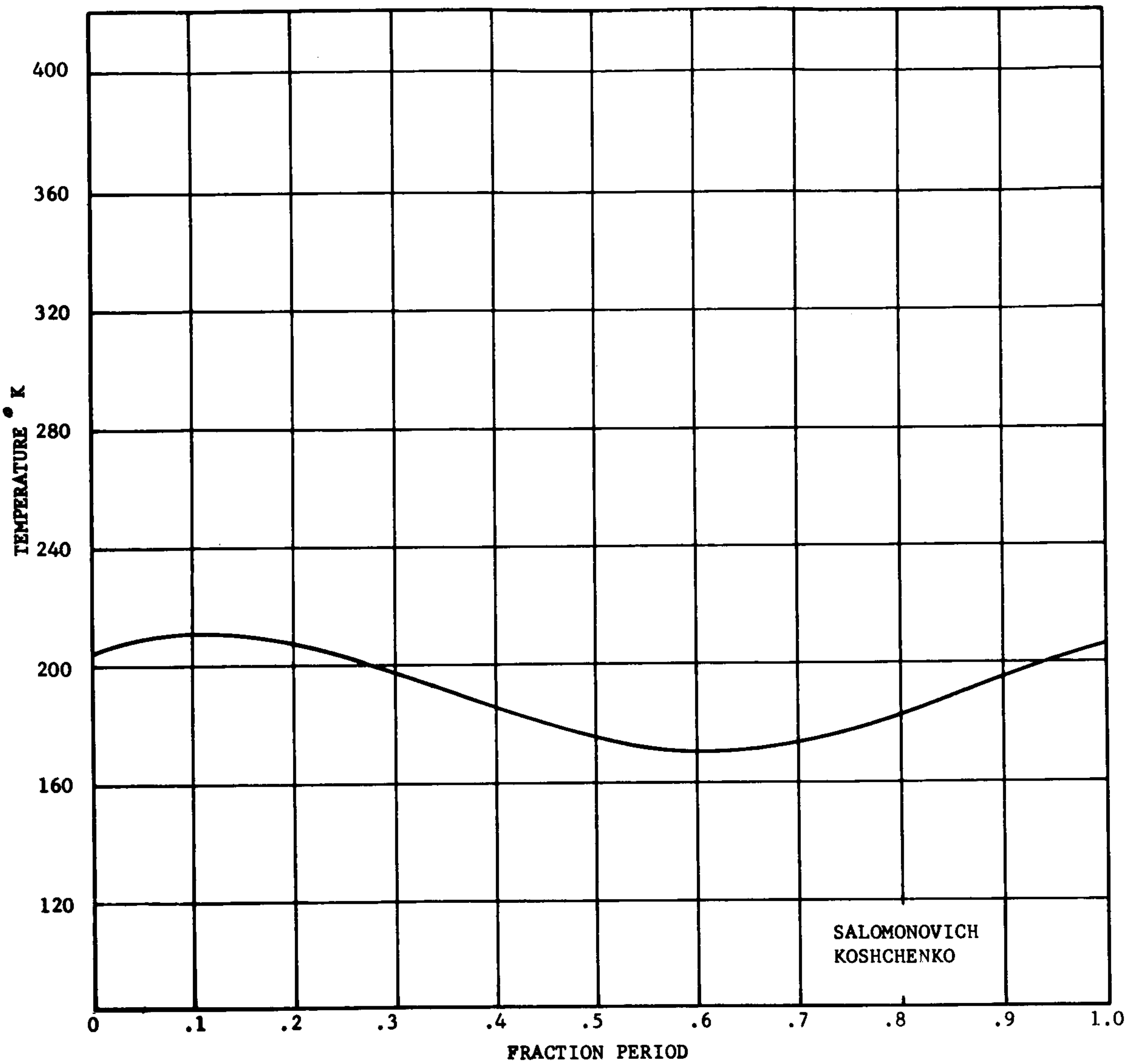

FIGURE 16 - LUNAR BRIGHTNESS TEMPERATURE AT 2 cm WAVELENGTH

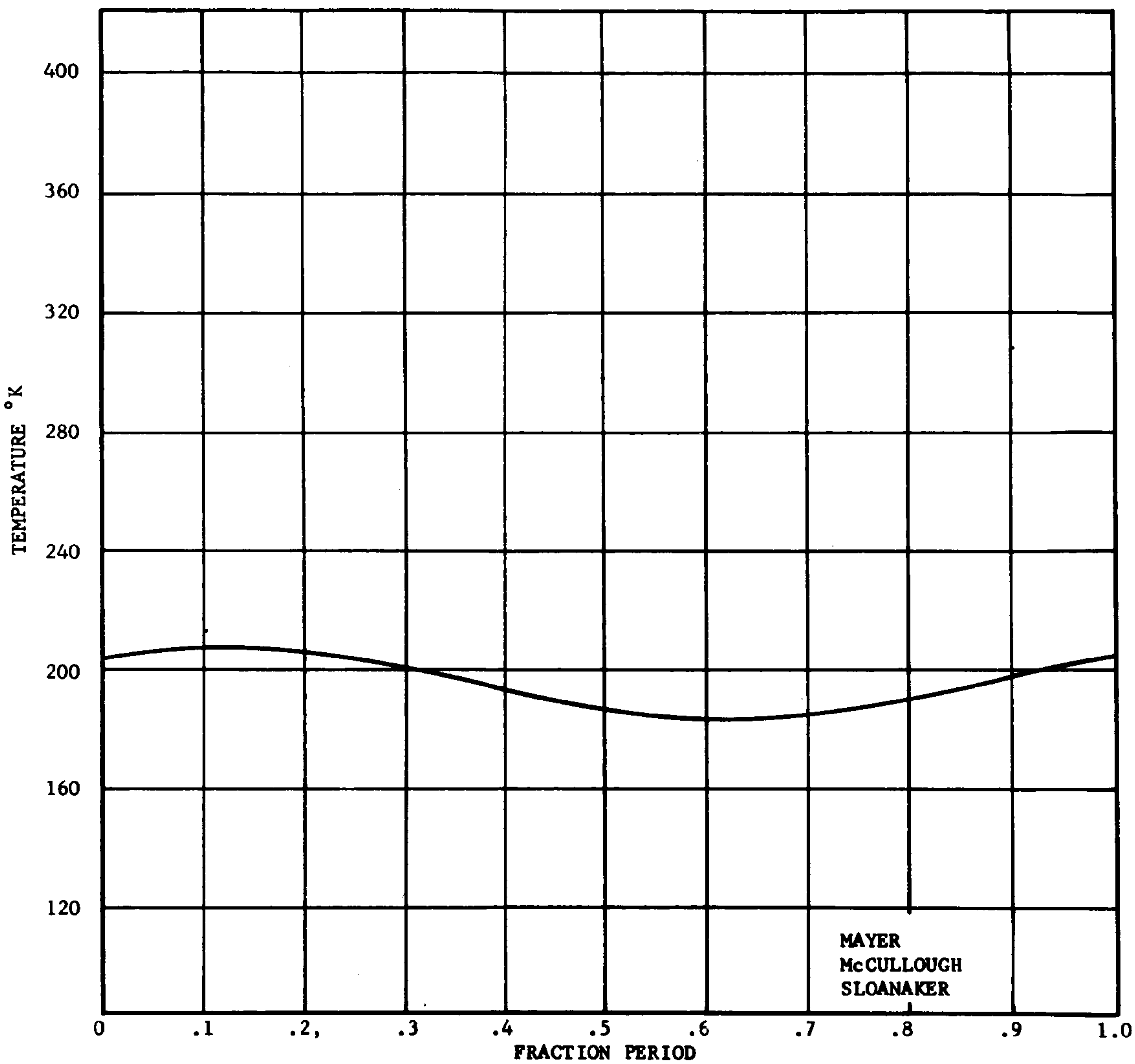

FIGURE 17 - LUNAR BRIGHTNESS TEMPERATURE AT 3.15 cm WAVELENGTH

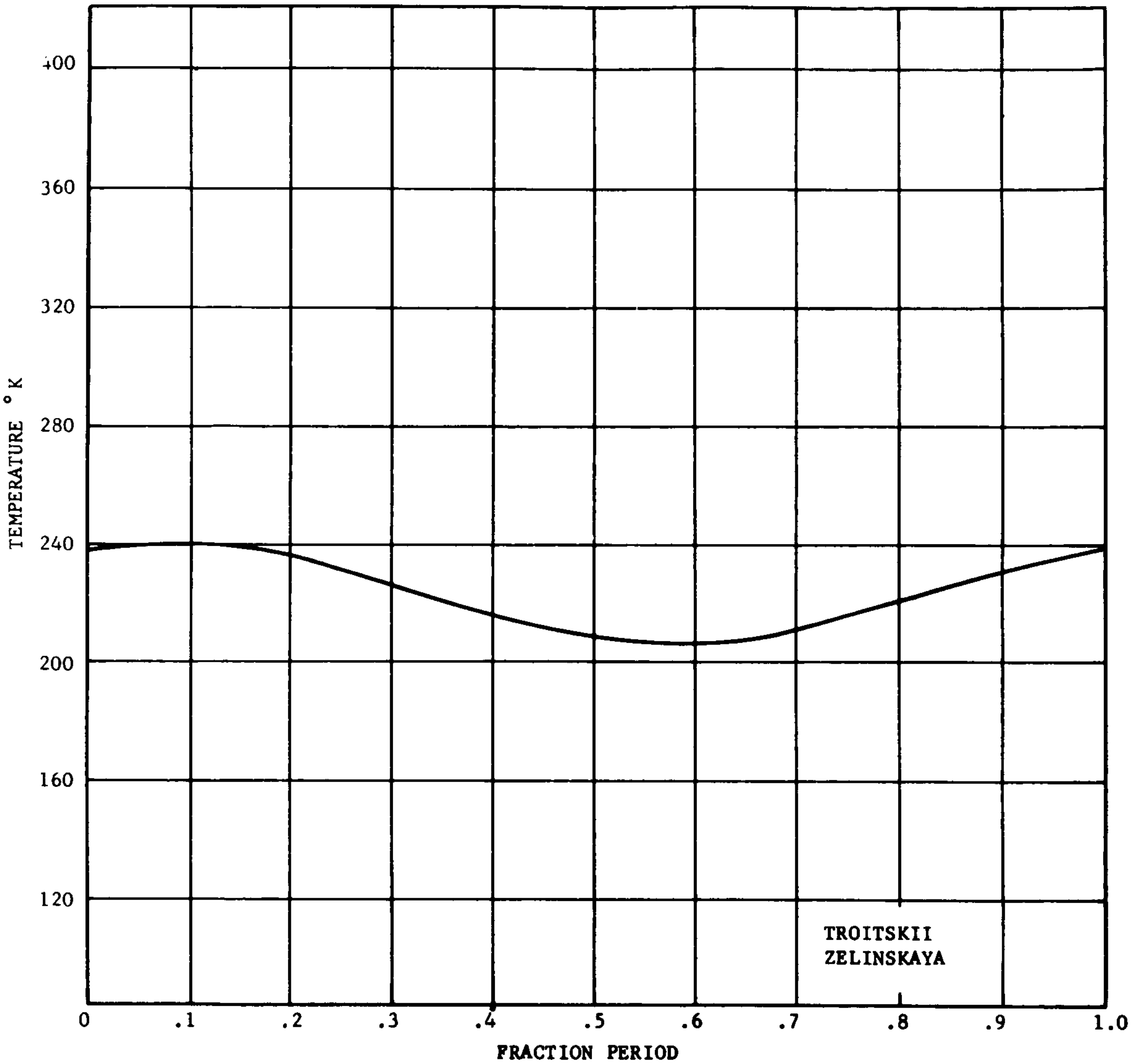

FIGURE 18 - LUNAR BRIGHTNESS TEMPERATURE AT 3.2 cm WAVELENGTH

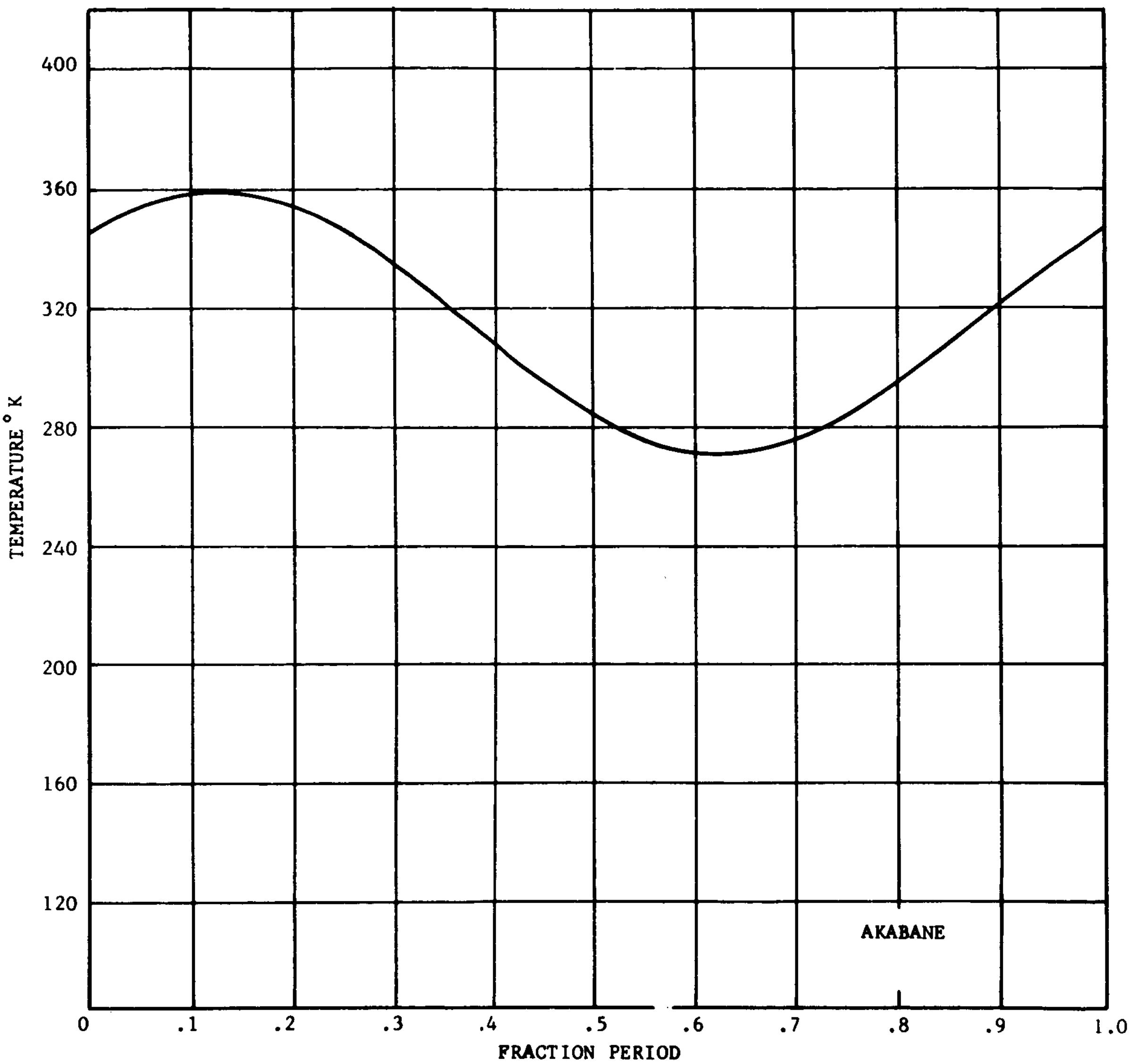

FIGURE 19 - LUNAR BRIGHTNESS TEMPERATURE AT 10 cm WAVELENGTH

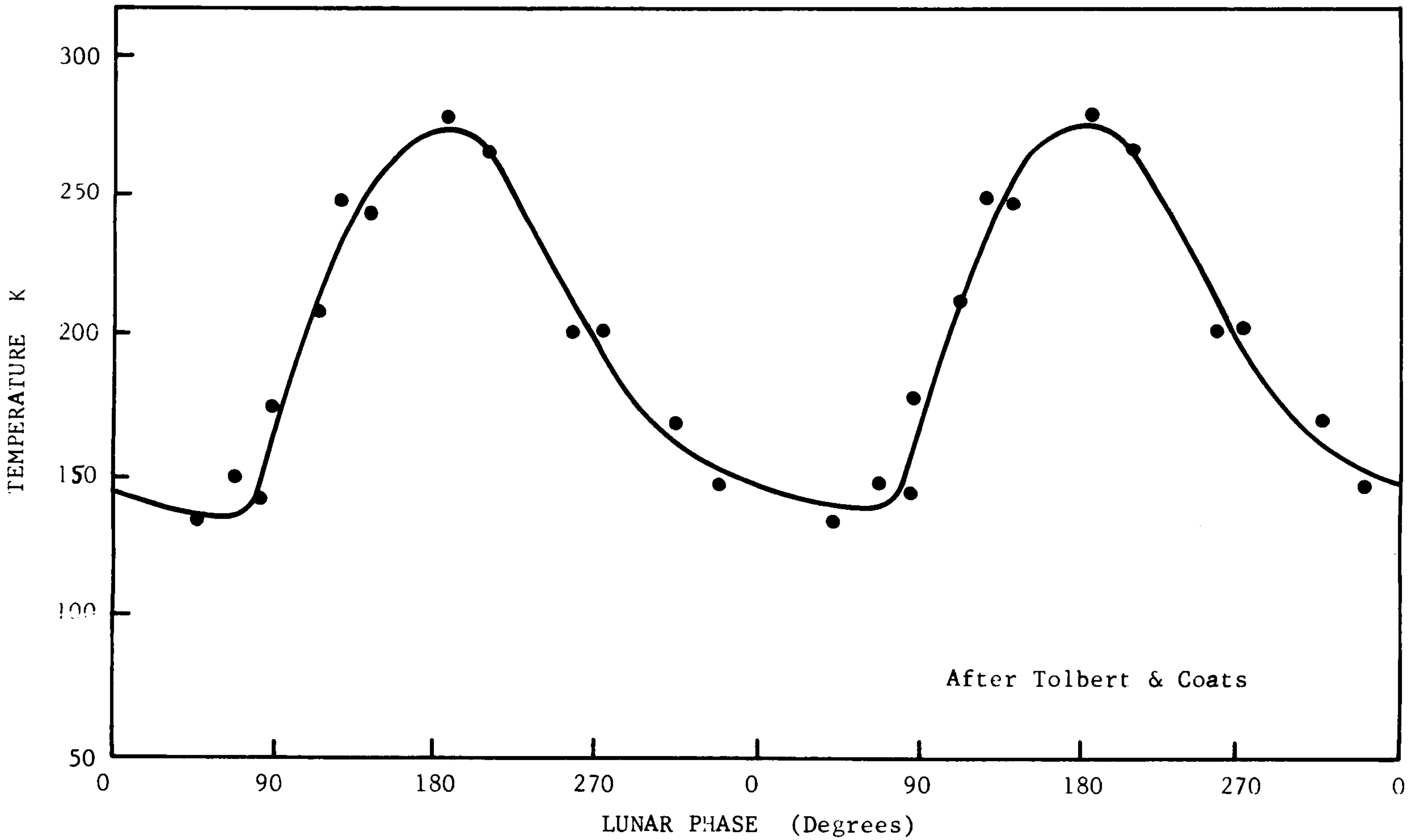

FIGURE 20 - 3.2 mm CENTRAL LUNAR AREA TEMPERATURE VERSUS LUNAR PHASE

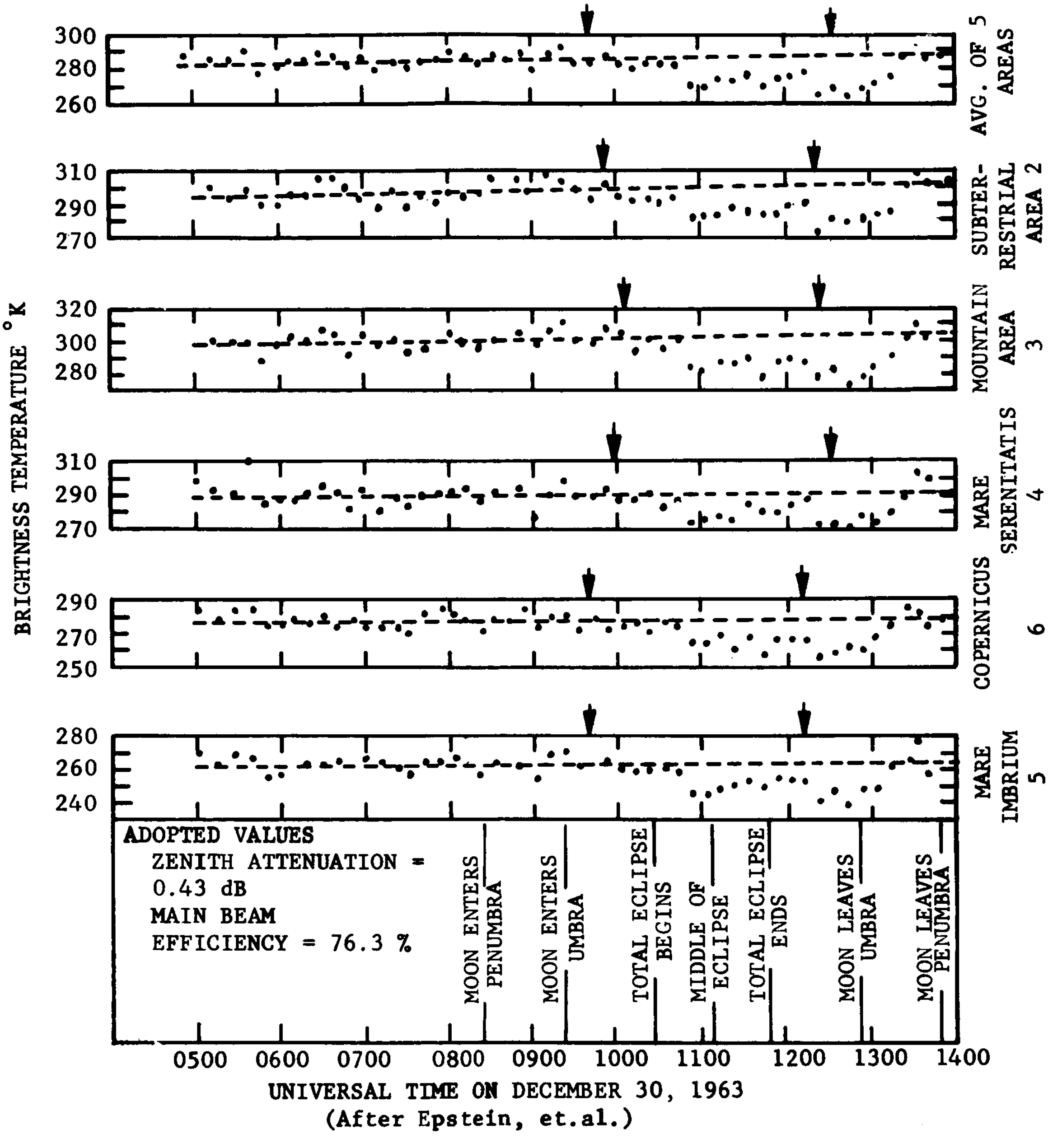

FIGURE 21 - LUNAR TEMPERATURE MEASUREMENTS DURING THE DECEMBER 30, 1963 LUNAR ECLIPSE

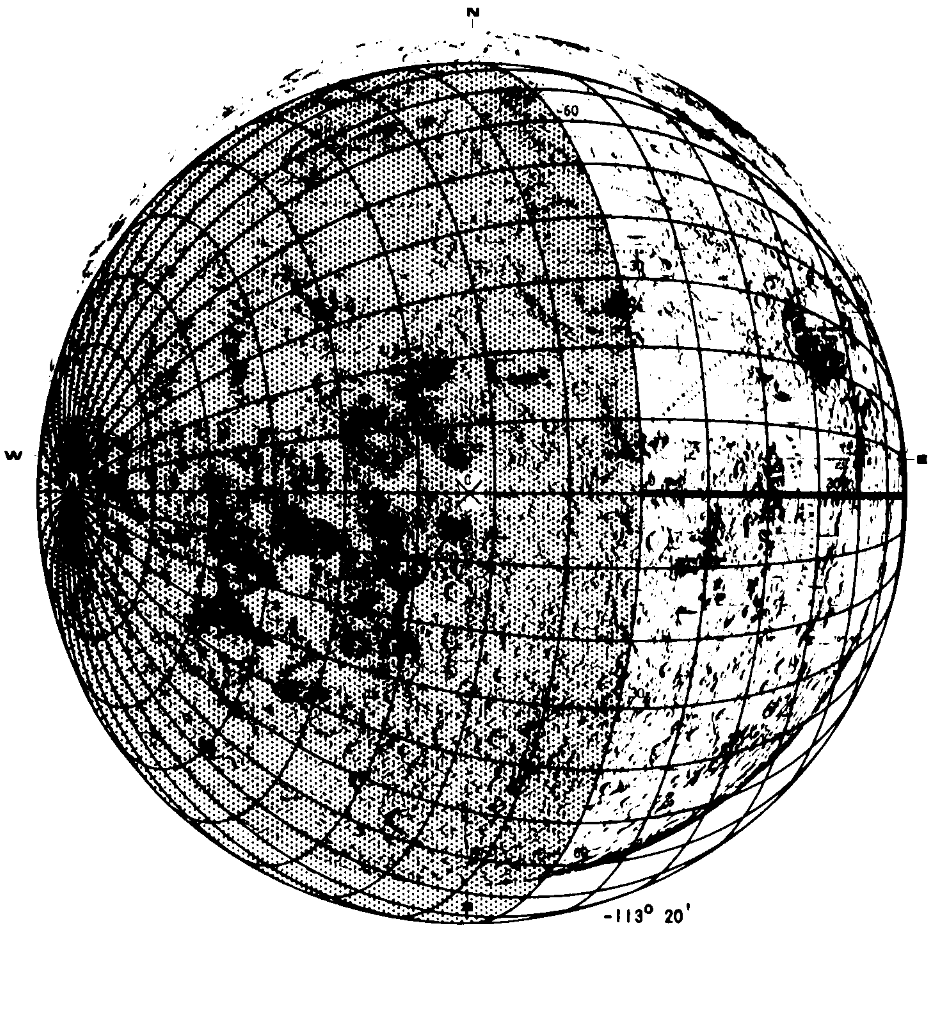

FIGURE 22 - THERMAL COORDINATES

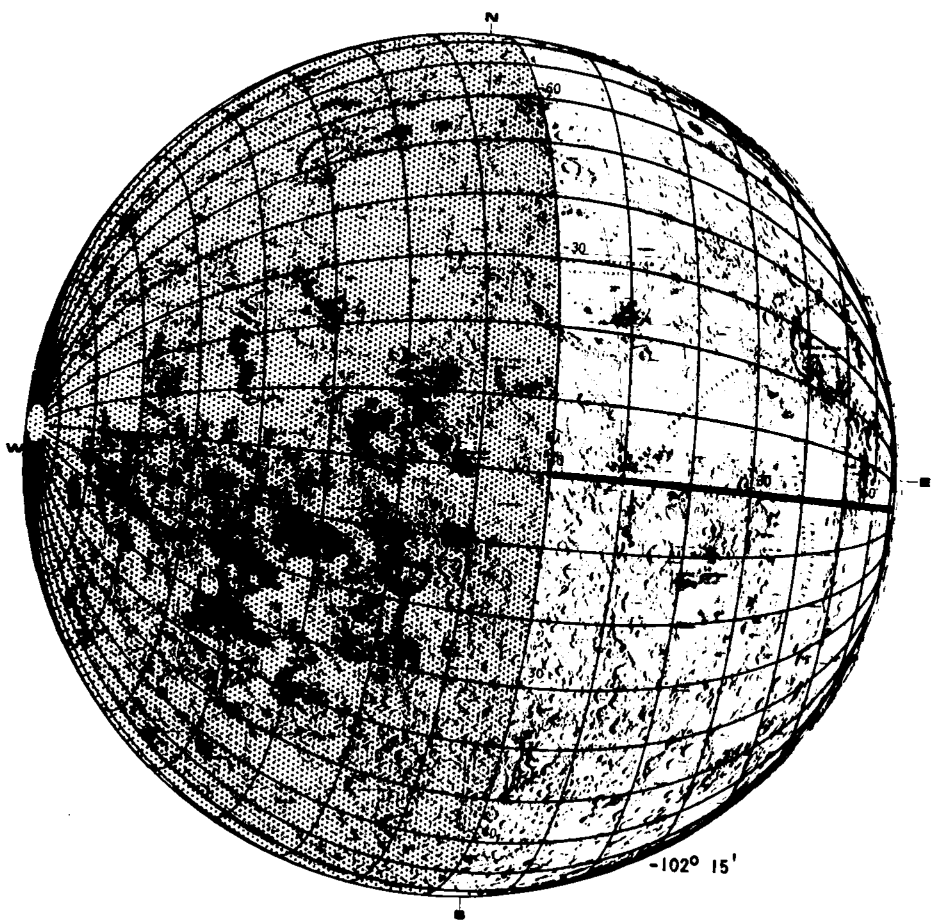

FIGURE 23 - THERMAL COORDINATES

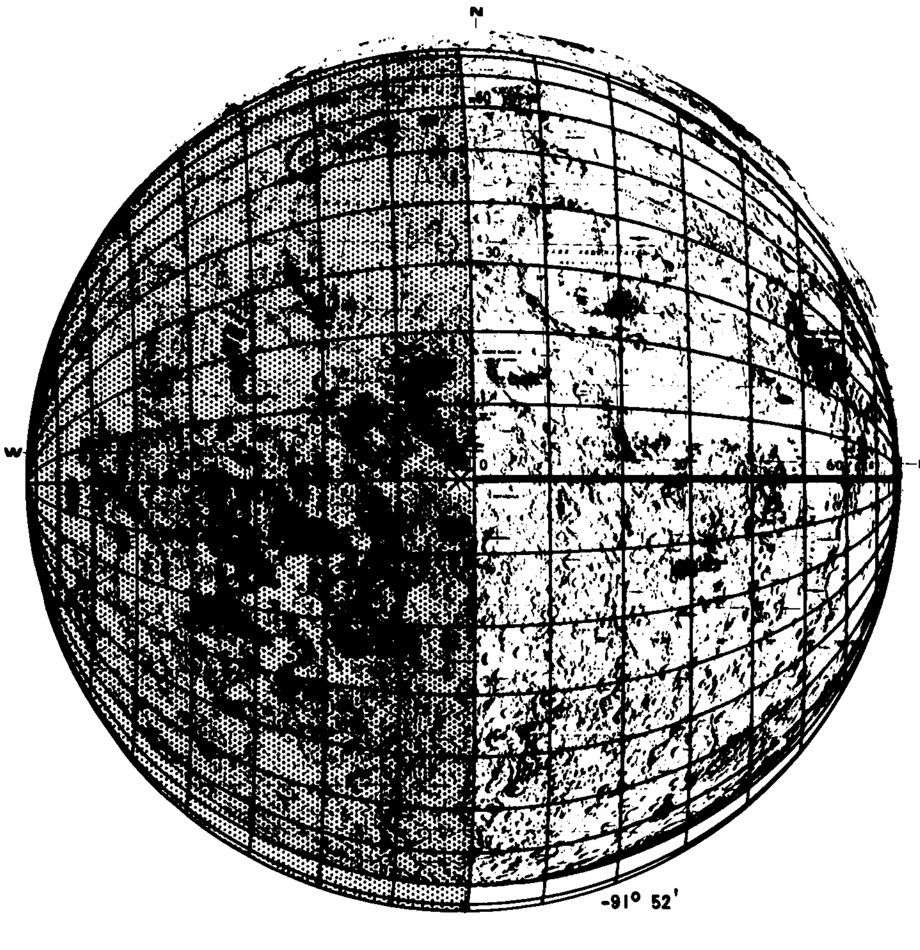

FIGURE 24 - THERMAL COORDINATES

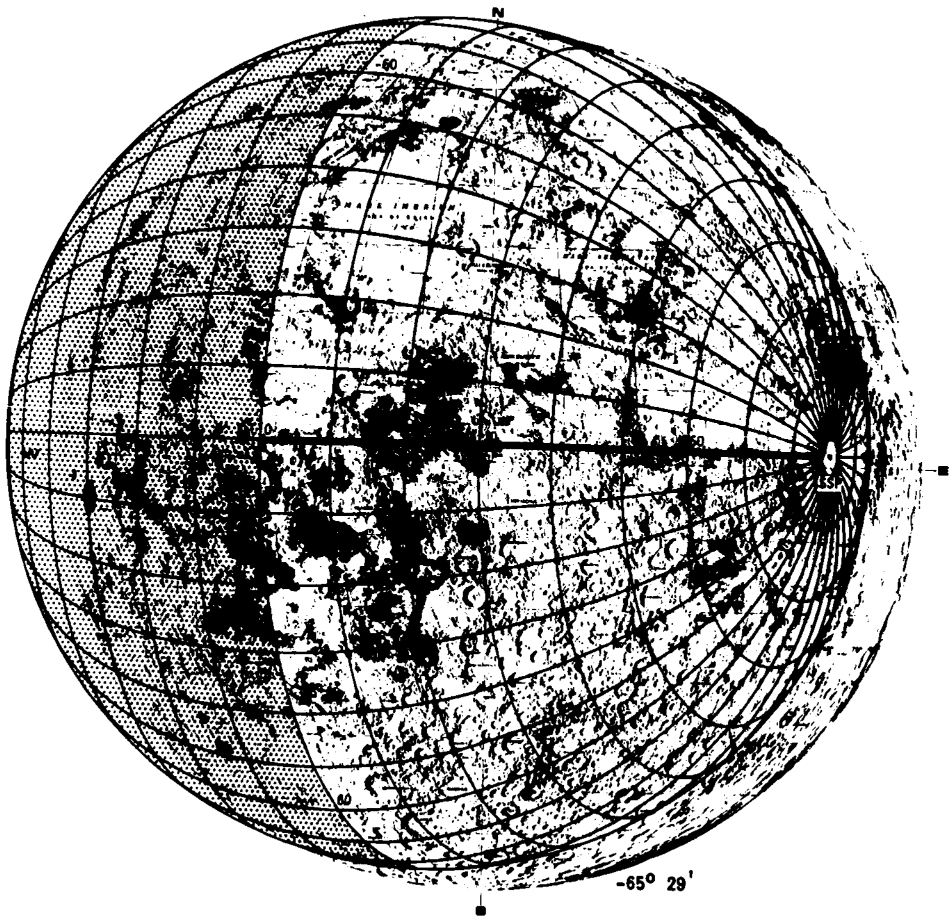

FIGURE 25 - THERMAL COORDINATES

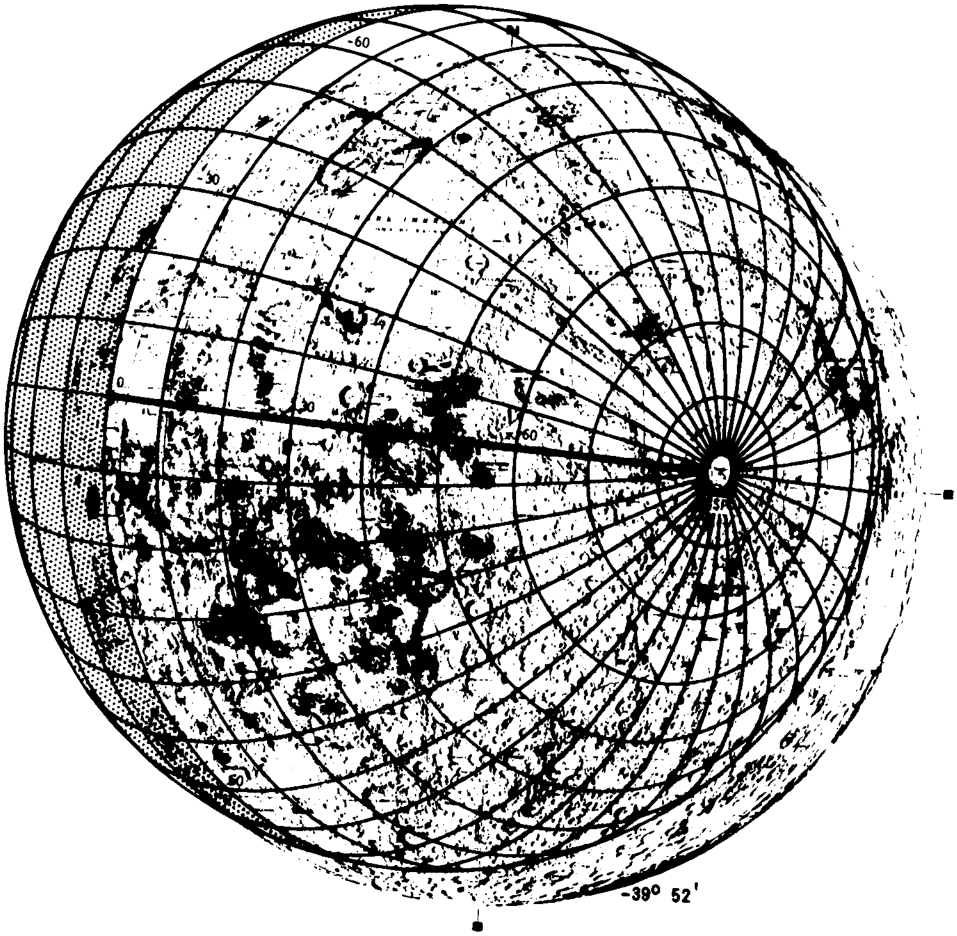

FIGURE 26 - THERMAL COORDINATES

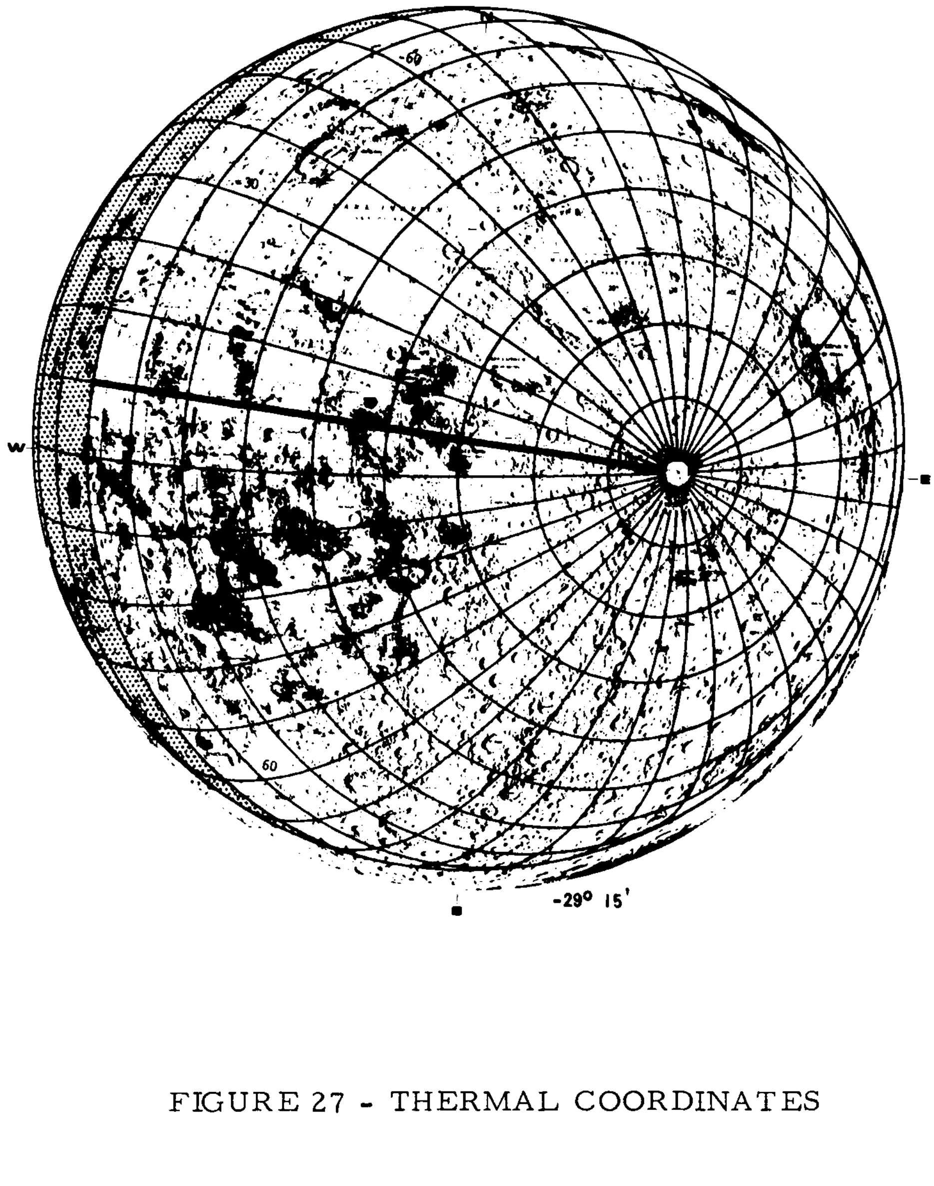

FIGURE 27 - THERMAL COORDINATES

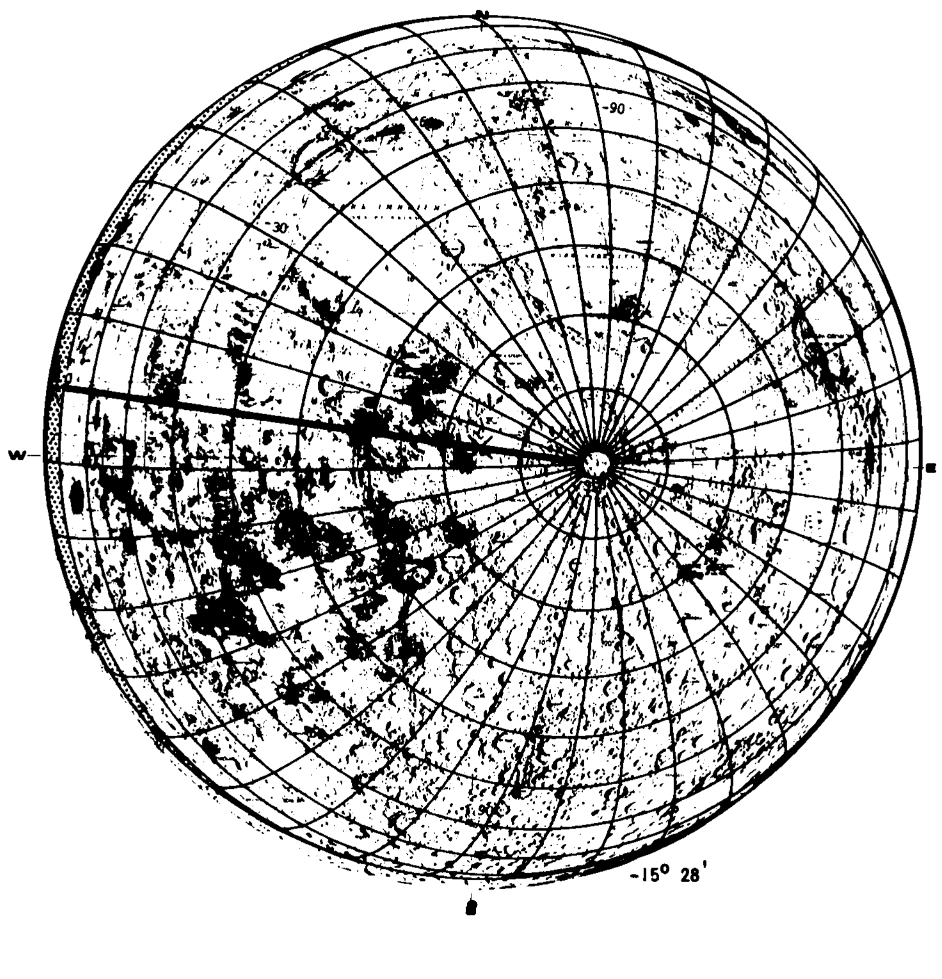

FIGURE 28 - THERMAL COORDINATES

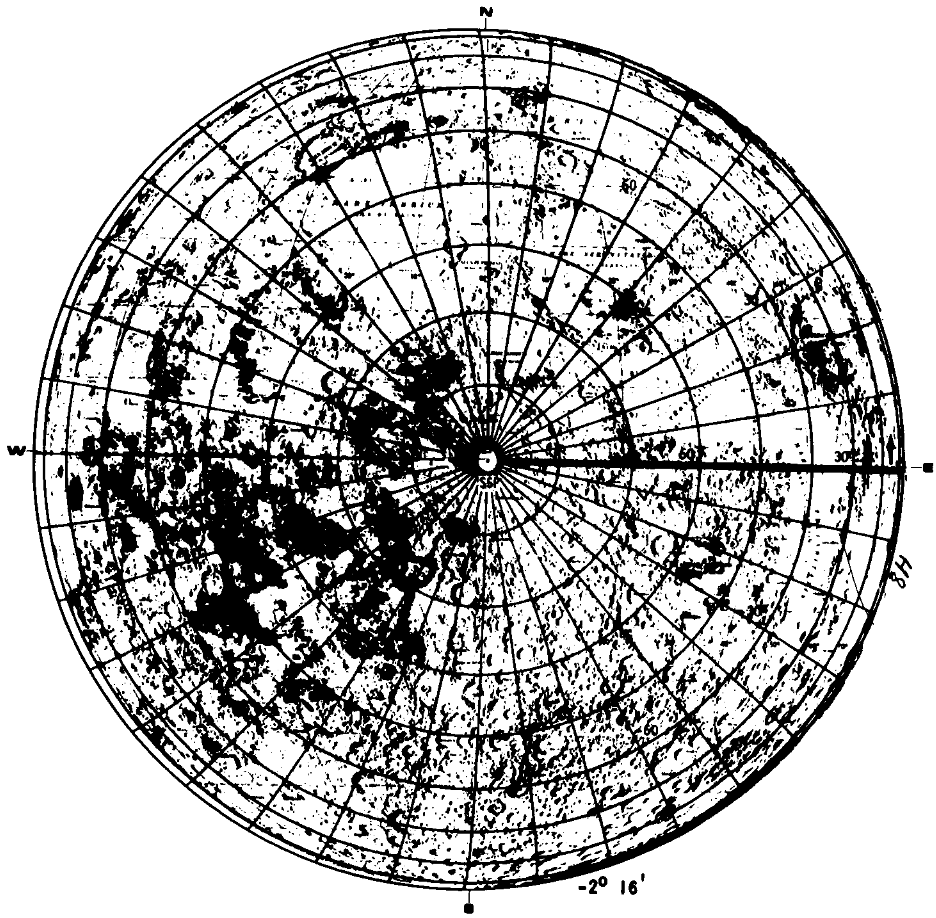

FIGURE 29 - THERMAL COORDINATES

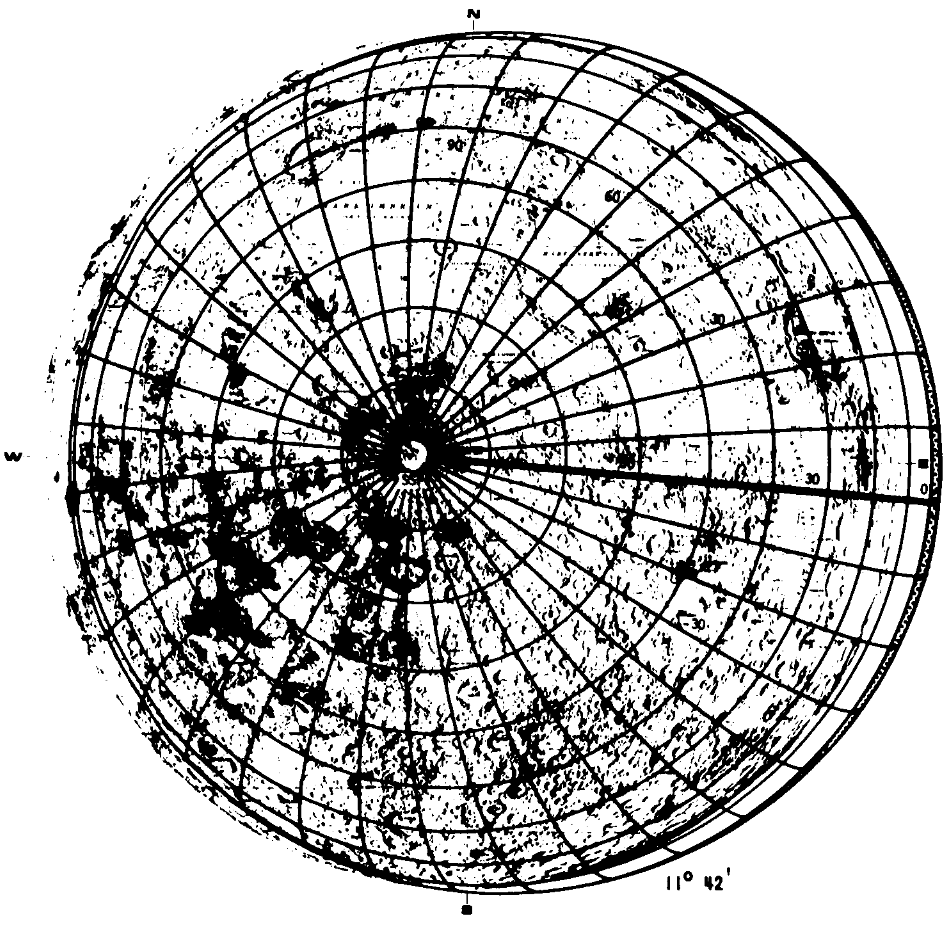

FIGURE 30 - THERMAL COORDINATES

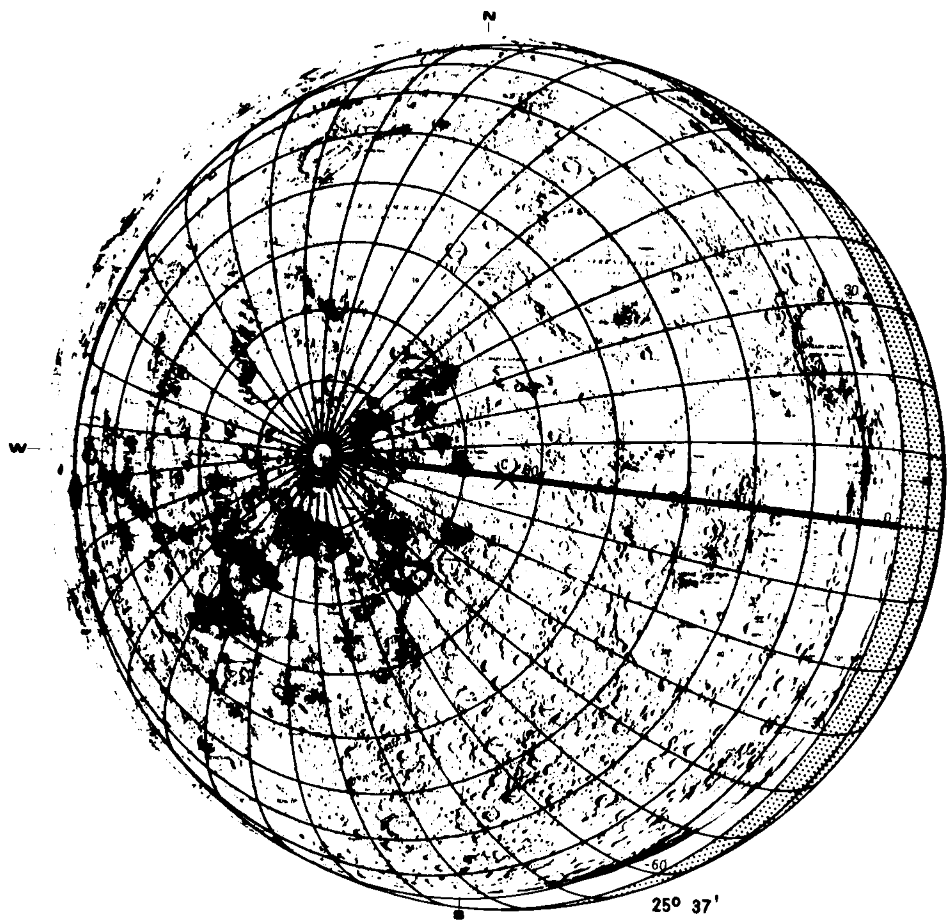

FIGURE 31 - THERMAL COORDINATES

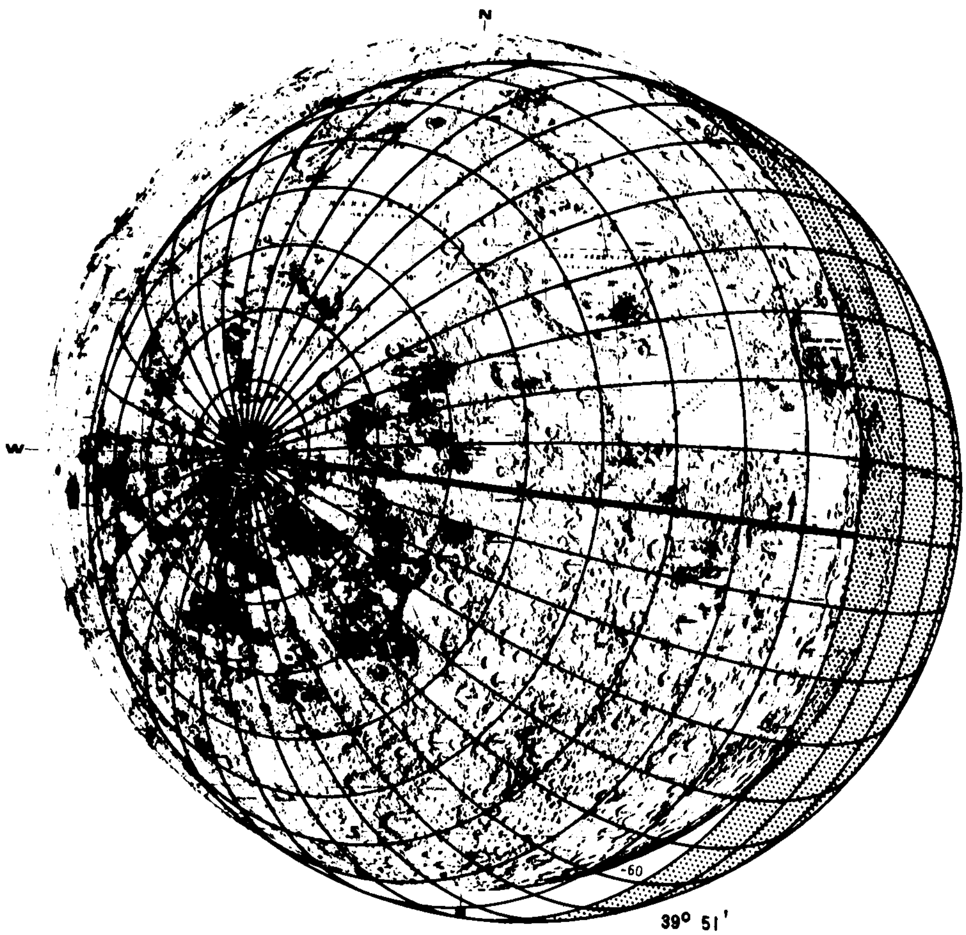

FIGURE 32 - THERMAL COORDINATES

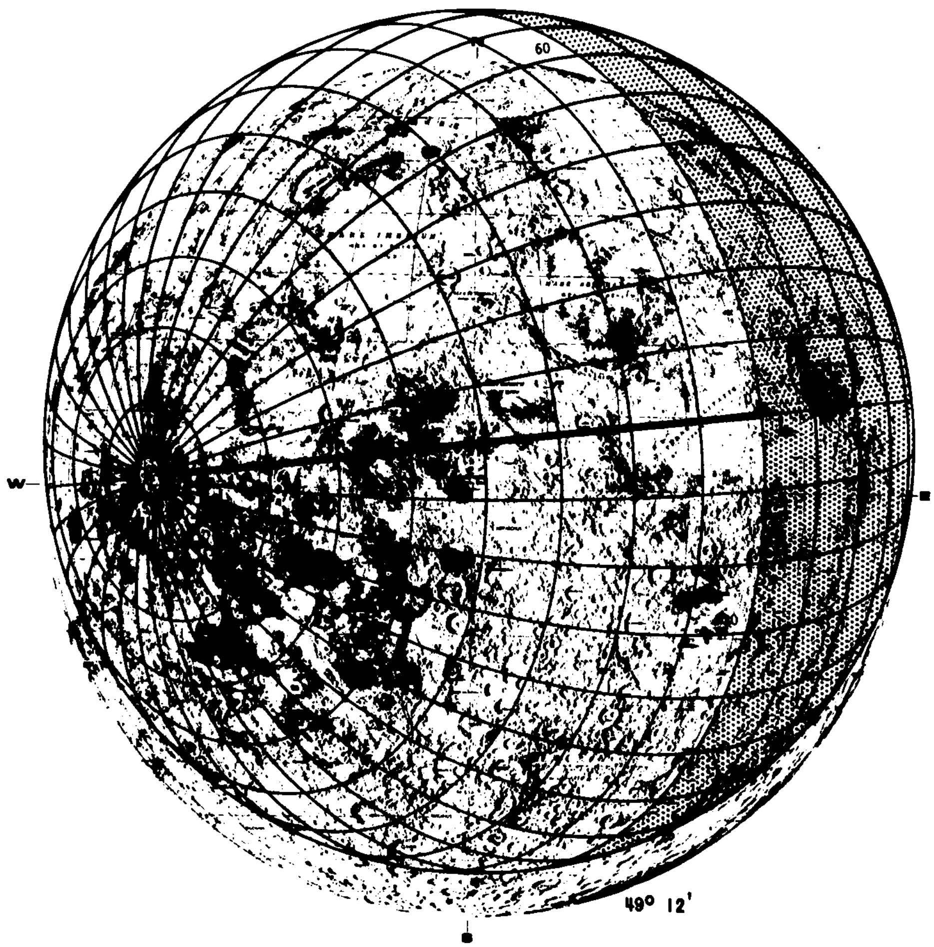

FIGURE 33 - THERMAL COORDINATES

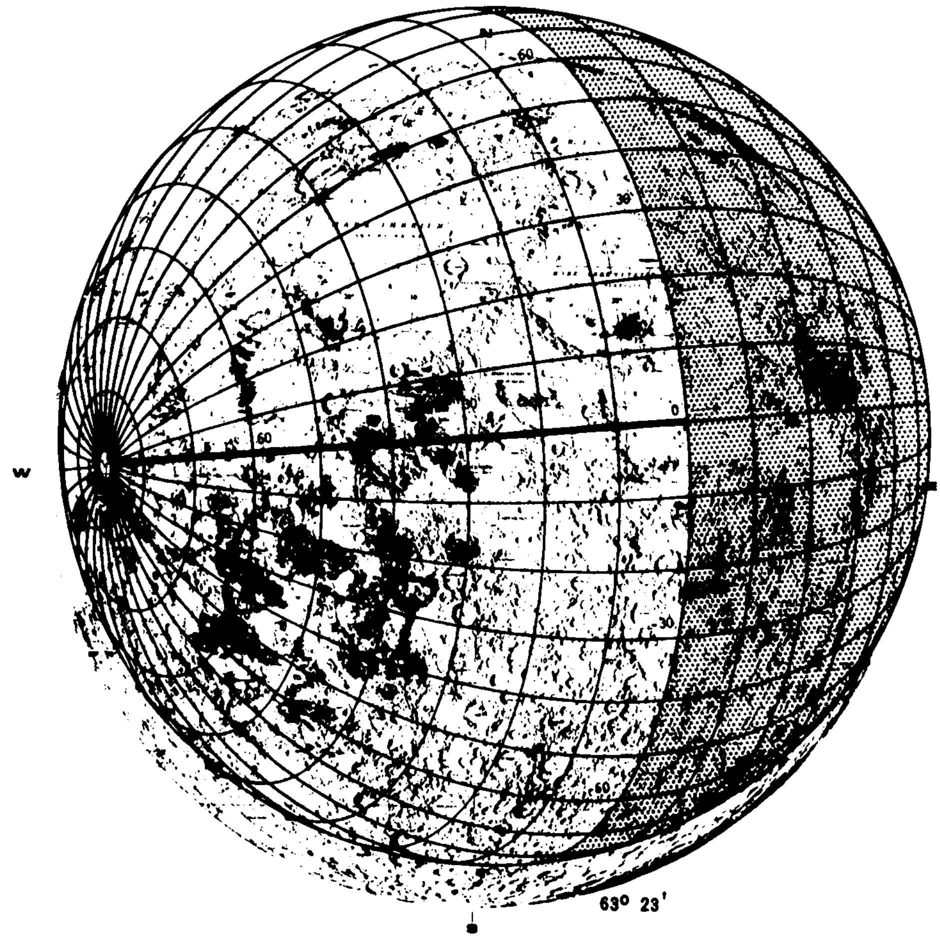

FIGURE 34 - THERMAL COORDINATES

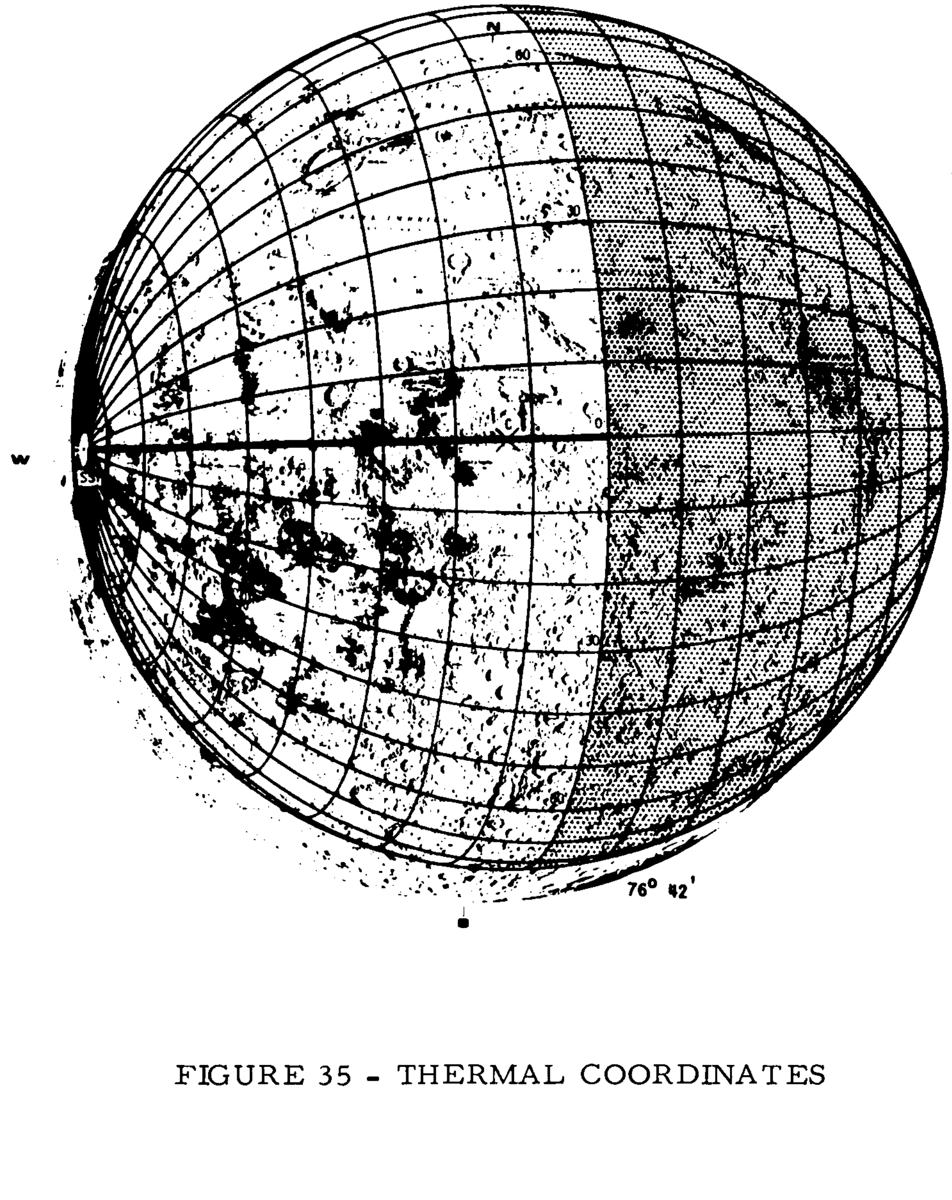

FIGURE 35 - THERMAL COORDINATES

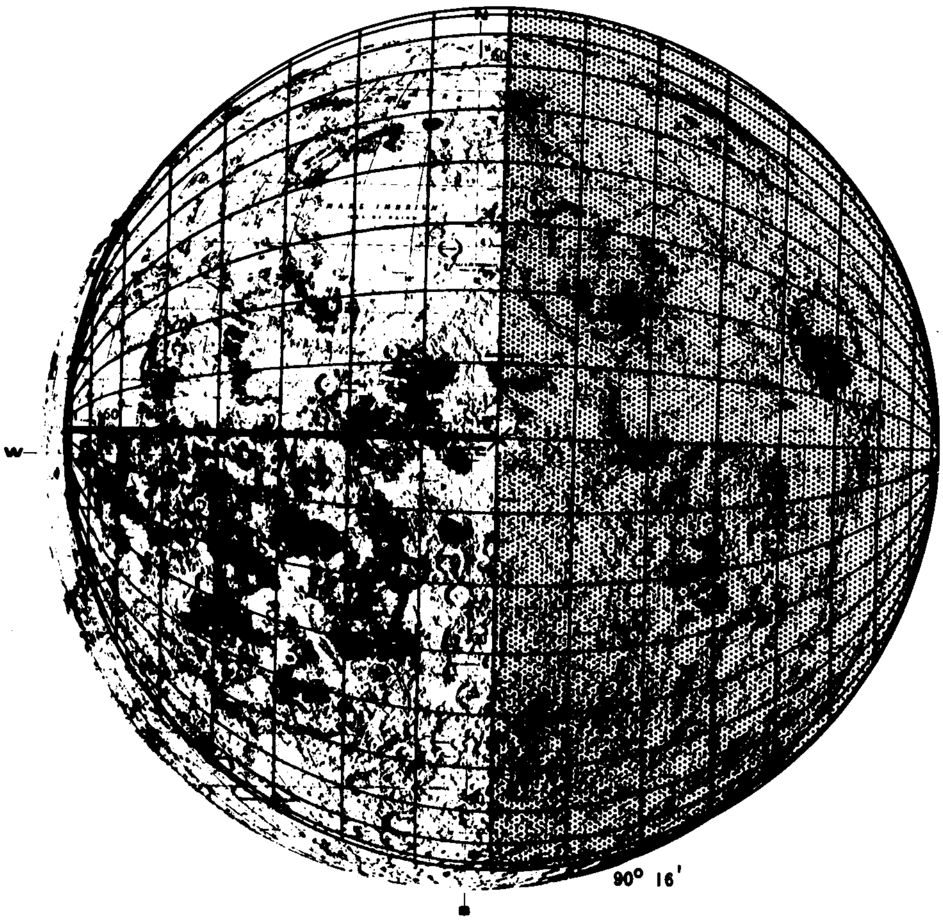

FIGURE 36 - THERMAL COORDINATES

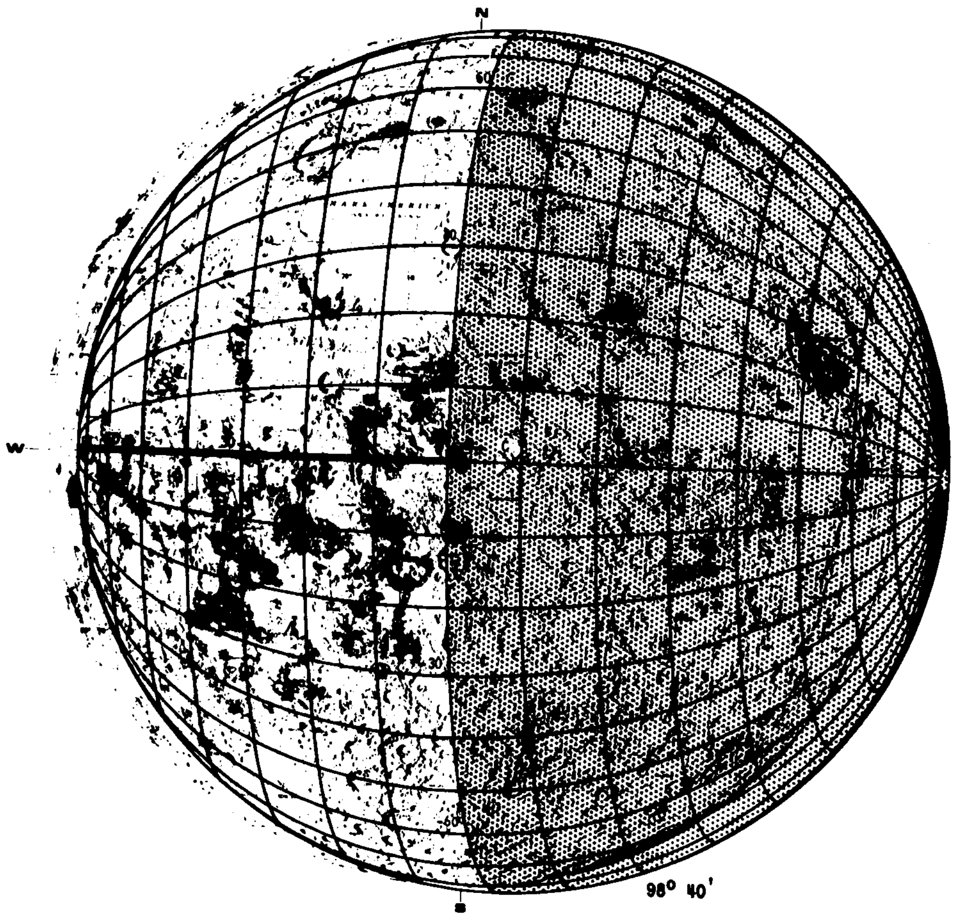

FIGURE 37 - THERMAL COORDINATES

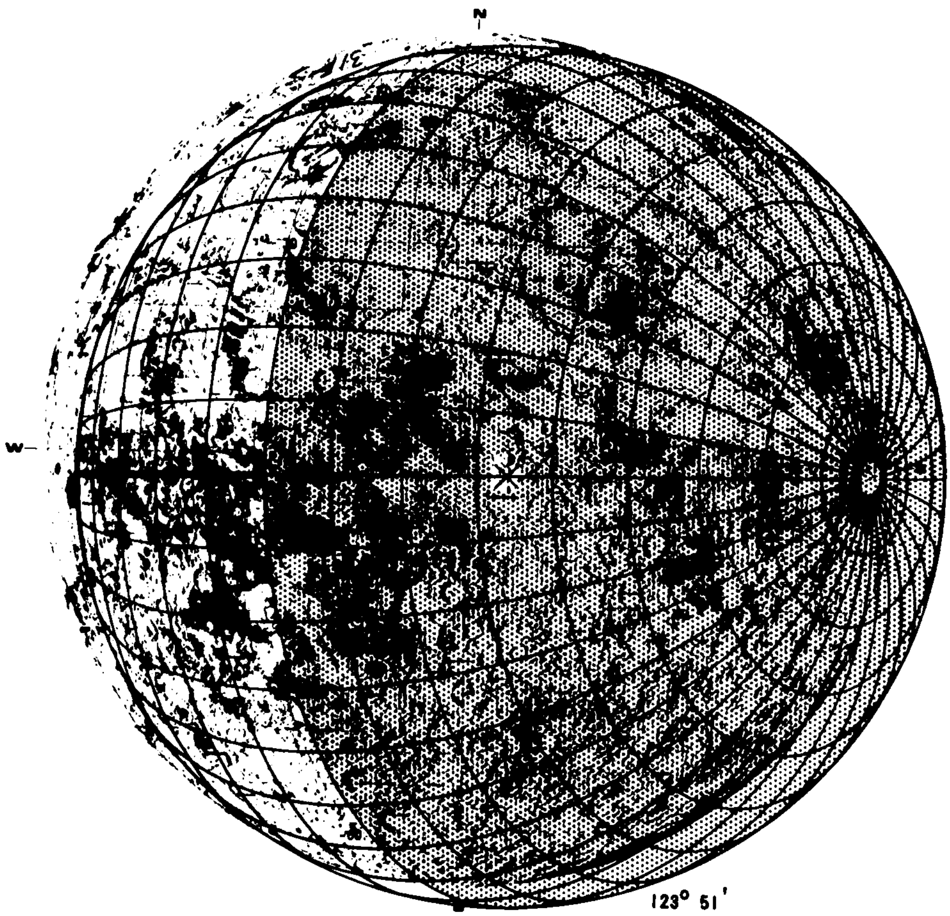

FIGURE 38 - THERMAL COORDINATES

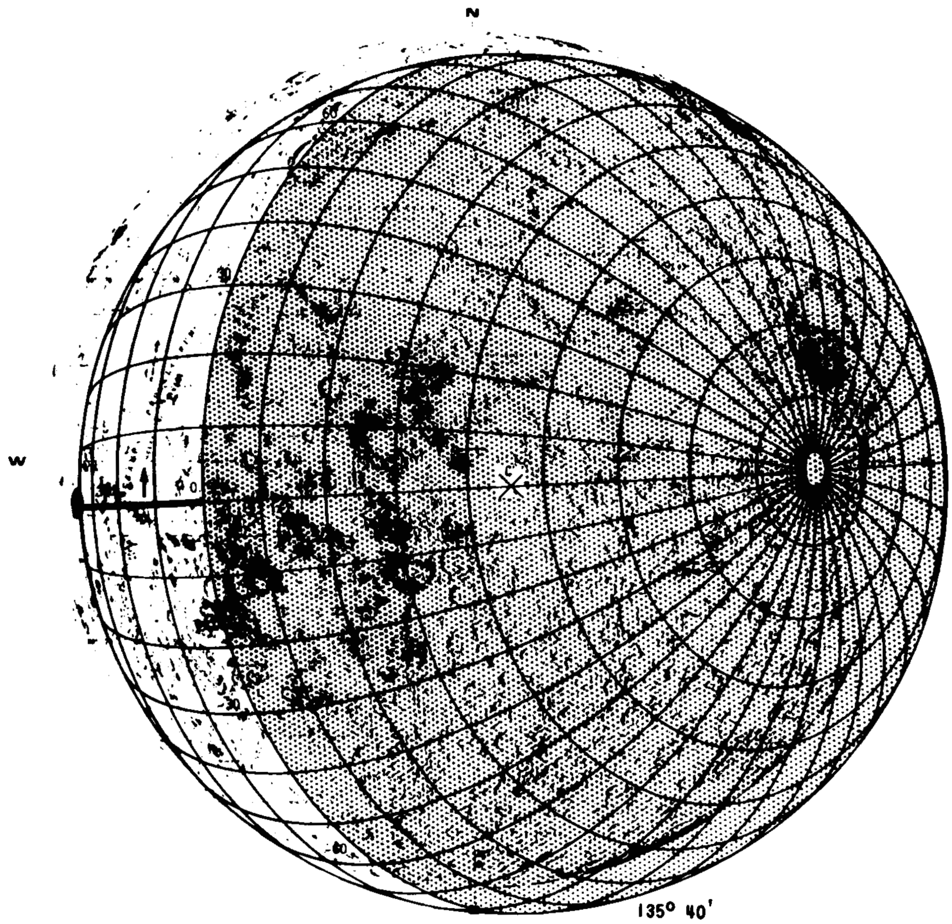

FIGURE 39 - THERMAL COORDINATES

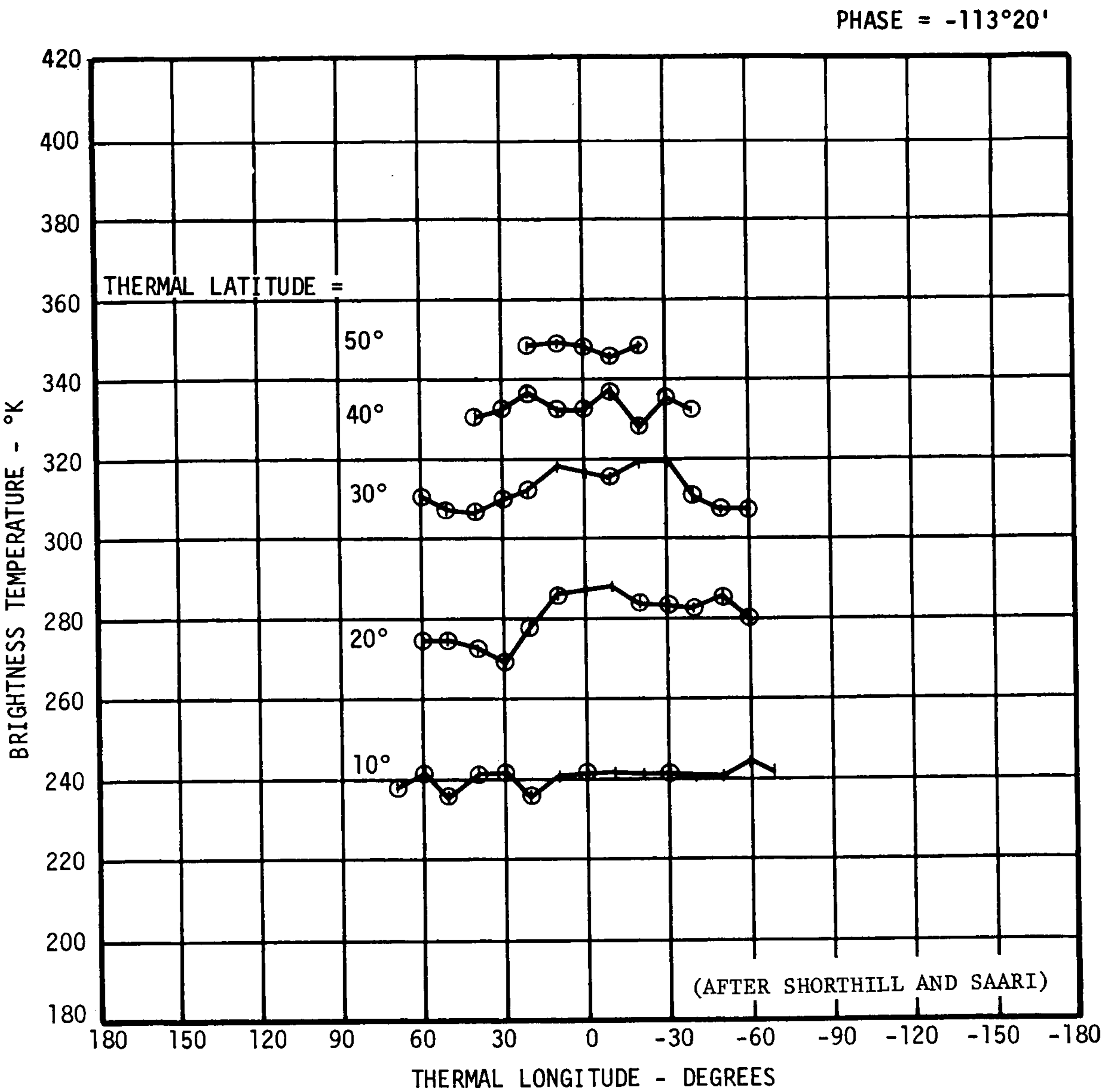

FIGURE 40 - TEMPERATURE FOR -113° 20' PHASE

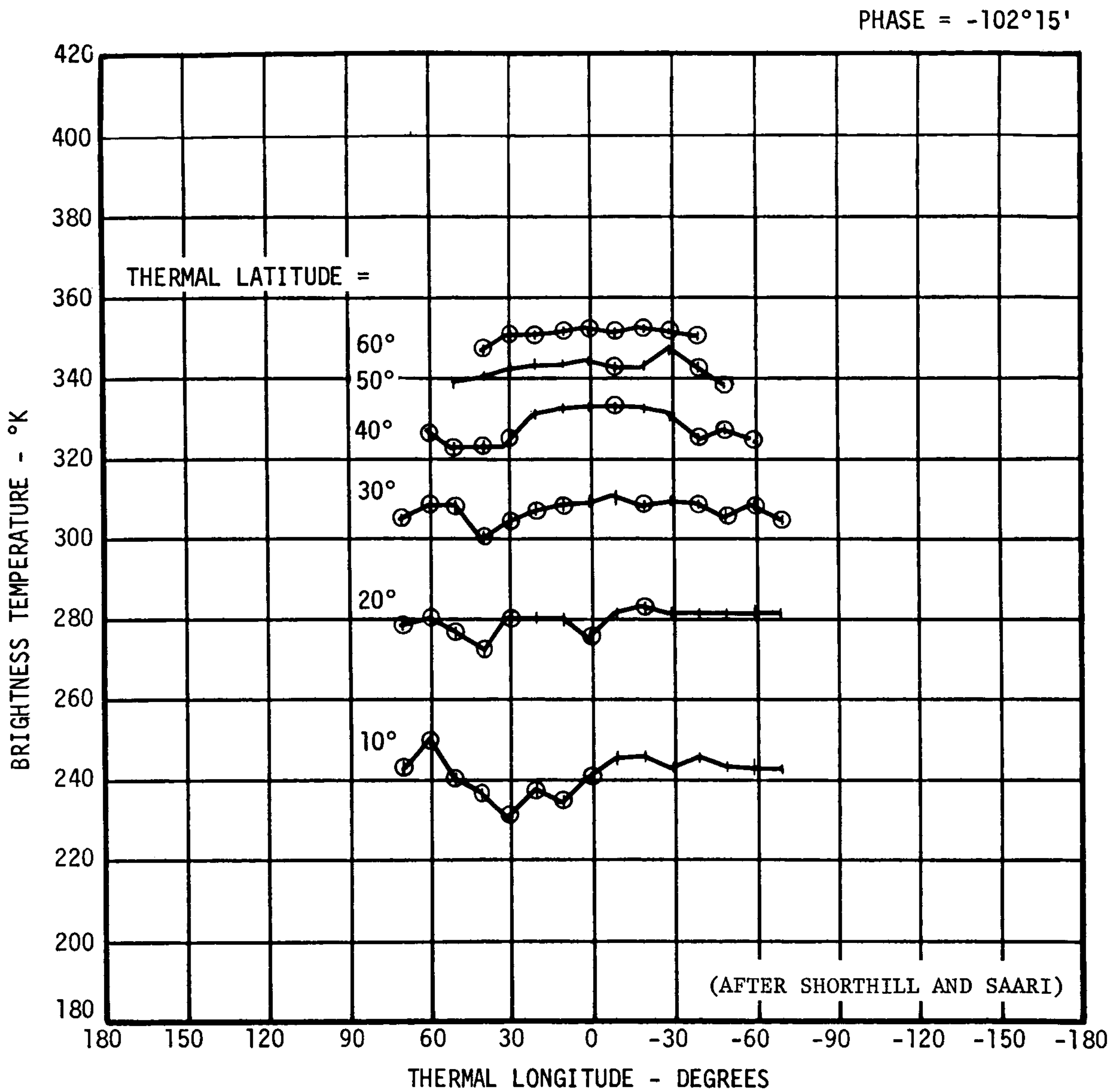

FIGURE 41 - TEMPERATURE FOR -102°15' PHASE

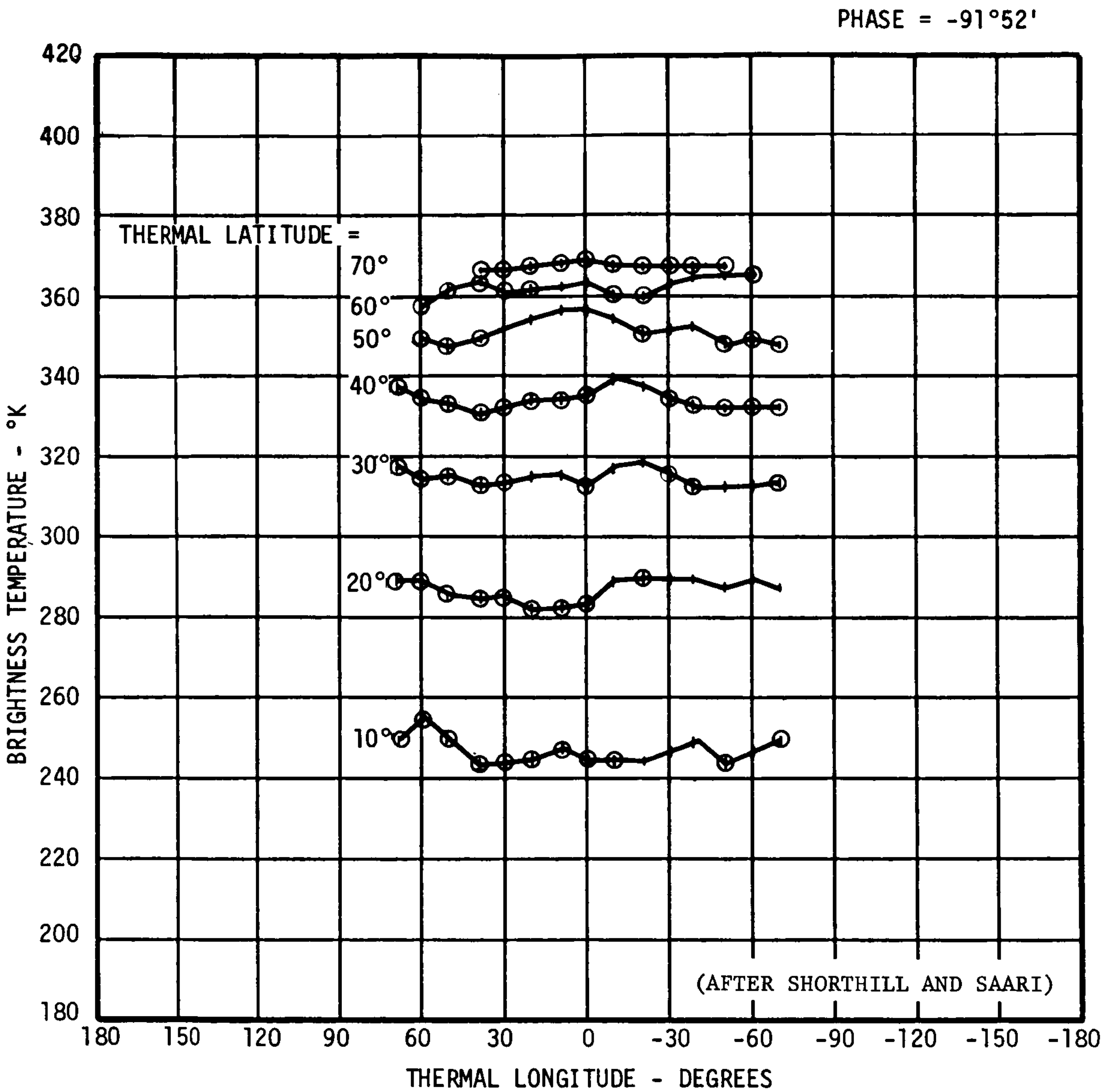

FIGURE 42 - TEMPERATURE FOR -91° 52' PHASE

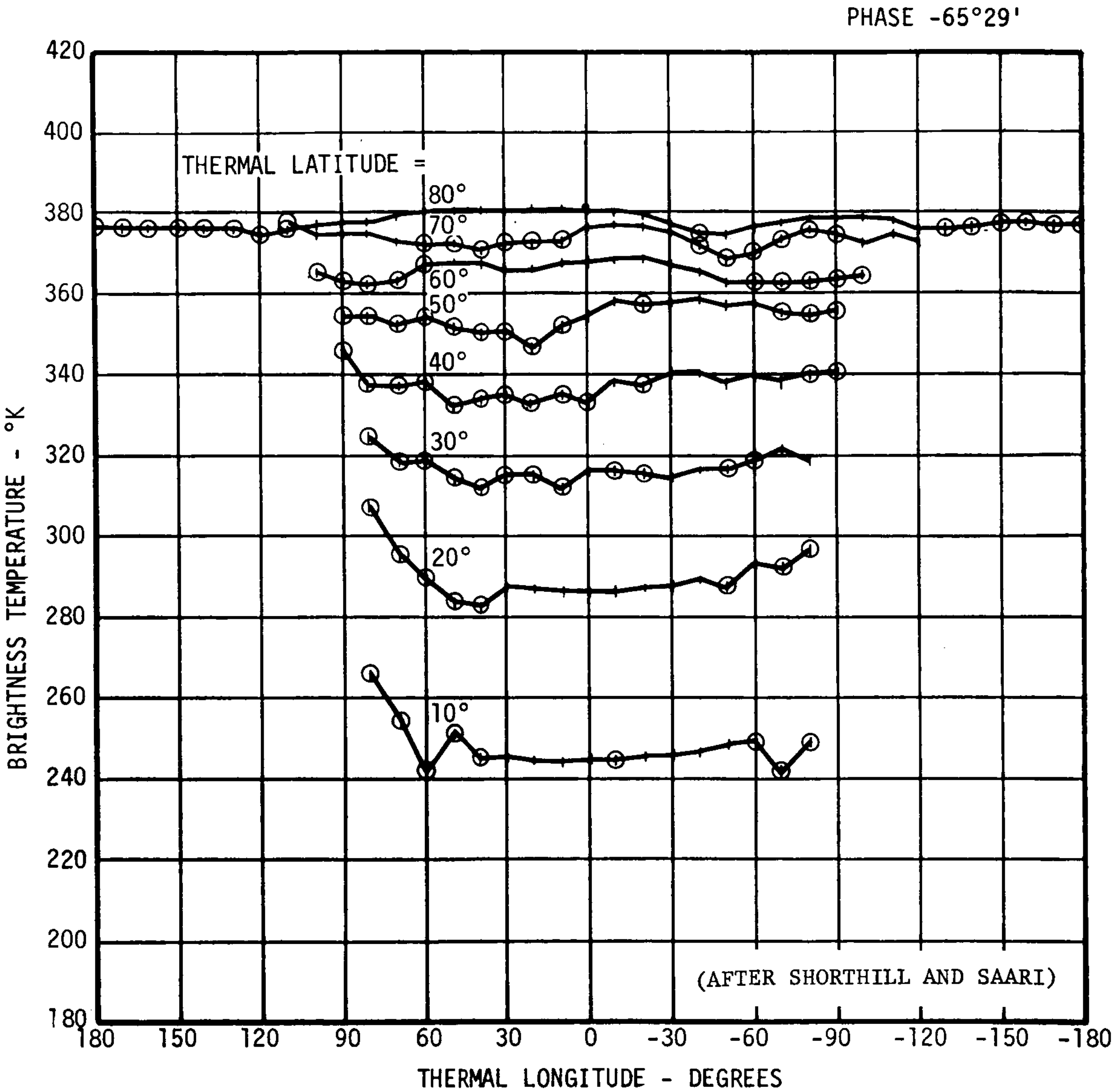

FIGURE 43 - TEMPERATURE FOR -65° 29' PHASE

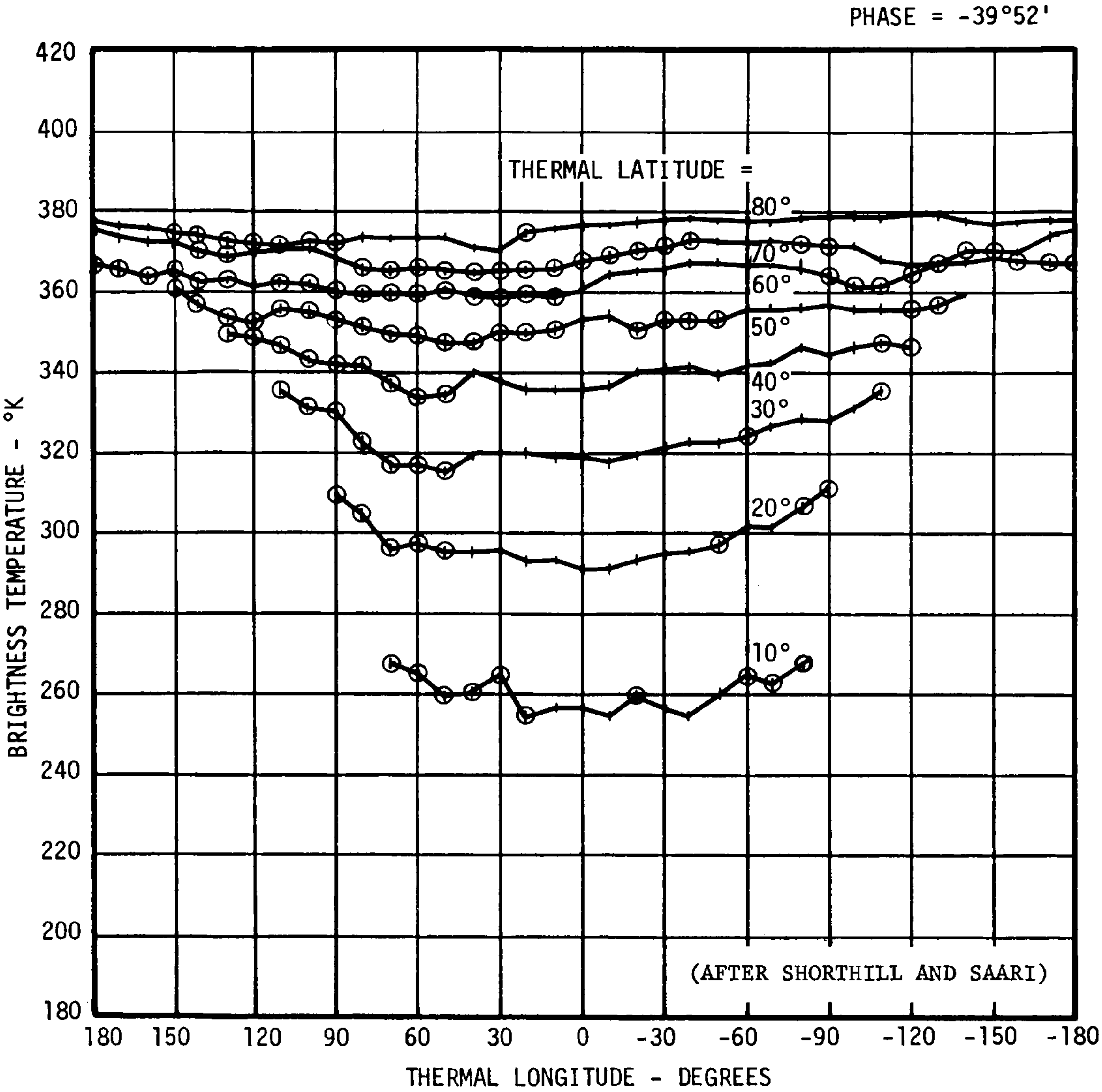

FIGURE 44 - TEMPERATURE FOR -39° 52' PHASE

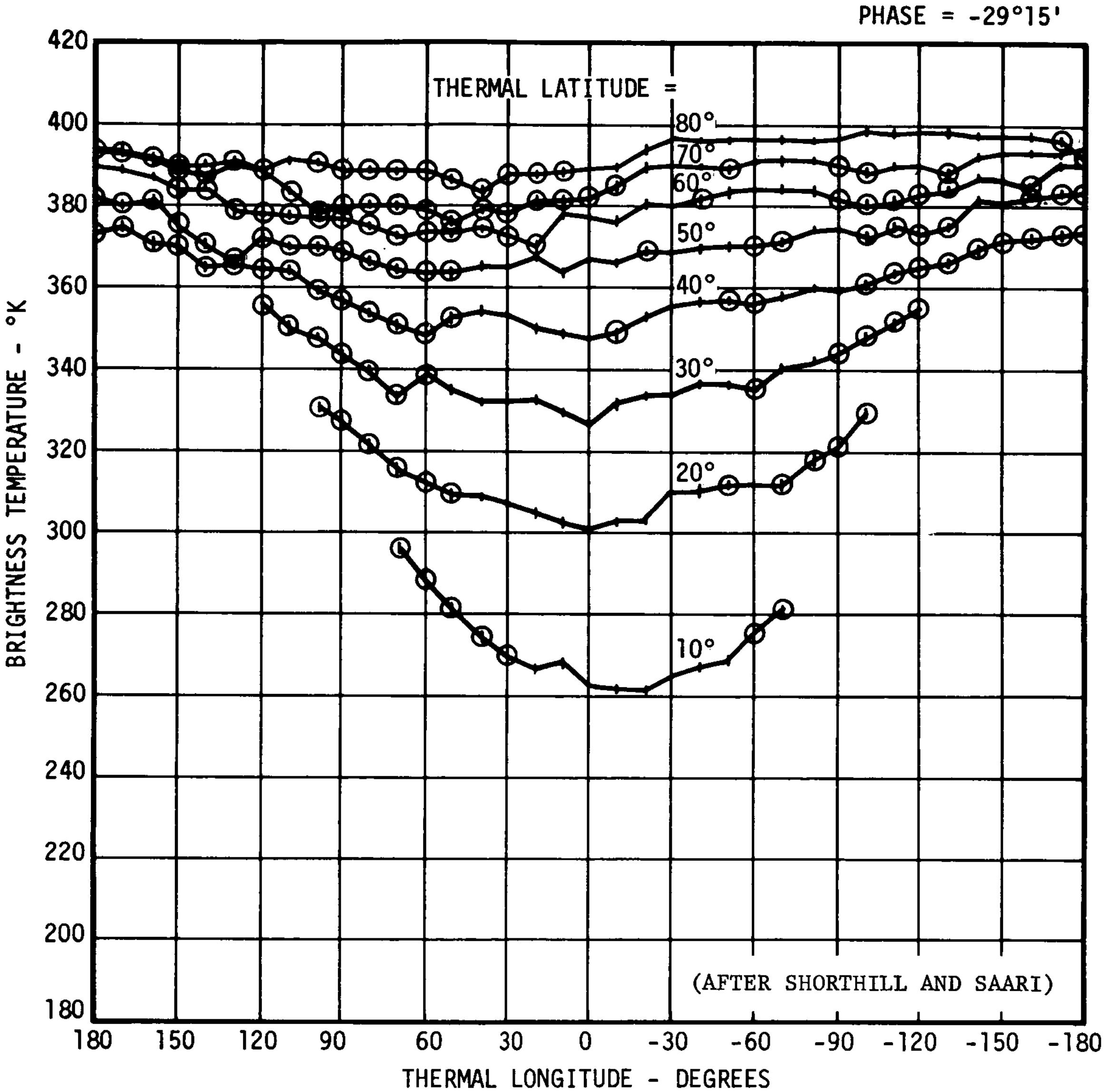

FIGURE 45 - TEMPERATURE FOR - 29^{o} 15' PHASE

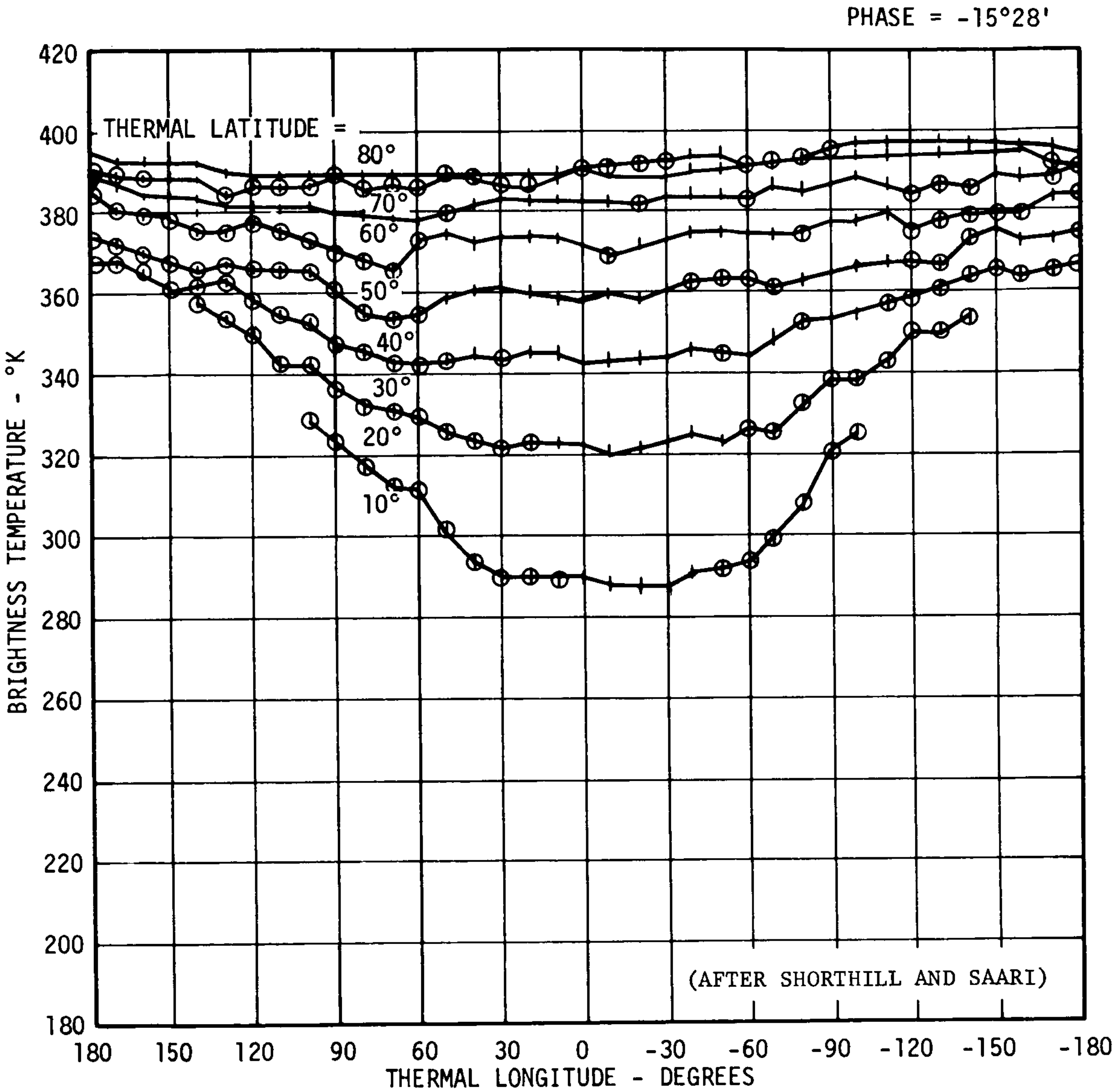

FIGURE 46 - TEMPERATURE FOR - 15° 28' PHASE

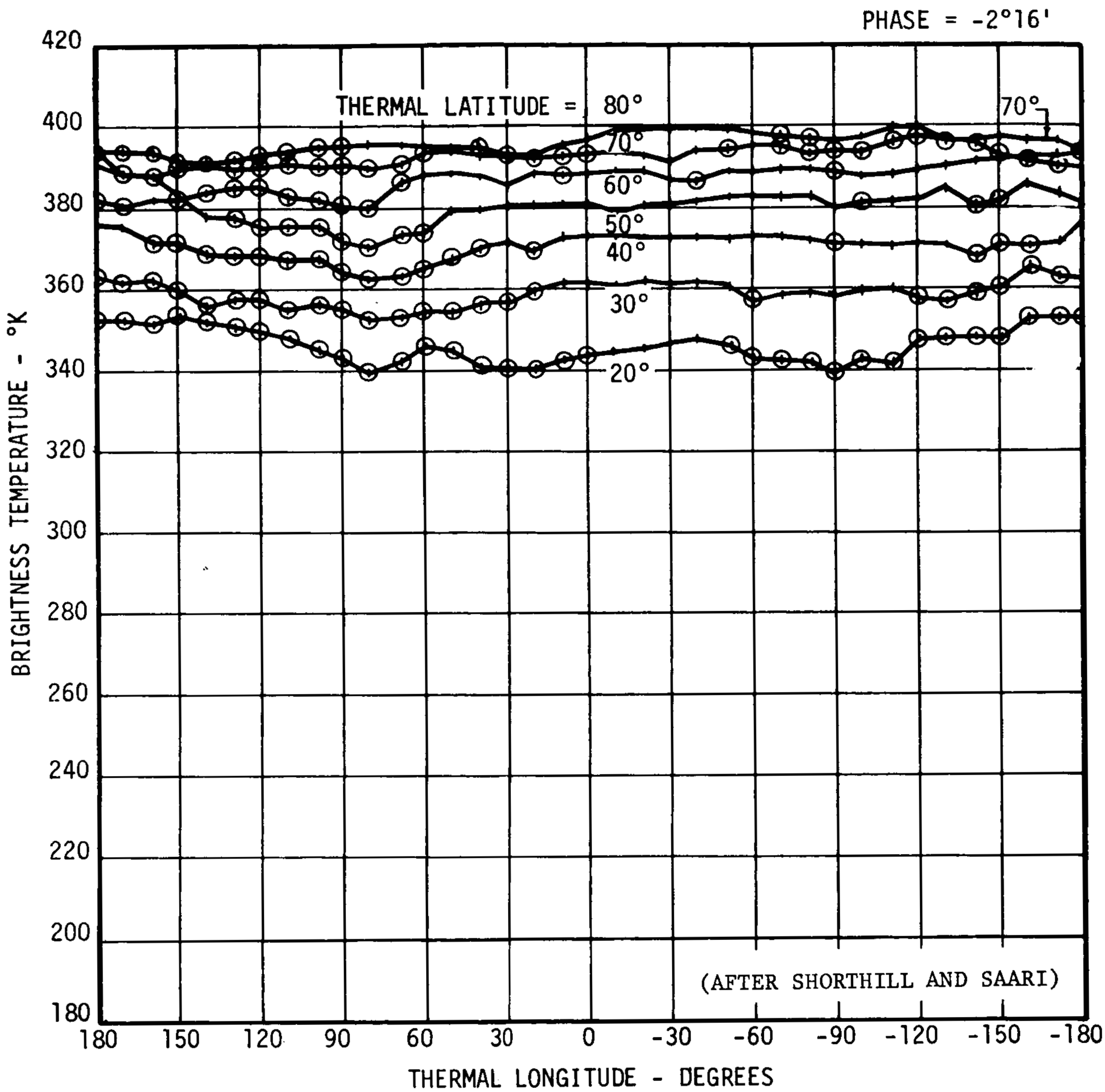

FIGURE 47 - TEMPERATURE FOR - 2^{o} 16' PHASE

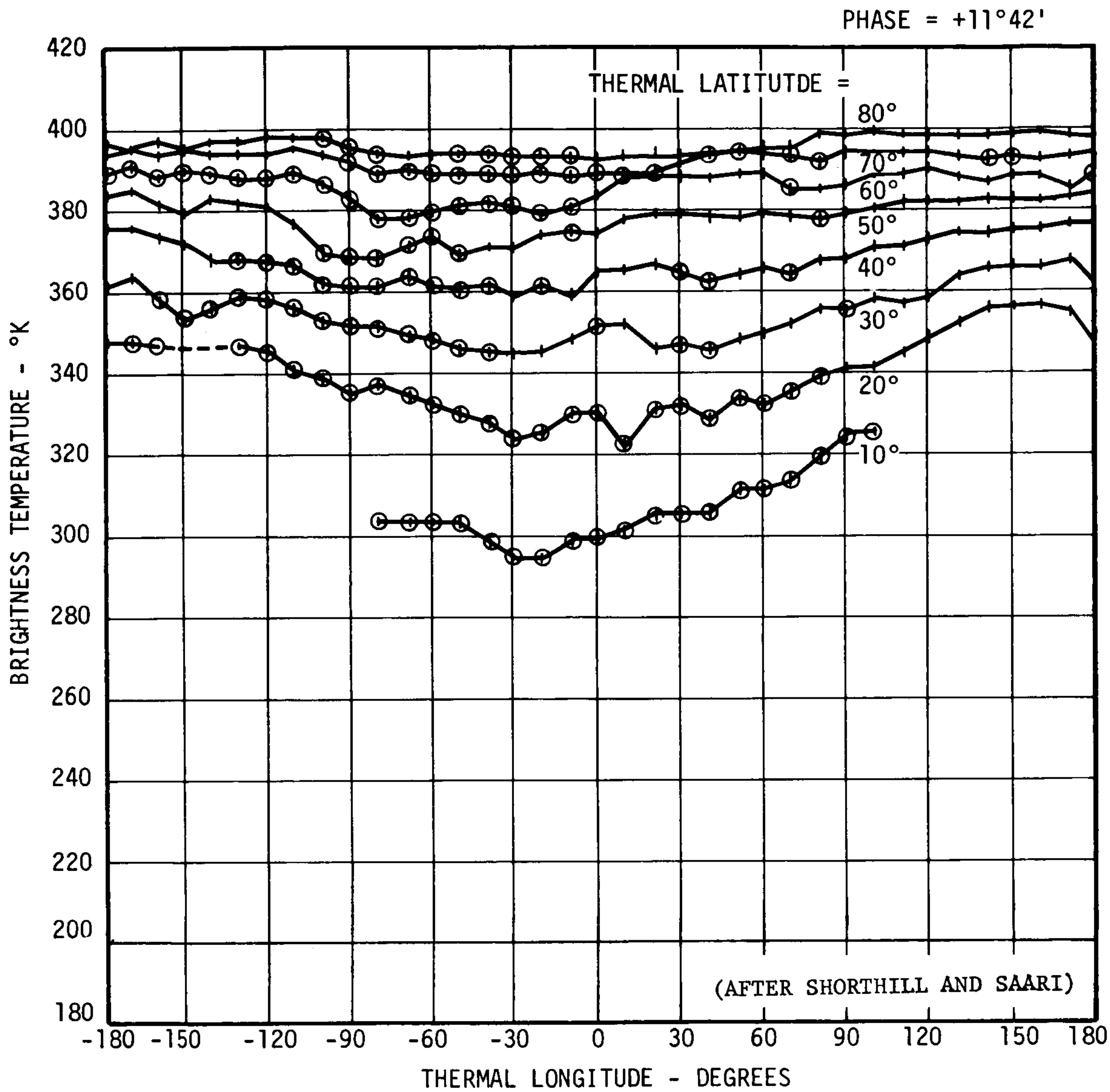

FIGURE 48 - TEMPERATURE FOR + 11° 42' PHASE

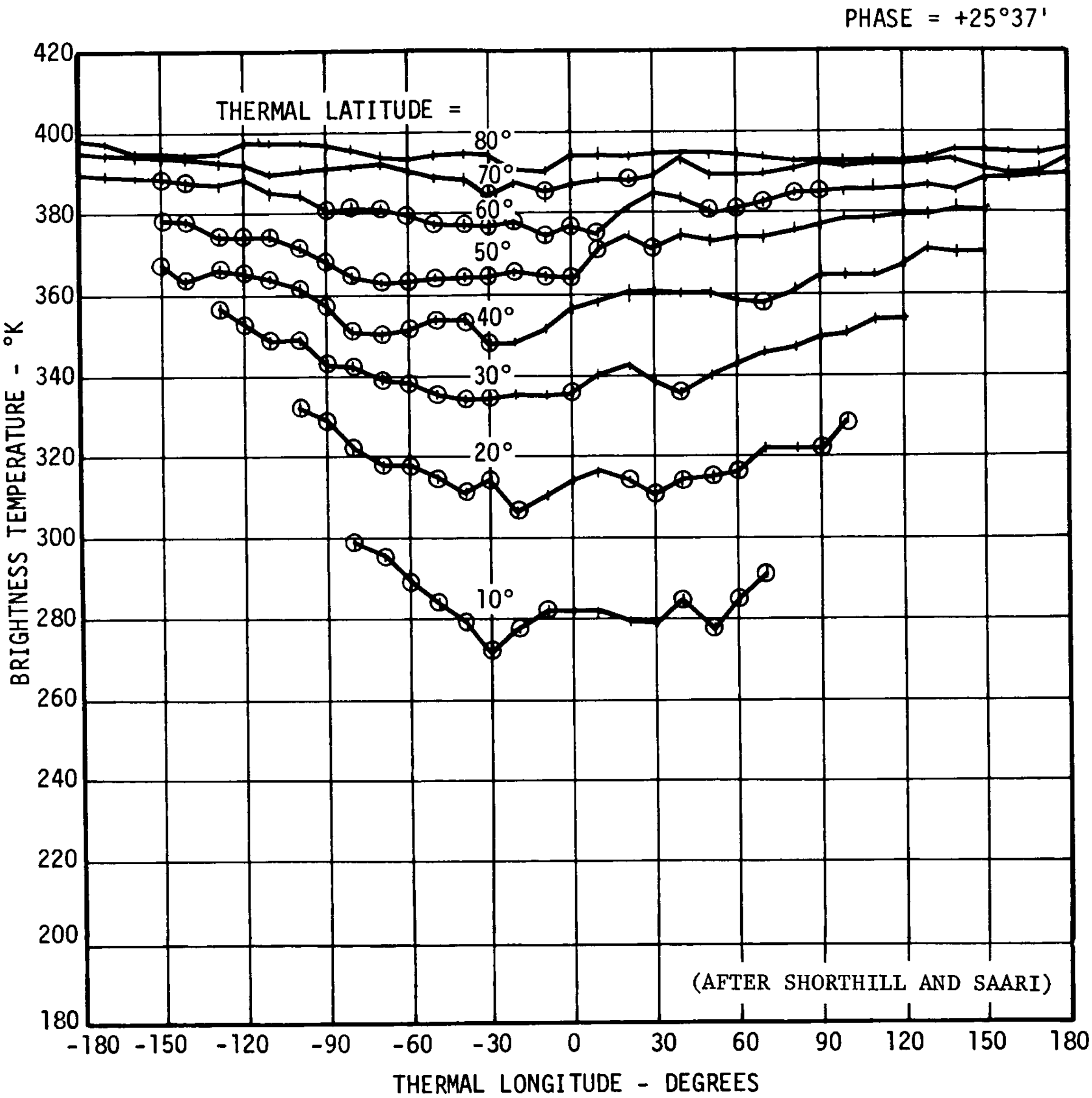

FIGURE 49 - TEMPERATURE FOR + 25° 37' PHASE

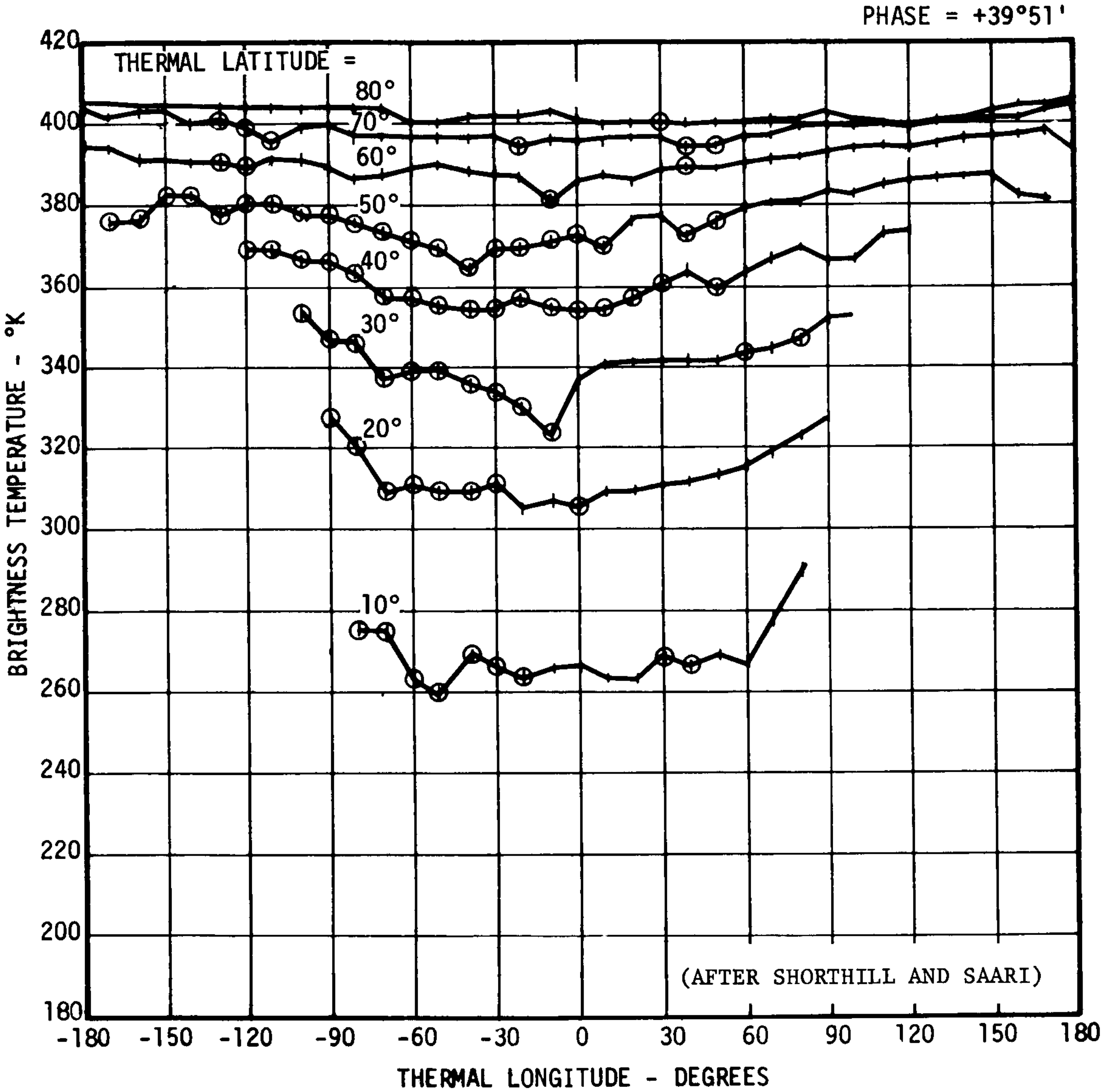

FIGURE 50 - TEMPERATURE FOR + 39° 51' PHASE

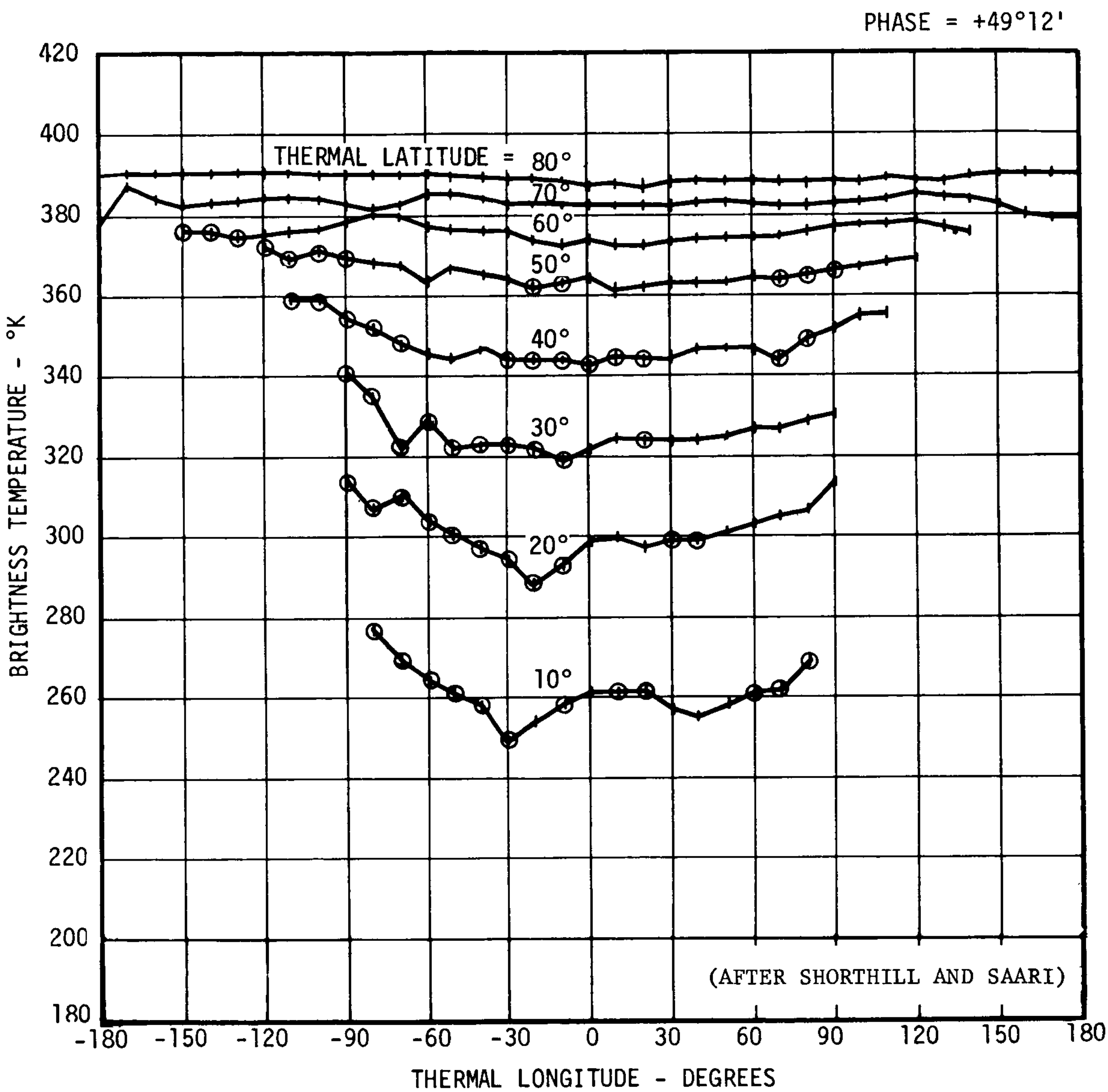

FIGURE 51 - TEMPERATURE FOR + 49° 12' PHASE

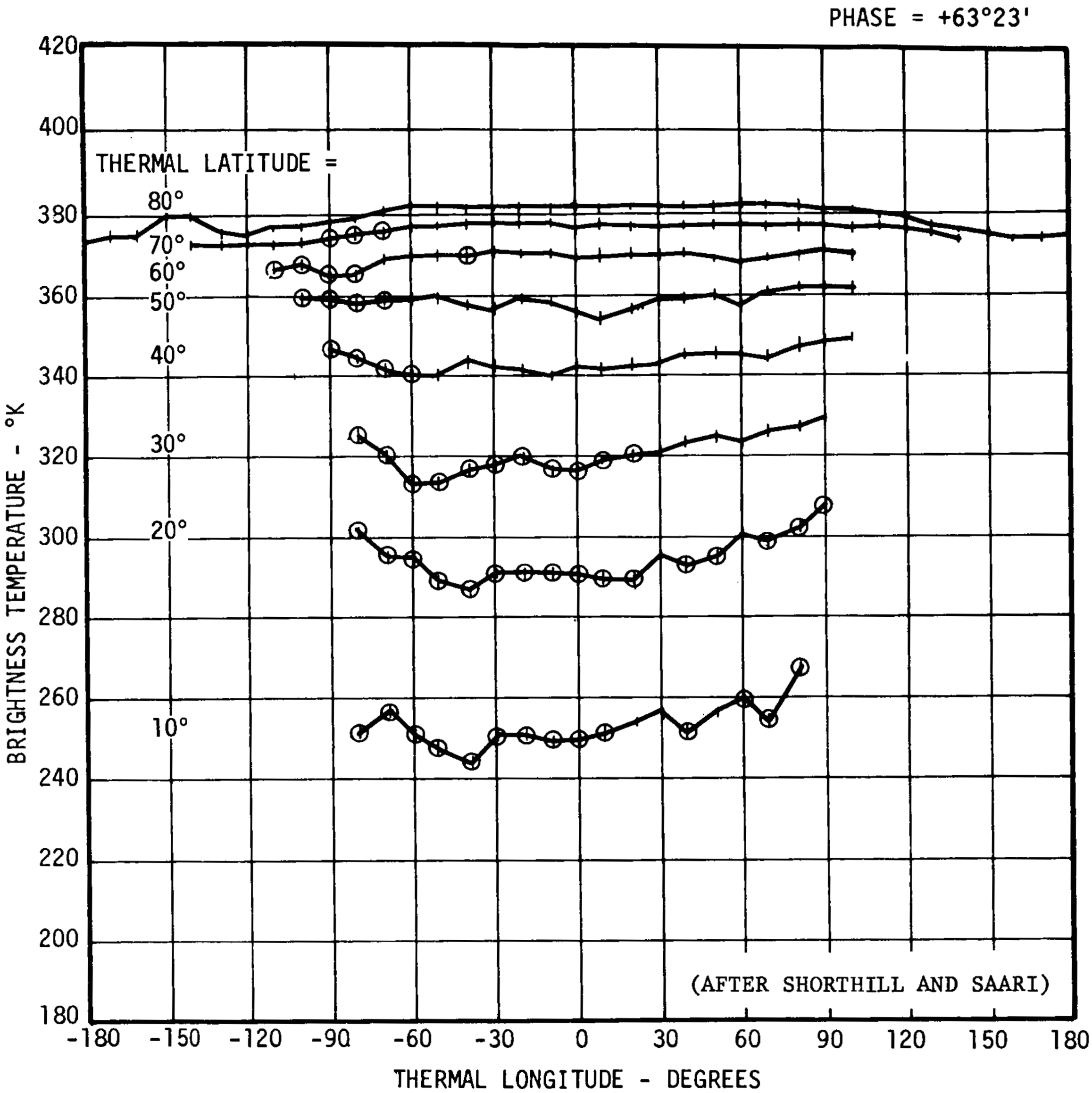

FIGURE 52 - TEMPERATURE FOR + 63° 23' PHASE

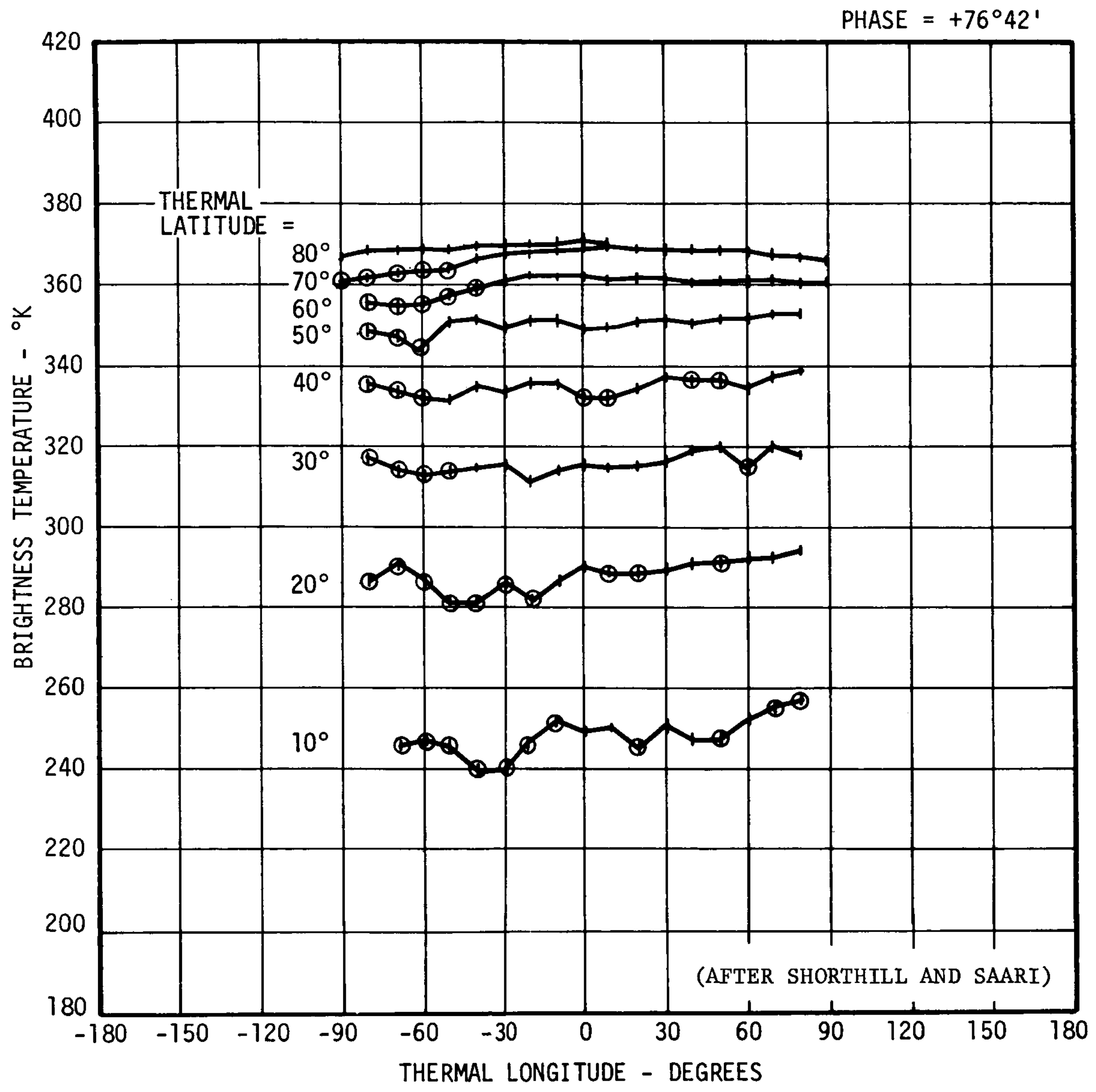

FIGURE 53 - TEMPERATURE FOR + 76° 42' PHASE

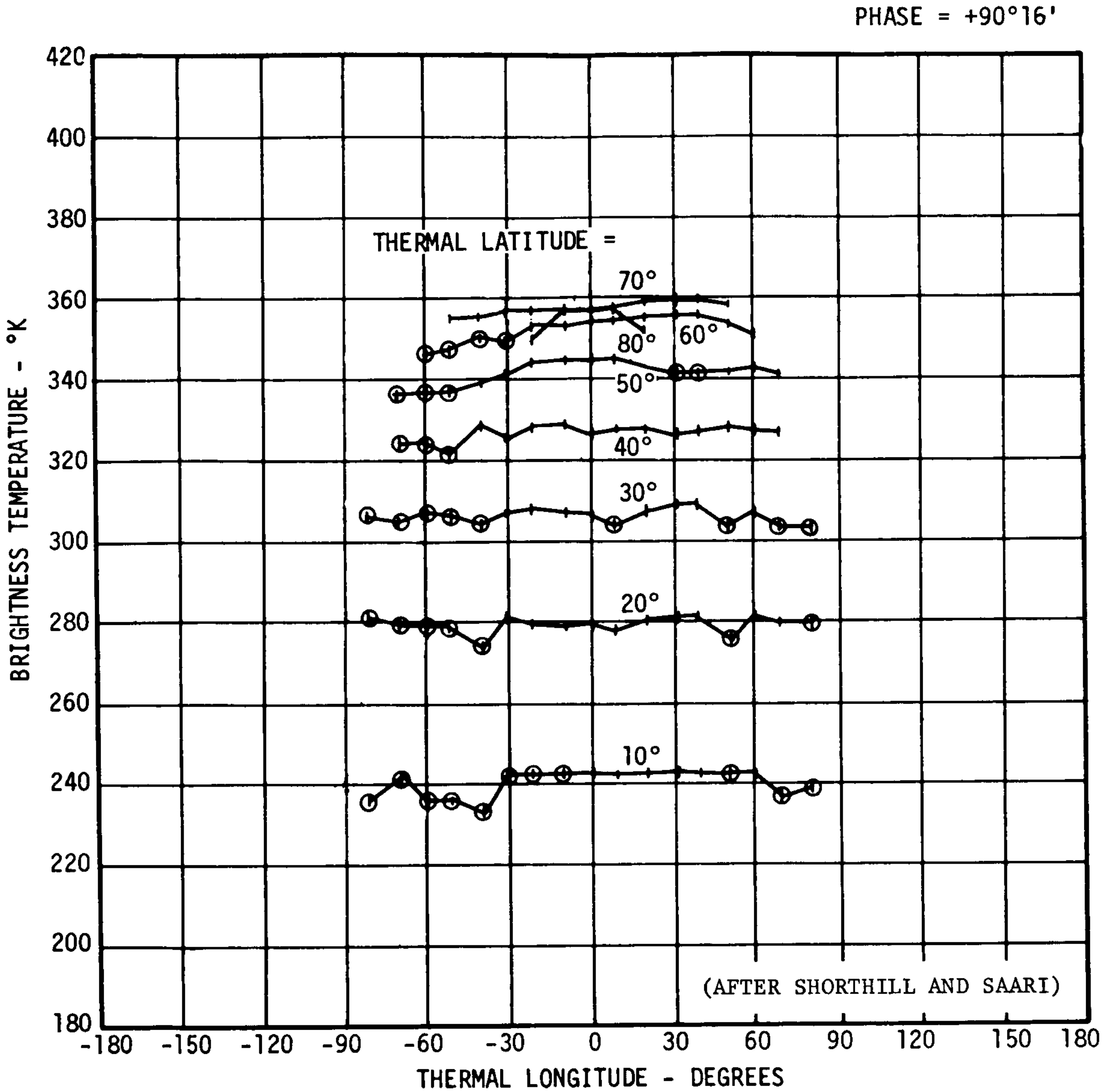

FIGURE 54 - TEMPERATURE FOR + 90° 16' PHASE

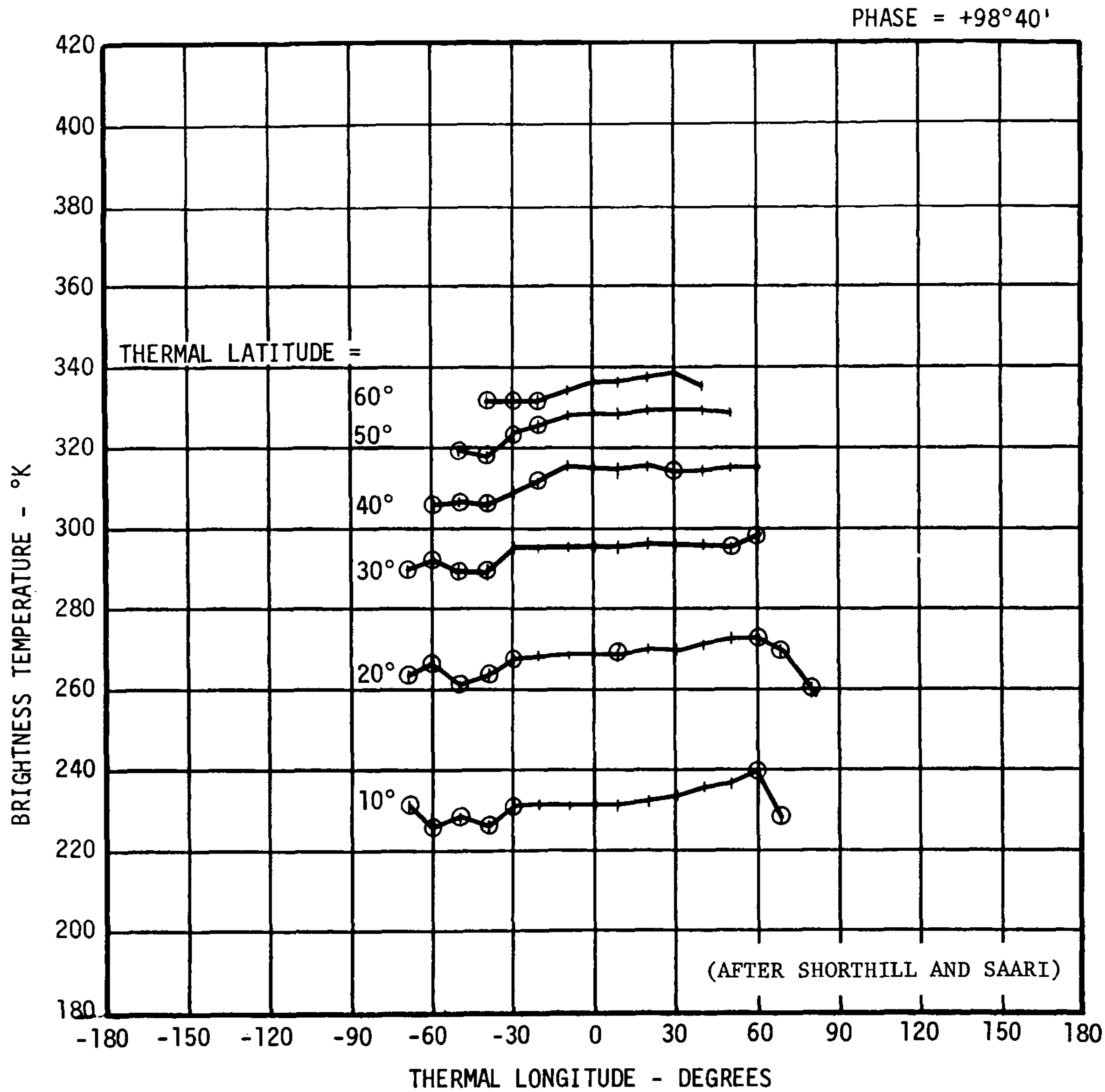

FIGURE 55 - TEMPERATURE FOR + 98° 40' PHASE

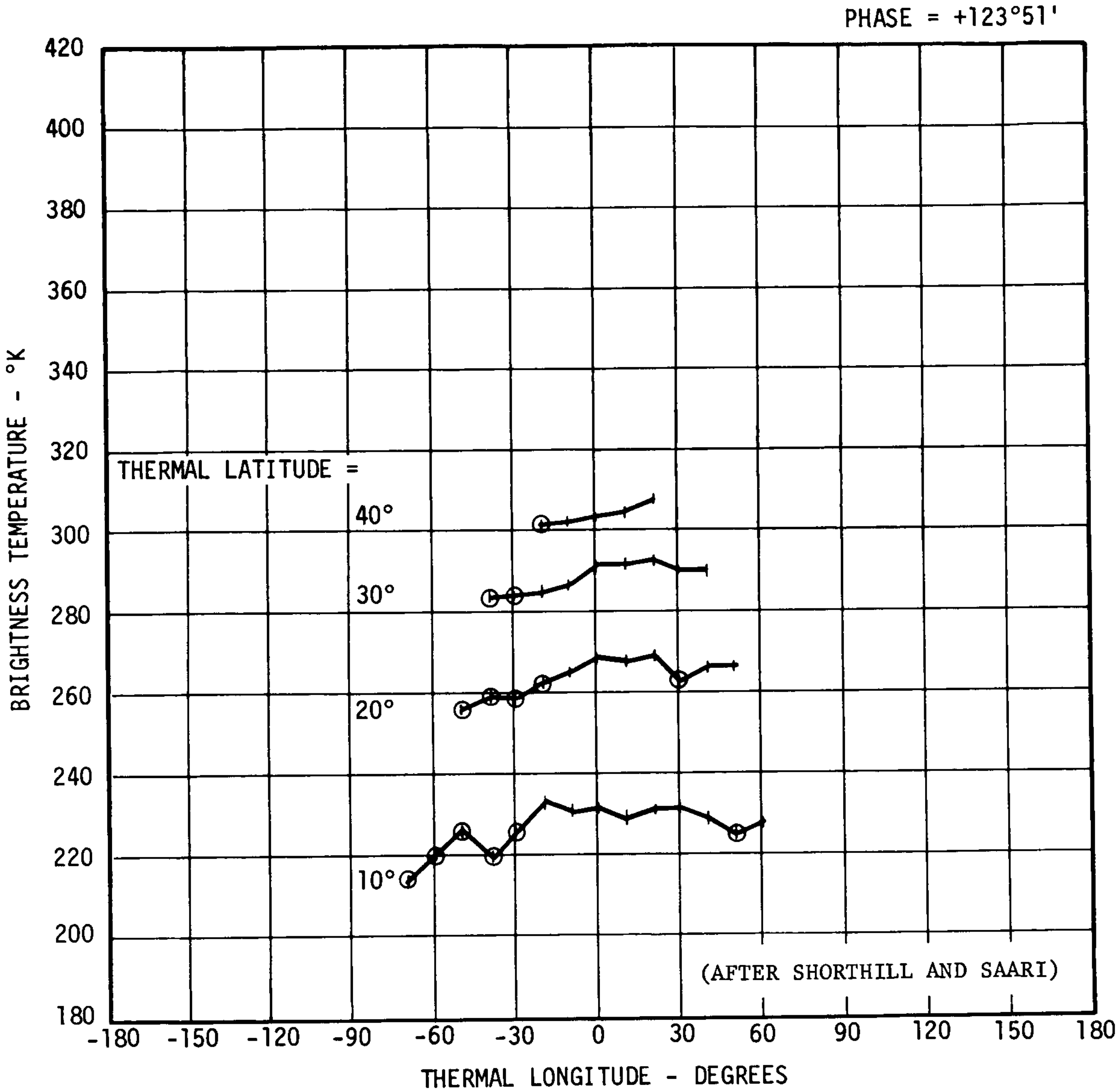

FIGURE 56 - TEMPERATURE FOR + 123° 51' PHASE

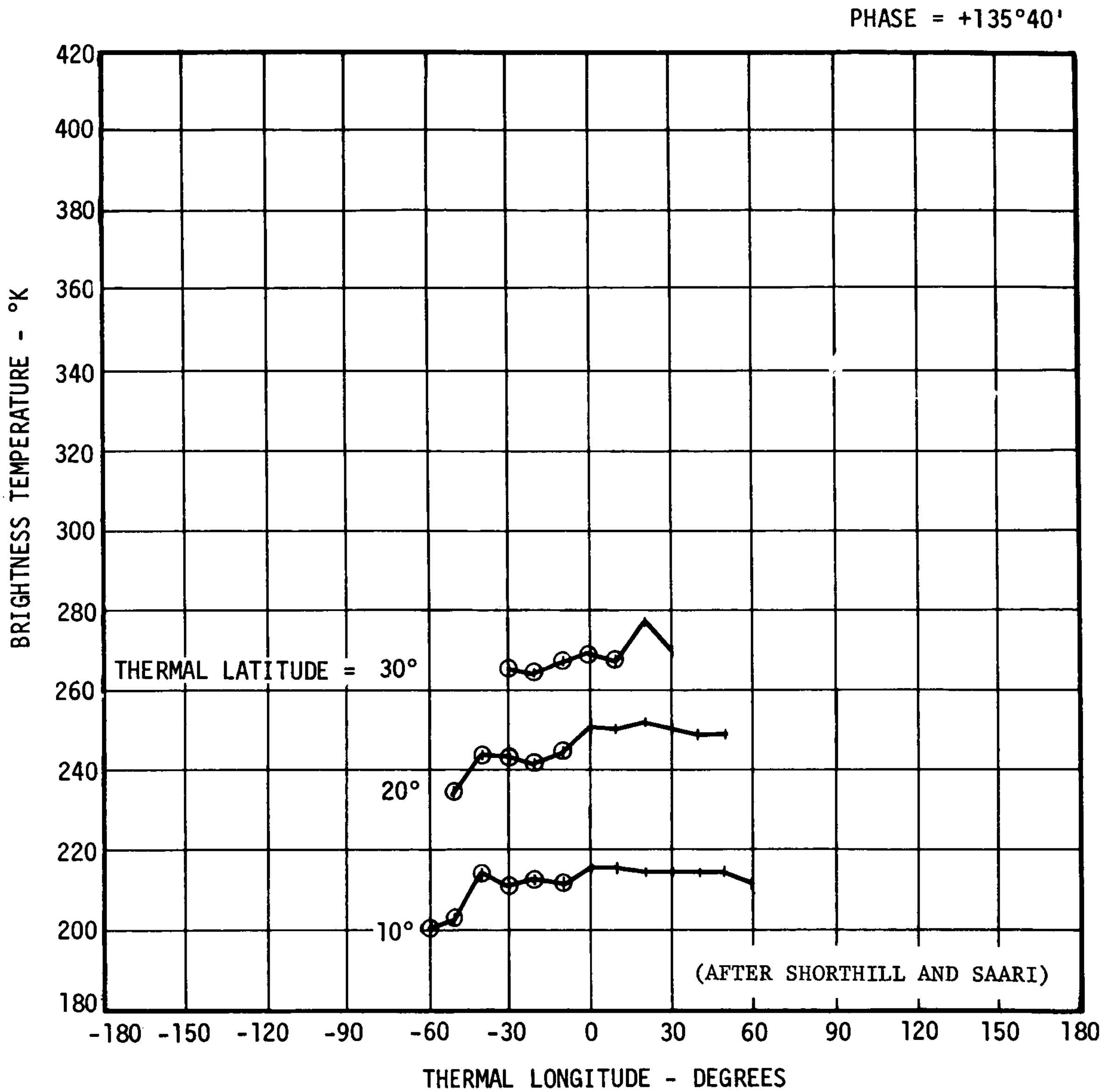

FIGURE 57 - TEMPERATURE FOR + 135° 40' PHASE

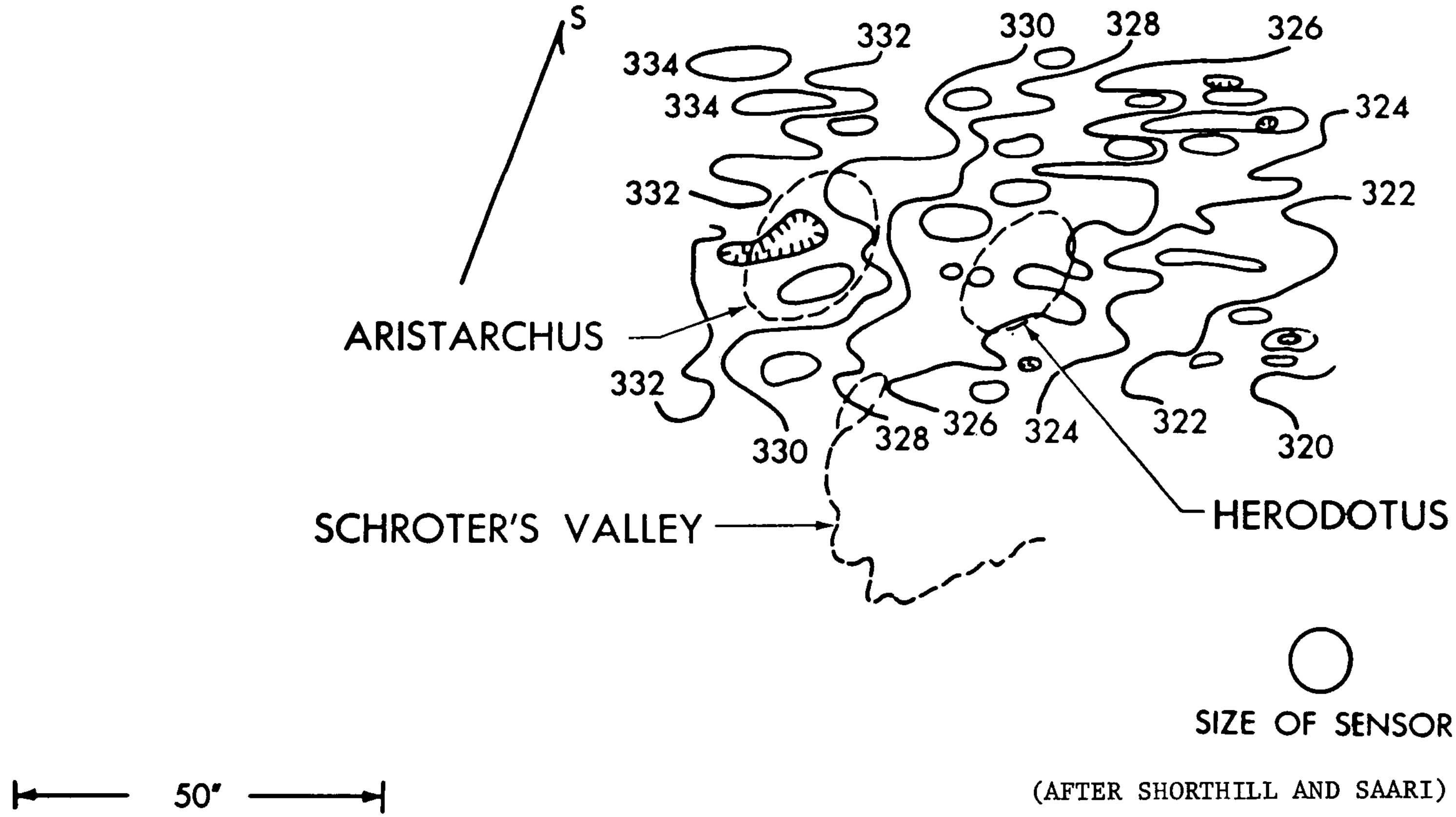

FIGURE 58 - ISOTHERMS IN THE REGION OF ARISTARCHUS SEPTEMBER 4, 1960, 10:30 UT

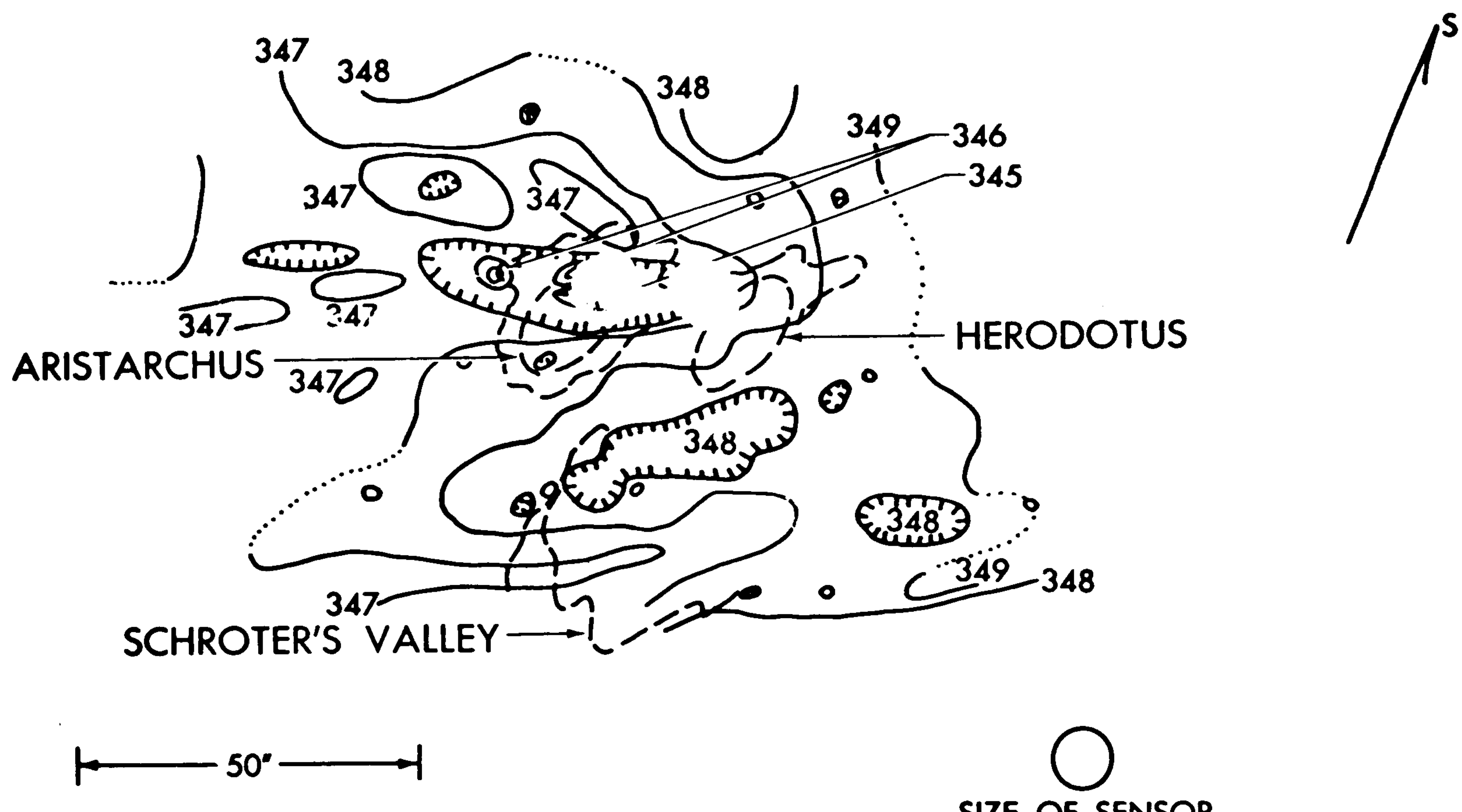

(AFTER SHORTHILL AND SAARI)

FIGURE 59 - ISOTHERMS IN THE REGION OF ARISTARCHUS RECTIFIED TO REMOVE THE EFFECT OF THE CURVATURE OF THE SURFACE, SEPTEMBER 5, 1960, 6:57 UT

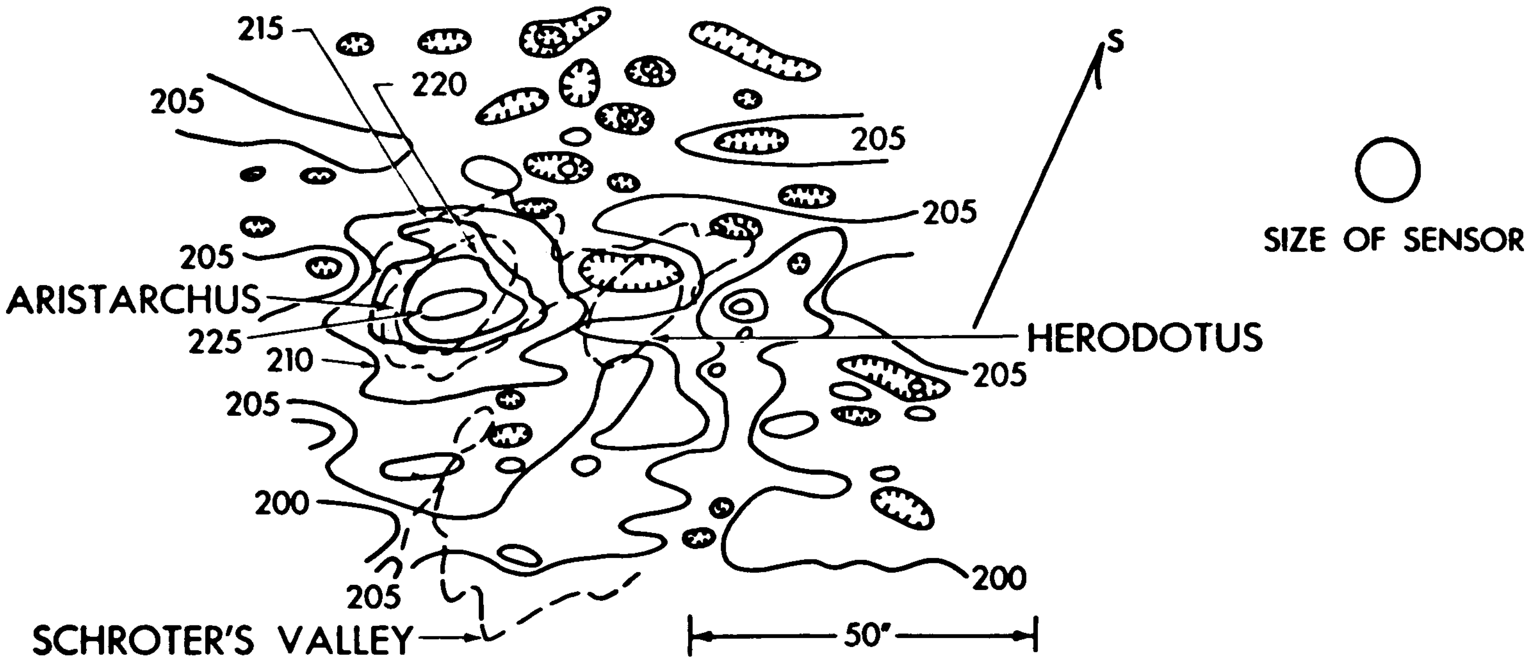

(AFTER SHORTHILL AND SAARI)

FIGURE 60 - ISOTHERMS IN THE REGION OF ARISTARCHUS DURING ECLIPSE, SEPTEMBER 5, 1960, 10:12 UT

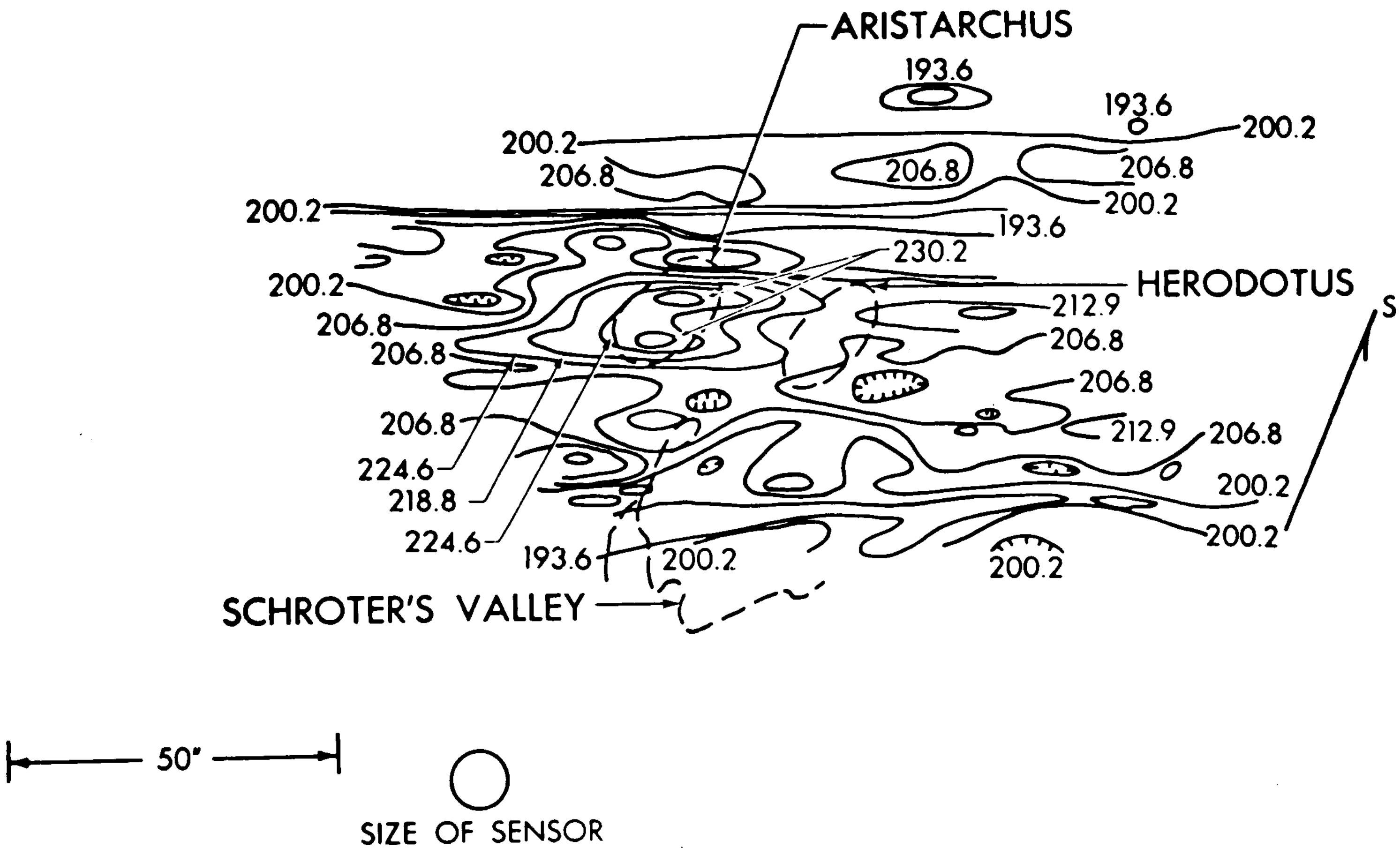

(AFTER SHORTHILL AND SAARI)

FIGURE 61 - ISOTHERMS IN THE REGION OF ARISTARCHUS DURING ECLIPSE, SEPTEMBER 5, 1960, 11:04 UT

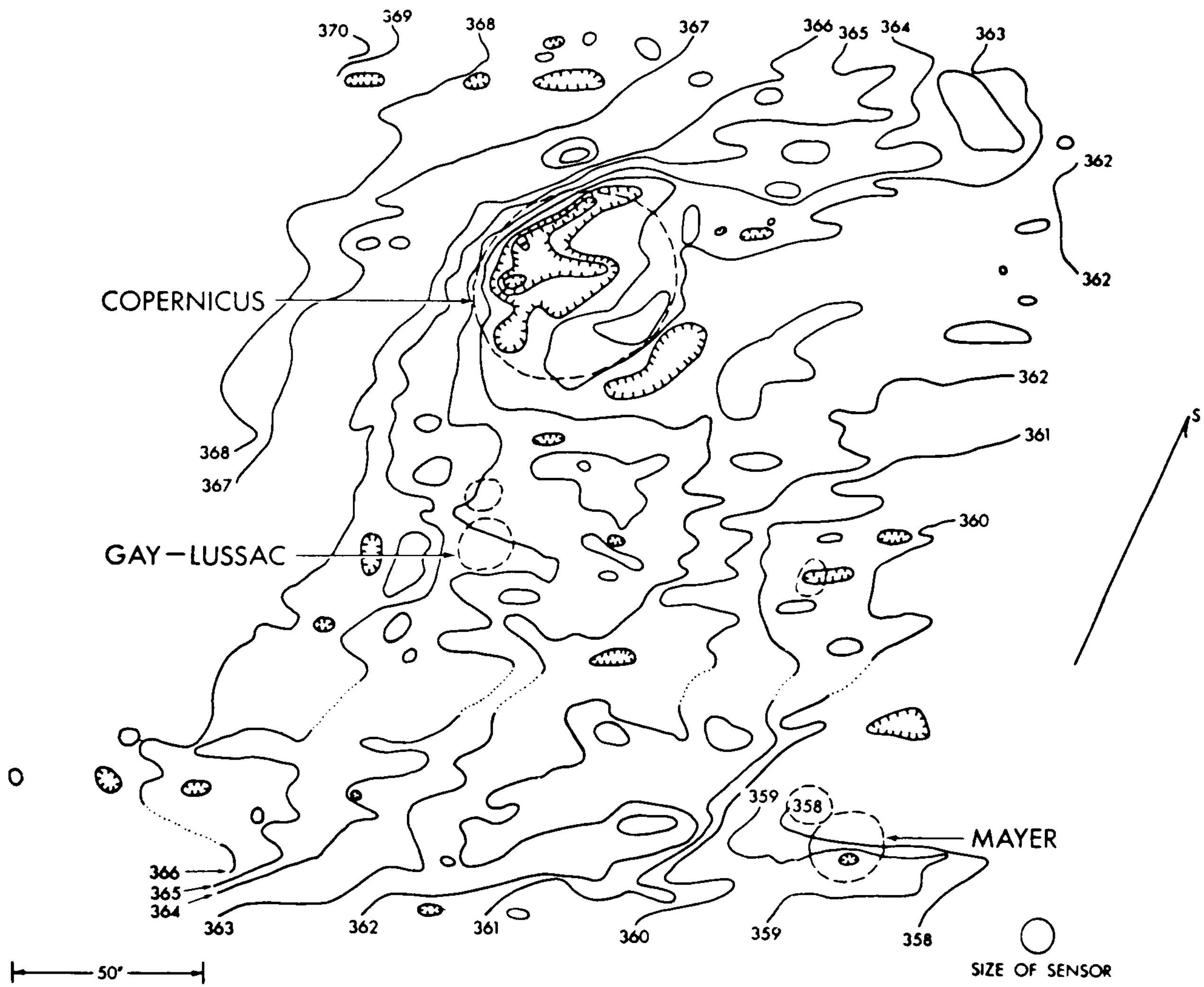

(AFTER SHORTHILL AND SAARI)

FIGURE 62 - ISOTHERMS IN THE REGION OF COPERNICUS SEPTEMBER 5, 1960, 5:48 UT

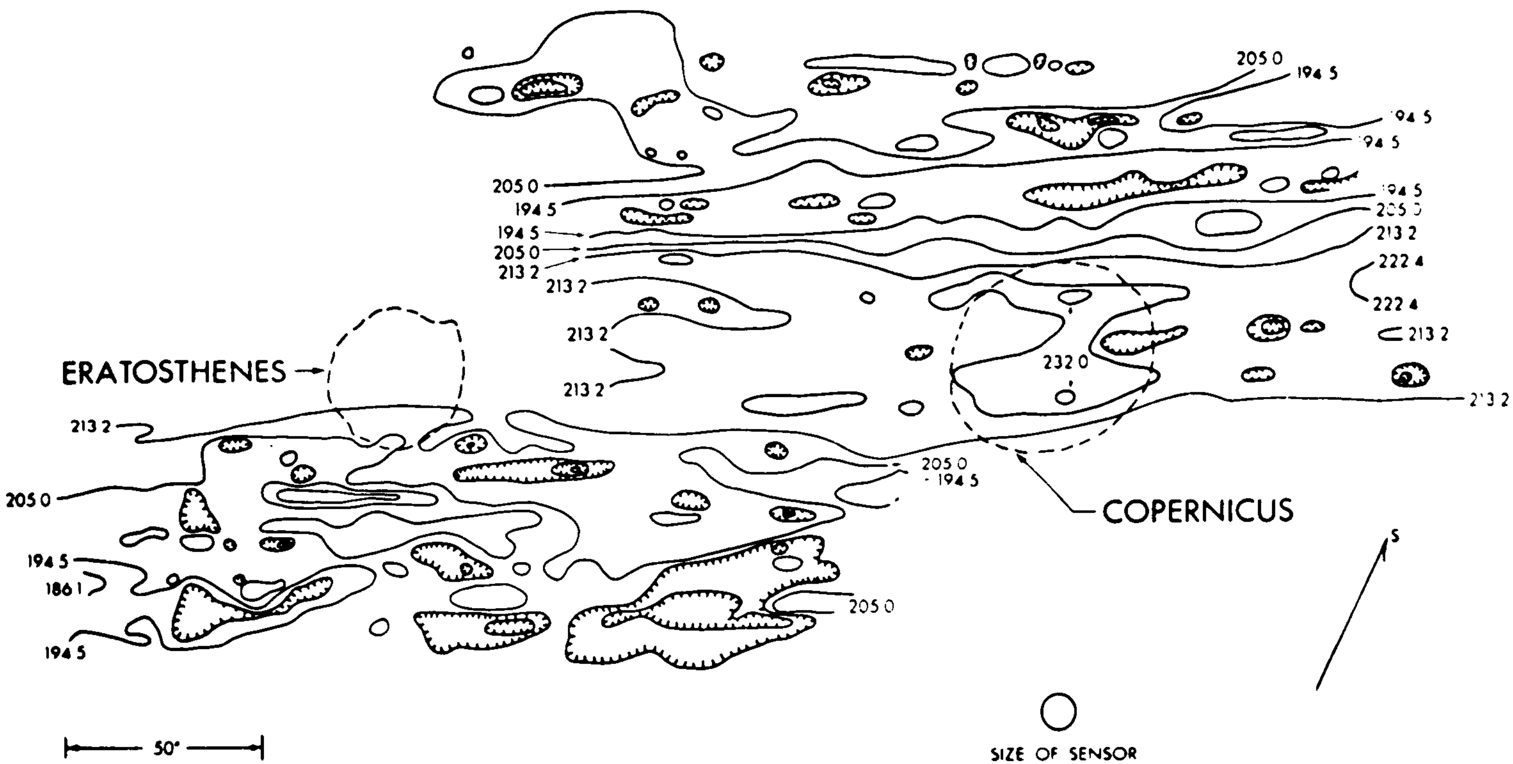

(AFTER SHORTHILL AND SAARI)

FIGURE 63 - ISOTHERMS IN THE REGION OF COPERNICUS DURING ECLIPSE SEPTEMBER 5, 1960, 11:30 UT

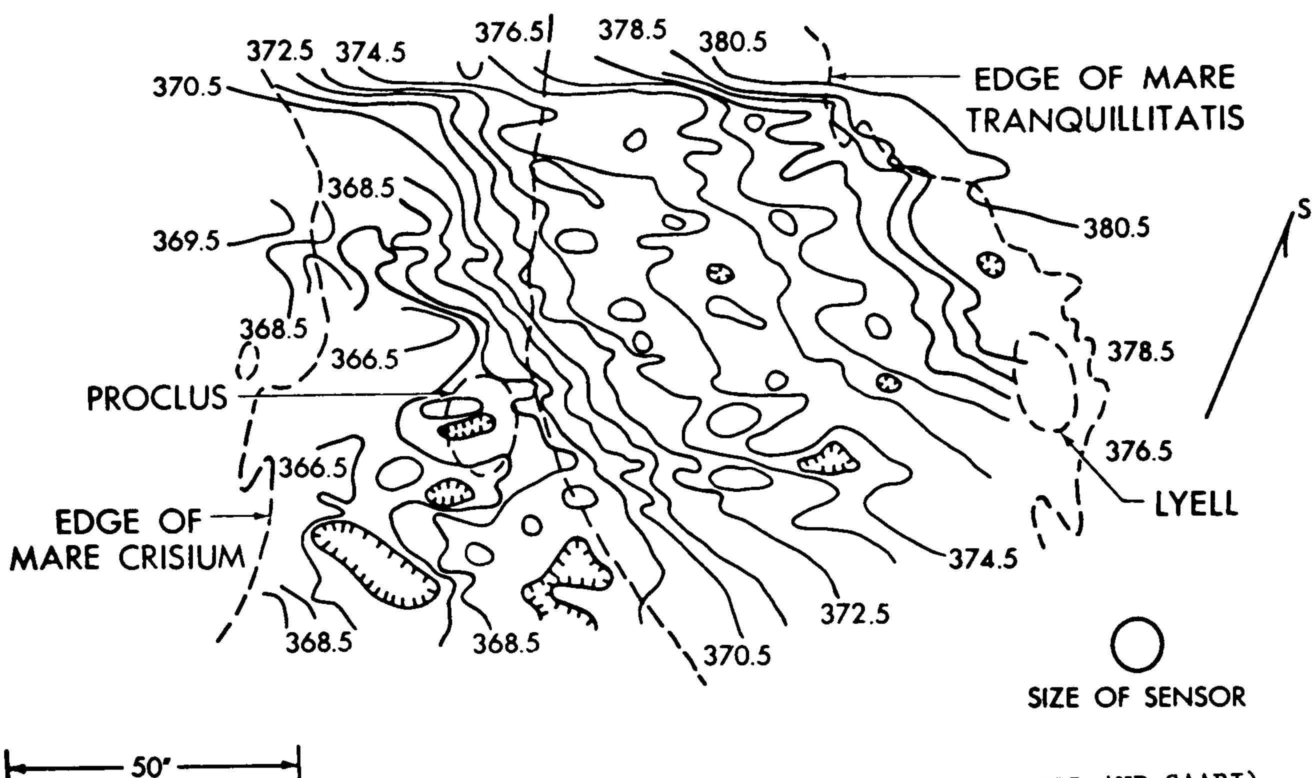

(AFTER SHORTHILL AND SAARI)

FIGURE 64 - ISOTHERMS IN THE REGION OF PROCLUS SEPTEMBER 5, 1960, 7:20 UT

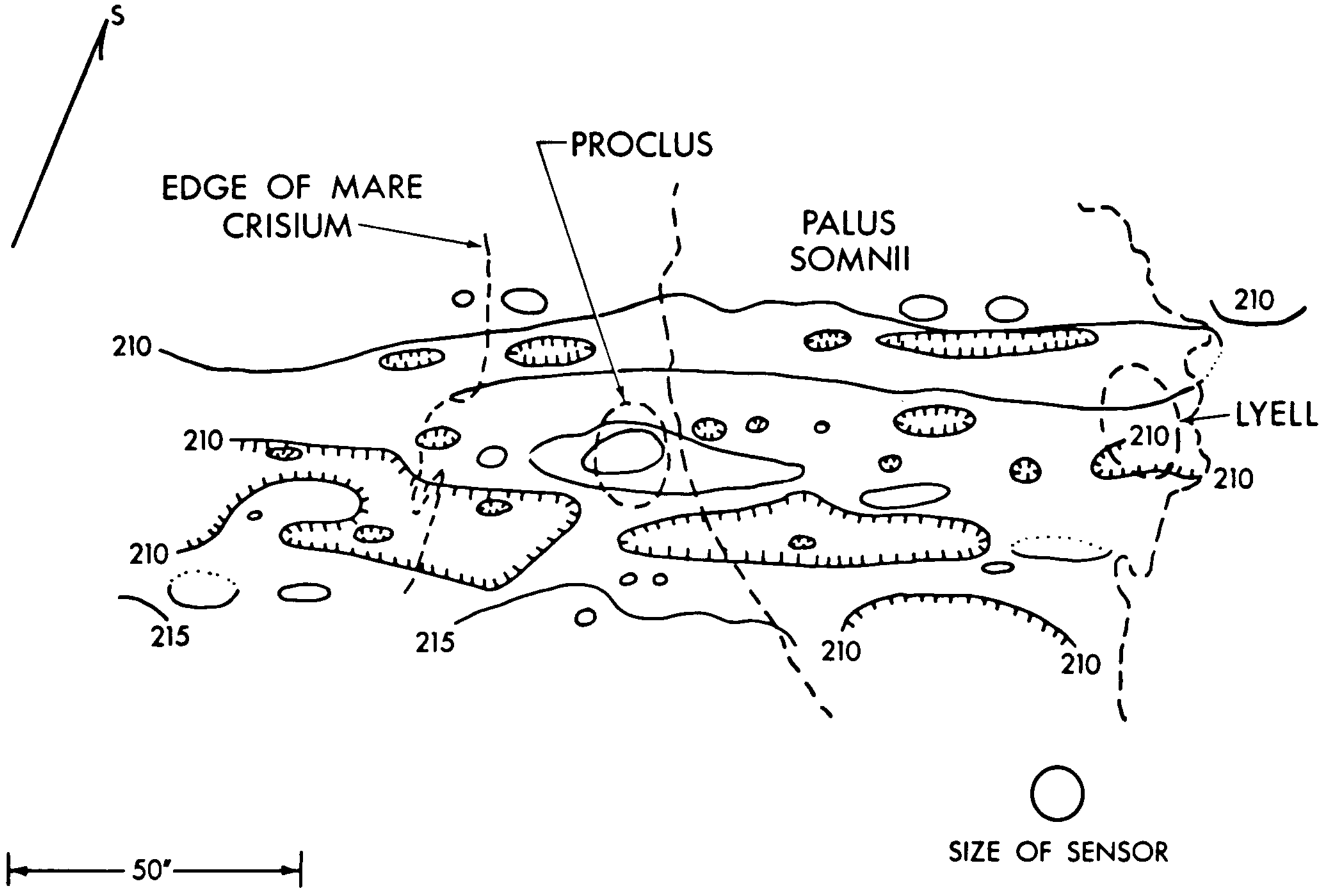

(AFTER SHORTHILL AND SAARI)

FIGURE 65 - ISOTHERMS IN THE REGION OF PROCLUS DURING ECLIPSE, SEPTEMBER 5, 1960, 11:56 UT

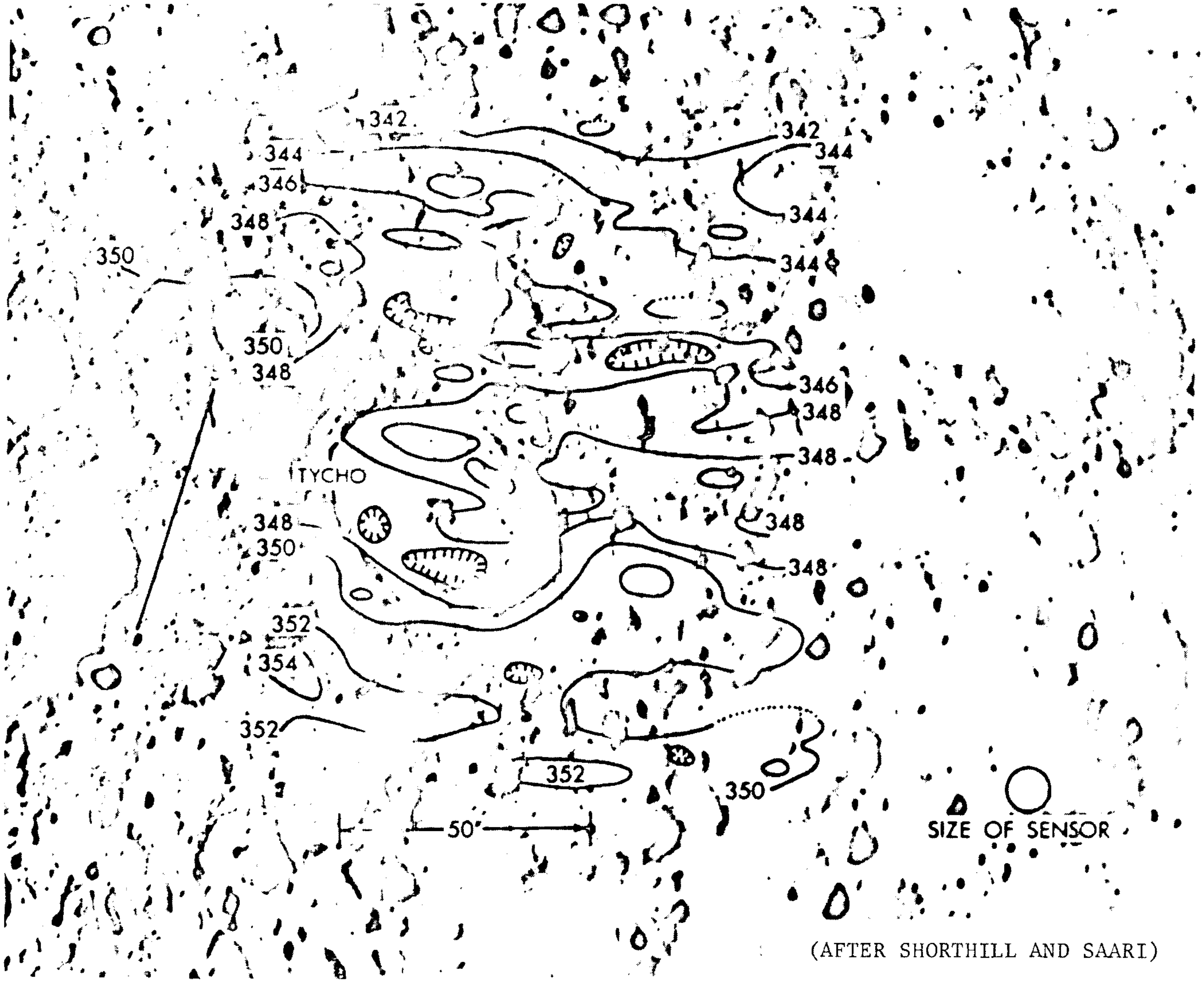

(AFTER SHORTHILL AND SAARI)

FIGURE 66 - ISOTHERMS IN THE REGION OF TYCHO SEPTEMBER 6, 1960, 5:50 UT

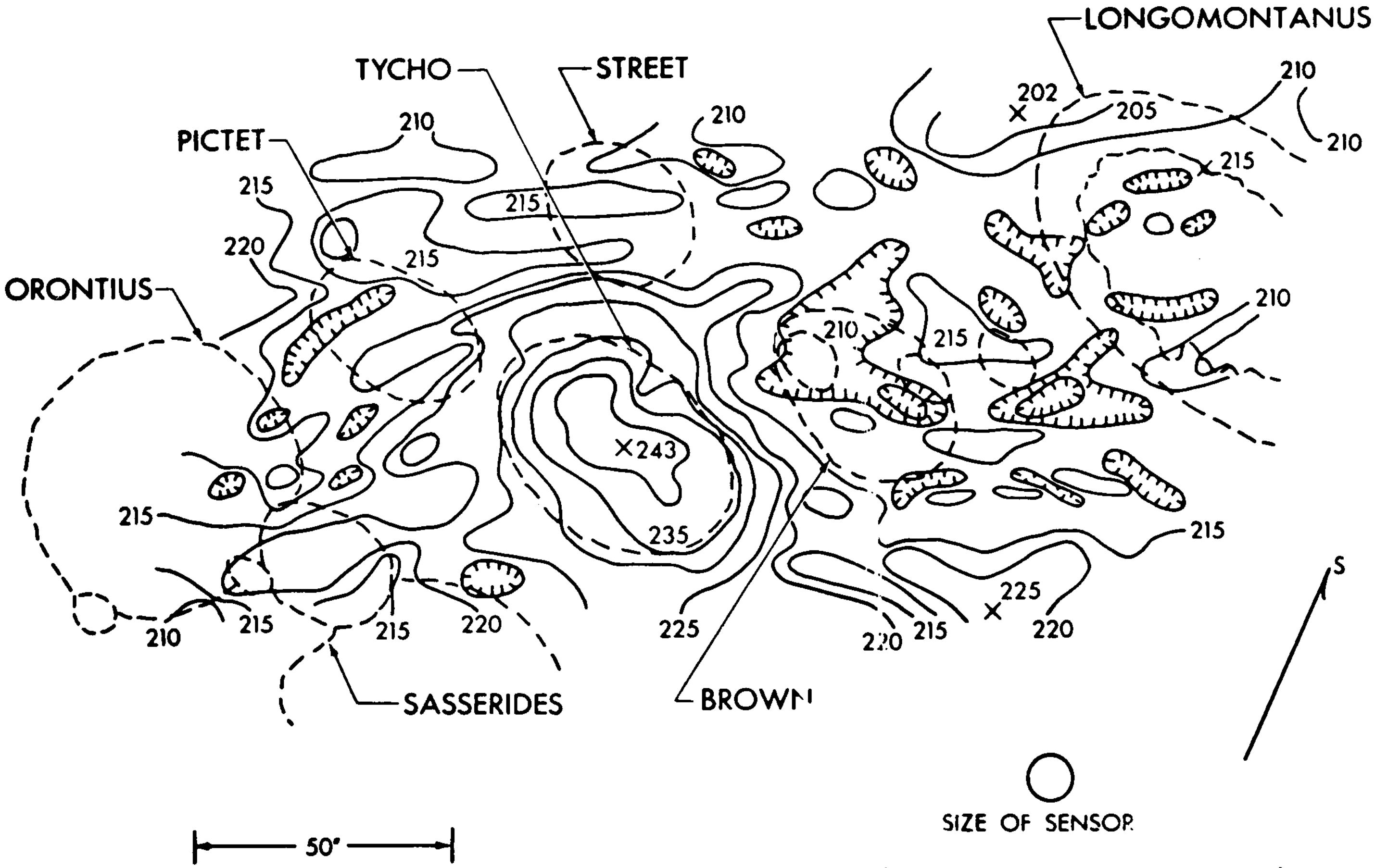

(AFTER SHORTHILL AND SAARI)

FIGURE 67 - ISOTHERMS IN THE REGION OF TYCHO DURING ECLIPSE, SEPTEMBER 5, 1960, 10:34 UT

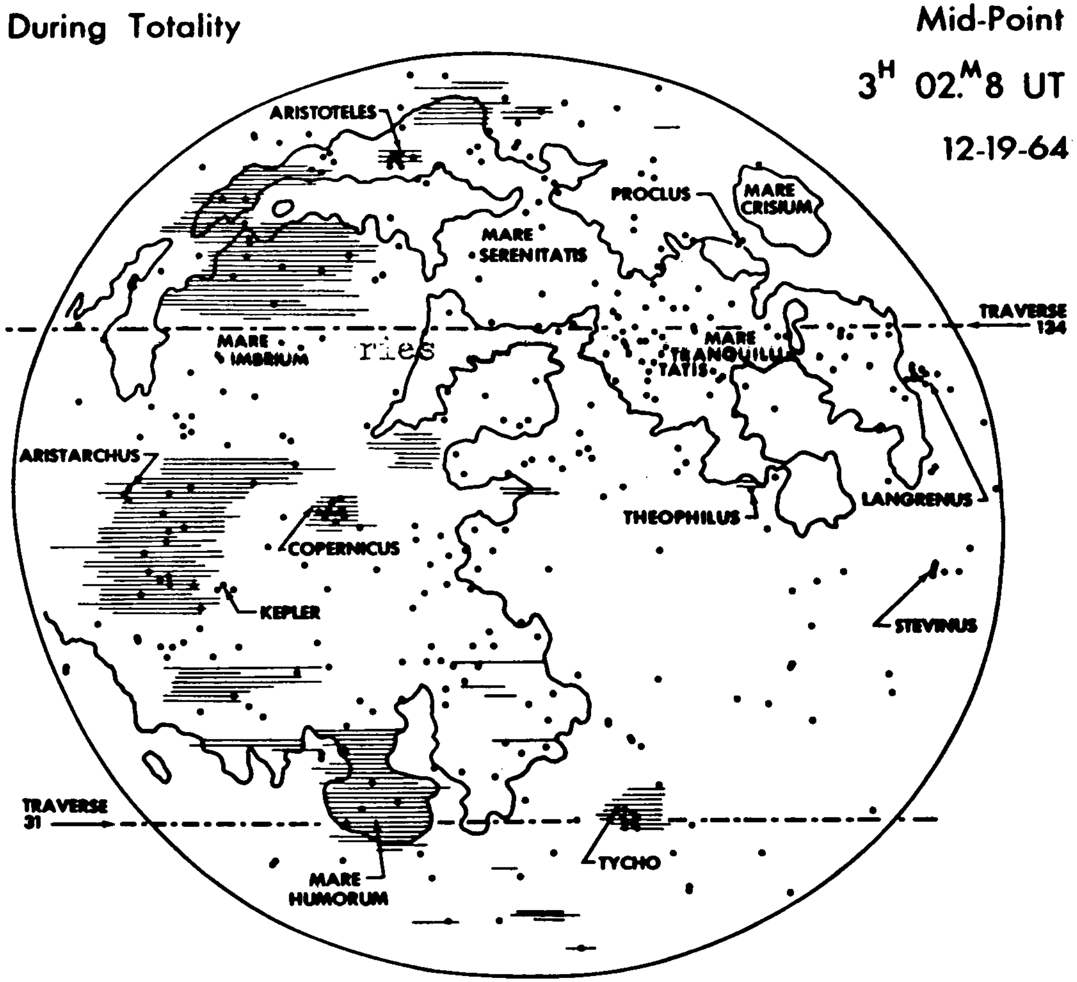

(AFTER SHORTHILL AND SAARI)

FIGURE 68 - HOT SPOT LOCATION INDICATED BY DOTS. SOME OF THE EXTENDED AREAS OF ENHANCEMENTS ARE INDICATED AS LINES ALONG THE SCAN DIRECTION.

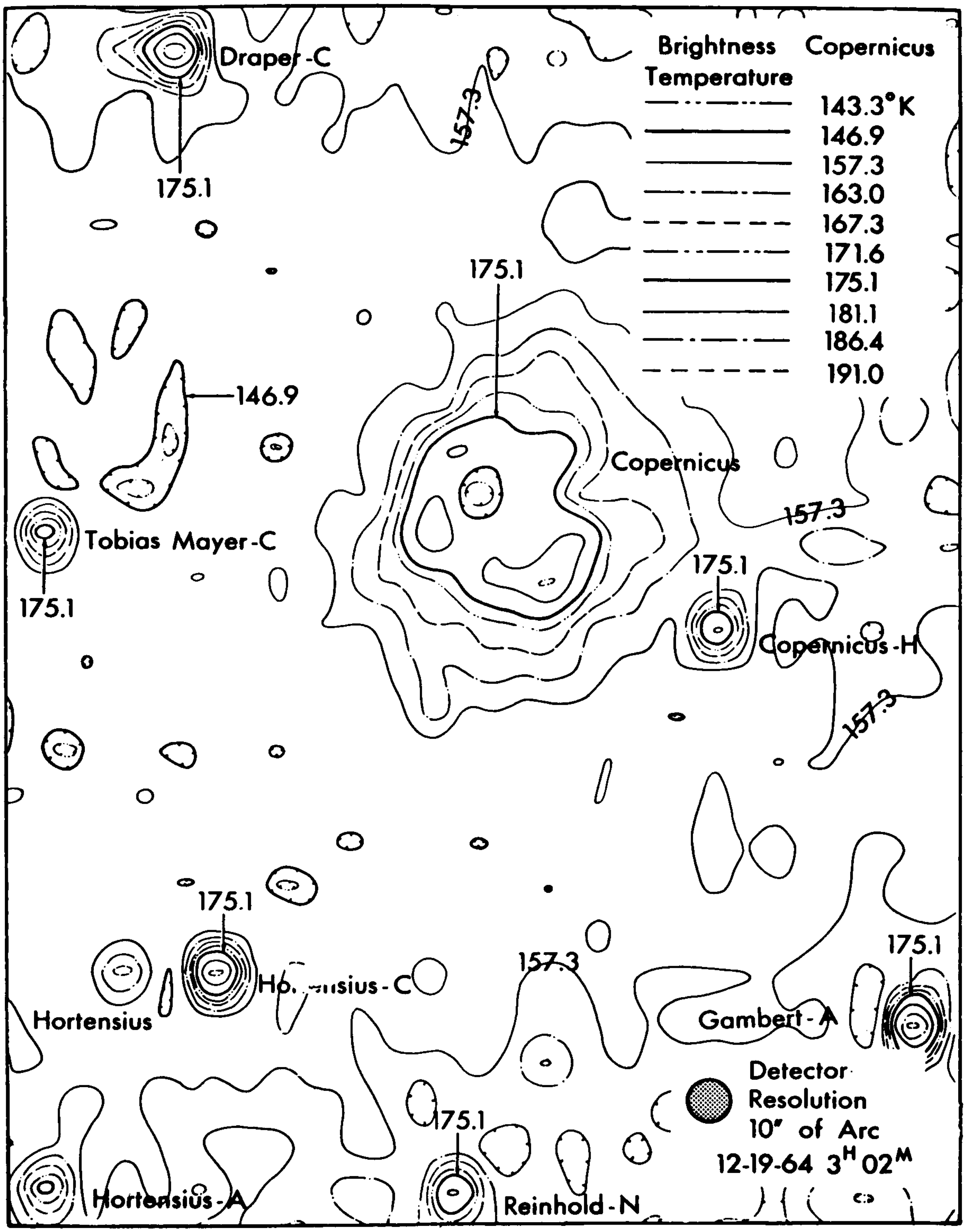

(AFTER SHORTHILL AND SAARI)

FIGURE 69 - CONTOURS OF BRIGHTNESS TEMPERATURE OVER THE REGION OF COPERNICUS DURING TOTALITY.

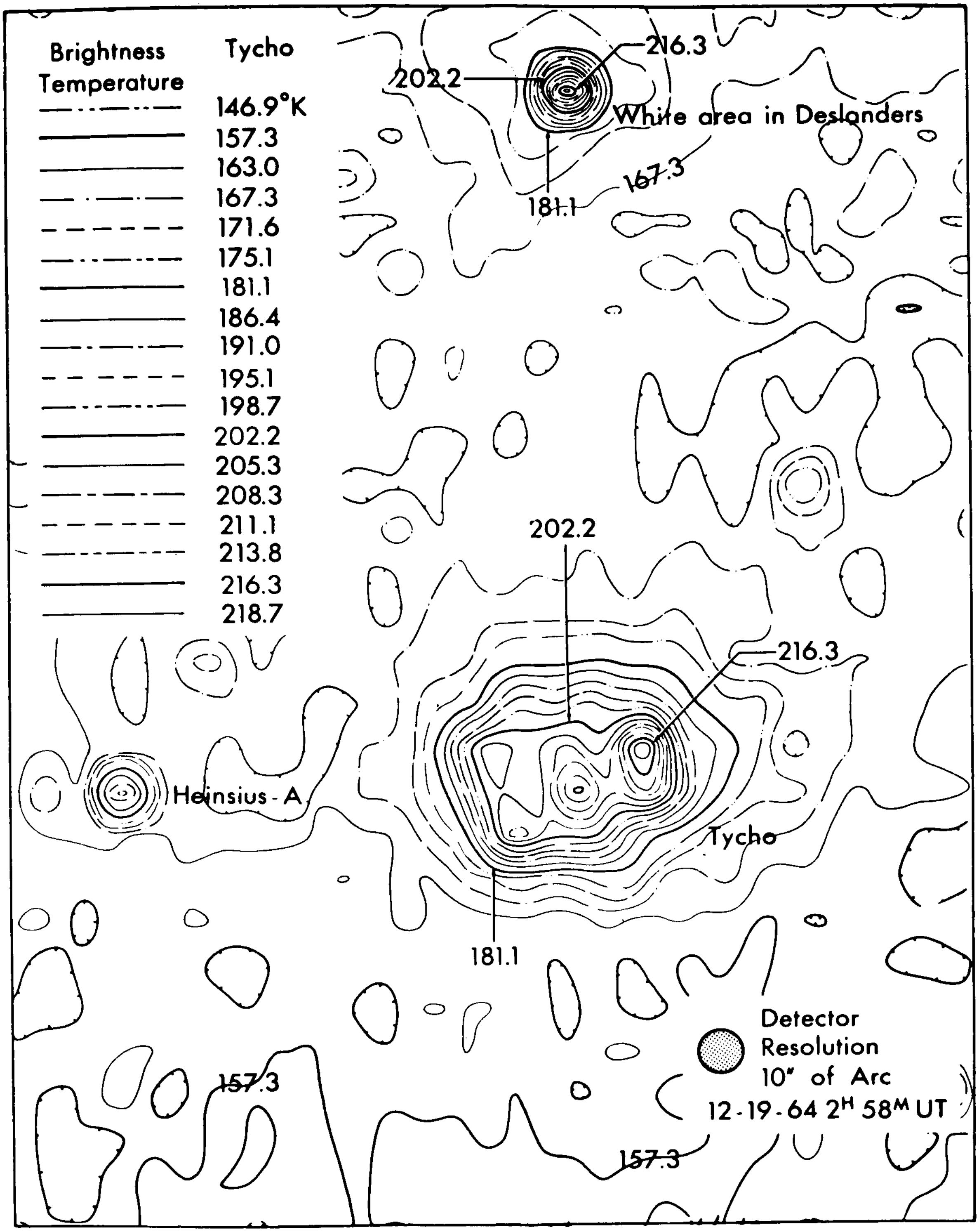

(AFTER SHORTHILL AND SAARI)

FIGURE 70 - CONTOURS OF BRIGHTNESS TEMPERATURE OVER THE REGION OF TYCHO DURING TOTALITY.

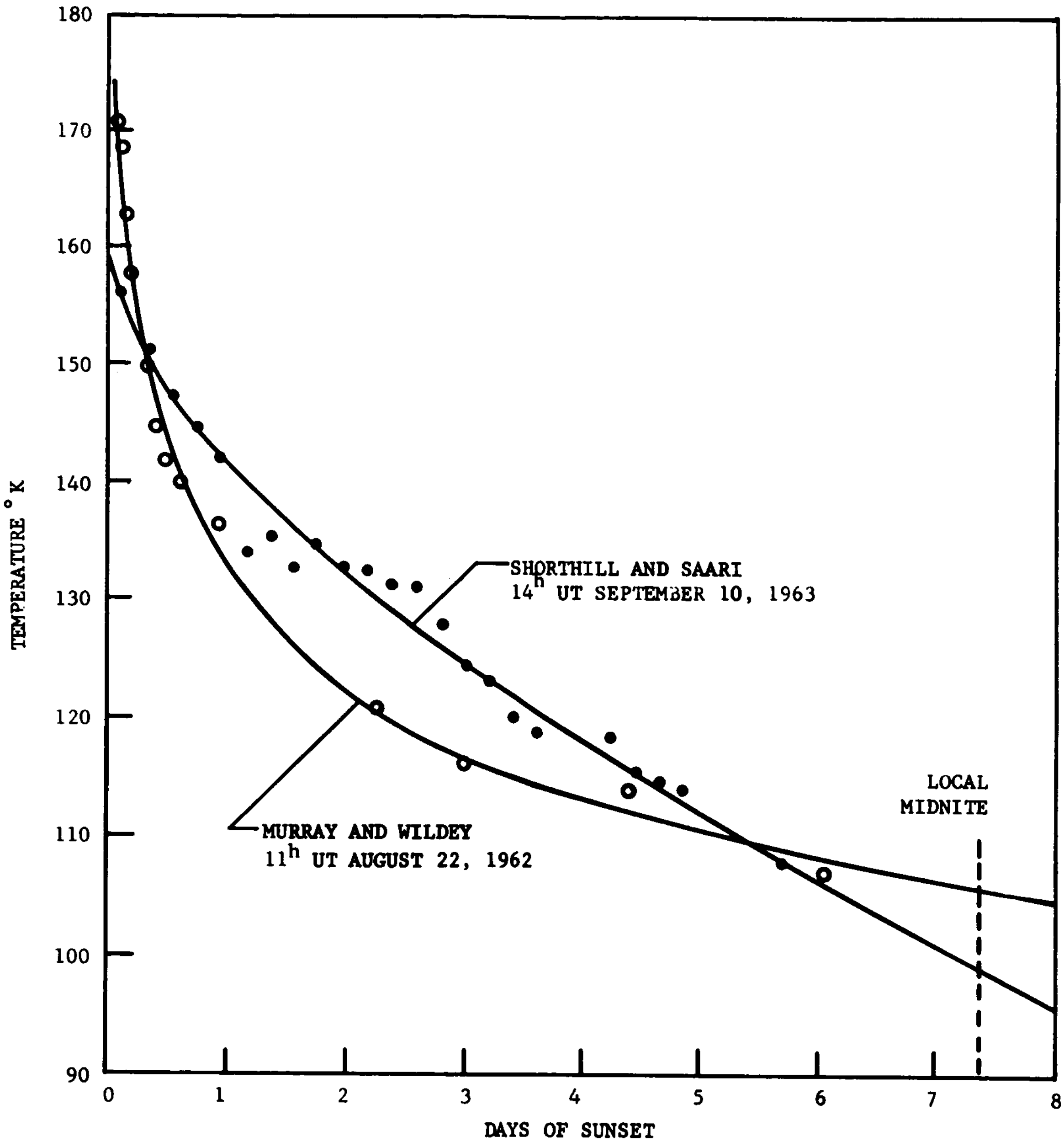

FIGURE 71 - ANTISOLAR POINT TEMPERATURE.

NASA TM X-53499 APPROVAL August 26, 1966

LUNAR THERMAL ENVIRONMENT

By James K. Harrison, Daniel W. Gates,
James R. Watkins, and Billy P. Jones

The information in this report has been reviewed for security classification. Review of any information concerning Department of Defense or Atomic Energy Commission programs has been made by the MSFC Security Classification Officer. This report, in its entirety, has been determined to be unclassified.

This report has also been reviewed and approved for technical accuracy.

Ernst Stuhlinger

ERNST STUHLINGER
Director, Research Projects Laboratory

DISTRIBUTION

INTERNAL

DEP-T

E-DIR

R-DIR

R-AS

F. L. Williams
J. Madewell

R-AERO-DIR

R-AERO-Y

W. W. Vaughan
R. Smith
O. Vaughn

R-ASTR-DIR

R-ASTR-A

J. L. Mack
F. E. Digesu

R-ASTR-N

F. B. Moore

R-ASTR-G

C. H. Mandel

R-ASTR-I

O. A. Hoberg
C. T. Paludan

R-ASTR-P

H. J. Fichtner
W. Angele

R-ASTR-R

J. C. Taylor

R-ASTR-M

J. Boehm

R-COMP-DIR

R-ME-DIR

R-ME-DIR

R-P&VE-DIR

R-P&VE-A

E. E. Goerner

R-P&VE-M

J. E. Kingsbury

R-P&VE-S

G. A. Kroll

R-P&VE-P

H. G. Paul

R-P&VE-PE

R. R. Head

DISTRIBUTION (continued)

R-P&VE-PT

C. C. Wood

R-P&VE-VA

J. C. Glover

R-P&VE-VS

W. A. Schulze

R-QUAL-DIR

R-TEST-DIR

B. R. Tessmann

R-RP-DIR

G. C. Bucher

R-RP-P

J. Dozier
R. Hembree

R-RP-N

R.D. Shelton
D. P. Hale
Patsy Lawrence
H. Stern

R-RP-S

J. Downey
H. Gierow
W. Duncan
D. Ruth
O.K. Hudson
N. Costes
C. Swanson
R. Jones

R-RP-T

G. B. Heller
K. Schocken
D. Gates (5)
J. Harrison (5)
B. Jones (5)
J. Watkins (5)
G. Arnett
H. Atkins
T. Bannister
D. Cochran
S. Fields
J. Fountain
R. Vun Kannon
R. Linton
R. Merrill
E. Miller
W. Snoddy
C. Schafer
H. Weathers
R. Lal

R-RP-C

Reserve (30)

I-DIR
Hans Hueter

I-MO-MGR

I-I/IB-MGR

I-SC-MGR

I-V-MGR

DISTRIBUTION (continued)

I-E-MGR

J. Waite

RSIC Documents (3)

MS-IL (8)

Scientific and Technical Information Facility (25)
P. O. Box 33
College Park, Maryland 20740
NASA Rep (S-AK/RKT)

MS-IP
MS-T (6)
CC-P
MS-H

EXTERNAL

Contractors and Universities

Northrop Space Laboratories
Huntsville, Alabama

Bellcomm, Inc.
1100 17th Street, N. W.
Washington, D. C.
Mr. William Elam
Mr. C. A. Pearse

A. D. Little, Inc.
Acorn Park
Cambridge Massachusetts
Dr. Aronson, Dr. P. Glaser
Dr. Simon, Dr. A. Wechsler

P.E.C. Research Associates
1001 Mapleton
Boulder, Colorado
Dr. Neil Ashby
Dr. Burkhard

DISTRIBUTION (continued)

Grummann Aircraft Engineering Corporation
Bethpage, L.I., New York
Mr. John Halajian
Dr. Neville Milford

Brown Engineering Company
Sparkman Drive
Huntsville, Alabama
Dr. Watson
Dr. F. Six

University of Alabama
Research Institute
Huntsville, Alabama
Dr. Rudolph Hermann

Division of Geological Sciences
California Institute of Technology
Pasadena, California
Dr. Bruce C. Murray

Dr. William M. Sinton
Astonomy Department
University of Hawaii
Honolulu, Hawaii

Boeing Scientific Research Laboratories
Seattle, Washington
Dr. R. Shorthill
Dr. J. Saari

Lunar and Planetary Laboratory
University of Arizona
Tuscon, Arizona
Dr. Gerard P. Kuiper
Dr. T. Gehrals
Dr. F. Low

DISTRIBUTION (continued)

Harvard College Observatory
Cambridge, Massachusetts
    Dr. Hector C. Ingrao
    Dr. Jeffrey L. Linsley

Department of Meteorology
University of Wisconsin
Madison, Wisconsin
    Dr. H. A. Lettau

U. S. Geological Survey
Flaggstaff, Arizona
    Dr. Eugene Shoemaker
    Dr. Kenneth Watson

Hughes Aircraft Company
Space Systems Division
Box 90919
Los Angeles, California 90009
    Dr. R. A. Fuchs

Electro-Mechanical Research, Inc.
Box 3041
Sarasota, Florida 33578
    Mr. A. D. Robinson

Texaco Experiments, Inc.
Richmond, Virginia 23202
    Mr. Ralph H. Chinard, Jr.

Westinghouse Electric Corporation
Box 1693
Baltimore, Maryland 21203
    Mr. V. B. Morris
    Dr. E. J. Sternglass

DISTRIBUTION (continued)

Air Force Cambridge Research Laboratories
Bedford, Massachusetts
Code CRFL
Dr. J. W. Salisbury

Lincoln Laboratory
Massachusetts Institute of Technology
Lexington, Massachusetts
Dr. J. V. Evans

Radio Astronomy Laboratory
University of California
Berkeley, California
Dr. Harold Weaver

Center for Radio Physics and Space Research
Clark Hall
Cornell University
Ithaca, New York 14850
Dr. J. Gold
Dr. M. Harwit
Dr. Bruce Hapke

Space Sciences Laboratory
Space and Information Systems Division
North American Aviation, Inc.
Downey, California
Dr. J. Green

Columbia University
New York, N. Y.
Dr. Langseth

Yale University
New Haven, Connecticut
Dr. Clark

DISTRIBUTION (continued)

University of Minnesota
Department of Electrical Engineering
Minneapolis, Minnesota
Mr. T. A. Holl

Princeton University
Department of Physics
Princeton, New Jersey
Dr. J. J. Hapfield

NASA HEADQUARTERS

Mr. J. J. Gangler, Code RRM

Dr. Leo Werner, Code RV-1

Mr. D. Beattie, Code MTL

Mr. V. Wilmarth, Code SL

Mr. M. Ames, Code RV

Dr. Homer Newell, Code S

Mr. O. Nicks, Code SL

Mr. W. Foster, Code SM

Dr. Hermann Kurzweg, Code RR

Dr. Raymond Wilson, Code RRA

Dr. J. G. Lundholm, Code MLA

NASA CENTERS

Jet Propulsion Laboratory
4800 Oak Grove Drive
Pasadena, California 91103
Dr. John Lucas
Mr. Elmer Christensen

Jet Propulsion Laboratory (contd)

Mr. W. F. Carroll
Technical Library (2)
Dr. Conway Snyder
Dr. L. D. Jaffe

Langley Research Center
Langley Station
Hampton, Virginia 23365
Dr. Samuel Katzoff
Mr. Charles Woerner
Library (2)
Dr. F. L. Thompson, Dir.

Goddard Space Flight Center
Greenbelt, Maryland 20771
Dr. H. Goett, Dir.
Mr. Milton Schach
Dr. J. O'Keefe
Dr. William Nordberg
Dr. Jacob Trombka
Mr. D. C. Kennard, Jr.
Dr. Wilmot Hess
Library (2)

Lewis Research Center
21000 Brookpark Road
Cleveland, Ohio 44135
Dr. Abe Silverstein, Dir.
Library (2)

Ames Research Center
Moffett Field, California 94035
Dr. S. J. DeFrance, Dir.
Mr. Carr B. Neel
Library (2)

DISTRIBUTION (concluded)

Manned Spacecraft Center
Houston, Texas 77058
- Dr. R. R. Gilruth, Dir.
- Technical Library (2)
- Mr. Robert L. Jones, ET33
- Mr. W. W. Mendell, ET33
- Mr. Curtis Mason, ET33
- Mr. William LeCroix, ET33
- Dr. J. Dornbach, ET33
- Mr. R. Piland, EX

John F. Kennedy Space Center
Kennedy Space Center, Florida 32931
- Dr. H. F. Gruene
- Col. Petrone, K-P
- Technical Library (2)